

IMPACTS OF CLIMATE VARIABILITY AND LAND USE CHANGE
ON THE HYDROLOGY OF THE AMAZON RIVER BASIN

By

Omid Bagheri

A DISSERTATION

Submitted to
Michigan State University
in partial fulfillment of the requirements
for the degree of

Civil Engineering – Doctor of Philosophy

2023

ABSTRACT

This dissertation investigates the intricate dynamics of hydrologic systems in the Amazon River basin (ARB) in the face of evolving climate patterns and human interventions. The ARB – a pivotal element of the global climate, hydrological, and biogeochemical systems – holds immense biodiversity and profoundly influences global water, energy, and carbon cycles. Climate variations and human activities, especially deforestation in the southern subbasins, have considerably altered the basin's functioning. Despite extensive research, critical scientific gaps remain regarding key processes that govern hydrologic dynamics and the resilience of the rainforest. This research disentangles the impacts of climate and land use/land cover (LULC) changes toward devising robust resource management strategies. Recent acceleration of the hydrological cycle of the ARB and the increase in the frequency of extreme events could be early indicators of the change in hydrological cycle in the region surpassing some irreversible thresholds. While some systematic tipping points are inferred over the ARB, no tipping points associated with dominant hydrological processes over the ARB are investigated. This inhibits the understanding of hydrological considerations needed for sustainable forest management under climatic change and growing human stressors. The dissertation employs high resolution (~2km), long-term simulations from a process-based hydrological model (LEAF-Hydro-Flood) to investigate the dominant hydrological processes across the ARB, their key roles in shaping basin functions, and the decadal evolutions therein. Further, by developing static and dynamics LULC scenarios, the impact of climate variability and LULC change are isolated. Finally, through a comprehensive area fraction analysis and using a corresponding tree cover dataset, the tipping points associated with dominant hydrological processes in the ARB are assessed. Results indicate that shallow groundwater (<5m deep) strongly modulates the seasonality of the surface

fluxes across the ARB and at least 34% of the Amazonian Forest is supported by groundwater during the dry season. This study reveals a two-month lag between seasonal peak evapotranspiration (ET) and river discharge as a crucial mechanism in preventing rainforest tipping into savanna. The ARB is dominantly energy limited; however, the results suggest that in the absence of groundwater support, and with less than ~125 mm/month of precipitation, the ARB could have become water-limited over some regions. The long-term basin-averaged ET—dominated by transpiration—changed with a split pattern of $\pm 9\%$ in the past three decades. Similarly, water table depth ($\pm 19\%$) and runoff ($\pm 29\%$) changed with a heterogeneous patterns across the ARB. The contribution of canopy interception loss and ground evaporation changed heterogeneously across the ARB in response to deforestation. River discharge did not change substantially due to the crucial buffering role of groundwater, but terrestrial water storage (TWS) decreased (increased) in the 2000s (2010s) compared to that in the 1990s. Although groundwater is the dominant contributor to total TWS, the dynamics of TWS over the major river channels are controlled by flood water, given relatively shallow groundwater. Despite extensive deforestation, climate variability remains the dominant influence on WTD dynamics; however, the impacts on ET varied across the basin. Runoff patterns were intricately tied to precipitation and water table dynamics, demonstrating regional variations influenced by both climate variability and LULC changes. The area fraction analysis of WTD seasonality confirms the existence of tipping points associated with groundwater dynamics in the ARB. This study provides crucial insights on (i) the dominant hydrological processes, (ii) isolated impacts of climate variability and LULC change on the water cycle of the ARB, and (iii) tipping points in the ARB that are associated with groundwater dynamics. These findings could be used to inform effective water resource management and sustainable environmental practices in this ecologically significant region.

Dedicated to my beloved parents.

ACKNOWLEDGEMENTS

This Ph.D. journey has profoundly transformed my life. Through the inevitable highs and lows, it would have been insurmountable without the invaluable guidance and unwavering support of numerous individuals. Foremost among them is my deep gratitude to Dr. Yadu Pokhrel, my Ph.D. advisor, whose exceptional mentorship, support, enlightening guidance, and constant encouragement were instrumental throughout my doctoral program. This dissertation owes its existence to his indispensable assistance, and I am fortunate to have collaborated with him. I also extend sincere appreciation to my committee members, Dr. Shu-Guang Li, Dr. Phanikumar Mantha, and Dr. Nathan Moore, for their consistent assistance, meticulous comments, and insightful suggestions. The completion of this dissertation was made possible in part by the support of the National Science Foundation (CAREER, Award #1752729 and INFEWS, Award #1639115). I acknowledge with gratitude the provision of high-performance computing by NCAR's Computational and Information Systems Laboratory (doi:10.5065/D6RX99HX). Special thanks go to Suyog Chaudhari and Mohammad Hassan Badizad for their technical insights in Python scripting, crucial for producing some of the figures in this dissertation. I express my thanks to dear friends and colleagues Farshid Felfelani, Sanghoon Shin, Tamanna Kabir, Amar Deep Tiwari, and Ahmed Elkouk for engaging in fruitful discussions and sharing joyful moments. My heartfelt appreciation goes to my parents, Ali and Fatemeh, for their boundless love and for guiding me in shaping my life.

TABLE OF CONTENTS

Chapter 1 Introduction	1
1.1 Research Motivation	1
1.1.1 Global significance of the Amazon River basin	1
1.1.2 Water cycle and climate variability in the ARB	2
1.1.3 LULC change in the ARB.....	6
1.1.4 Process-based analysis of climate variability and LULC change impacts	8
1.1.5 Separating the LULC change impacts from CV impacts.....	11
1.1.6 The ARB tipping points	14
1.2 Research Goal, Objectives, and Science Questions	16
1.3 Dissertation Outline.....	18
Chapter 2 Groundwater Dominates Terrestrial Hydrological Processes in the Amazon at the Basin and Subbasin Scales.....	19
2.1 Introduction	19
2.2 Methods.....	25
2.2.1 Model Description	25
2.2.2 Atmospheric Forcing	27
2.2.3 Land Use/Land Cover and Leaf Area Index	28
2.2.4 Simulation Setup.....	30
2.2.5 Trend Analysis	31
2.3 Results and Discussion.....	32
2.3.1 Validation.....	32
2.3.2 Dynamics of Key Hydrological Processes.....	39
2.3.3 Governing Hydrological Processes.....	60
2.3.4 Early/Late Warning Signals.....	68
2.3.5 Hydrological Implications for Forest Management.....	69
2.4 Conclusions	72
Chapter 3 Climatic and Anthropogenic Impacts on the Hydrology of the Amazon River Basin.	76
3.1 Introduction	76
3.2 Methods.....	80
3.2.1 Model Description	80
3.2.2 Atmospheric Forcing	82
3.2.3 Land Use/Land Cover and Leaf Area Index	83
3.2.4 Simulation Setup.....	84
3.3 Results and Discussion.....	85
3.3.1 Validation.....	85
3.3.2 Impacts on Groundwater.....	85
3.3.3 Impacts on Evapotranspiration	93
3.3.4 Impacts on Runoff.....	98
3.4 Conclusions	103
Chapter 4 Tipping Points Associated with Water Table Depth in the Amazon River Basin	106
4.1 Introduction	106
4.2 Methods.....	110
4.3 Results and Discussion.....	112

4.4 Conclusion.....	118
Chapter 5 Summary and Conclusion	120
REFERENCES	122

Chapter 1 Introduction

1.1 Research Motivation

1.1.1 Global significance of the Amazon River basin

With a total area of ~7.3 million km² (including the Tocantins) and diverse rivers, floodplains, and wetlands, the Amazon River basin (ARB) is home to the most extensive tropical forest biome on the planet (~40% of the global tropical forest) (L. E. O. C. Aragão et al., 2014; Junk et al., 2011; W. F. Laurance et al., 2001; Jose A. Marengo et al., 2018; Reis et al., 2019; Weng et al., 2018). It spans nine nations (i.e., Brazil, Bolivia, Peru, Ecuador, Colombia, Venezuela, Guyana, Suriname, and French Guiana) and hosts four of the 10 largest rivers in the world (i.e., Solimoes, Madeira, Negro, and Japura rivers) (Fassoni-Andrade et al., 2021). The Amazon River flows into the Atlantic Ocean with an average annual discharge of 206×10^3 m³/s (Callede et al., 2010), amounting to ~20% of the total global freshwater reaching the ocean annually (Nepstad et al., 2008) and transfers substantial amount of sediment to the ocean (1.1×10^9 tons/year) (Armijos et al., 2020). Further, ARB provides home to ~25% of all terrestrial species on earth, accounts for ~15% of global terrestrial photosynthesis and is referred to as “lungs of the earth” (Field et al., 1998; Malhi et al., 2008).

Further, the ARB is an important component of global biodiversity as well as global water, energy, and carbon cycles, and plays a key role in the global climate system through high rates of precipitation recycling and atmospheric moisture transport, and large variations in freshwater storage and river discharge (Arvor et al., 2017; Cox et al., 2004; Y. Fan & Miguez-Macho, 2010; Fassoni-Andrade et al., 2021; Gash, 1979; Gatti et al., 2021; William F. Laurance et al., 2002; Malhi et al., 2008; Nagy et al., 2016; Carlos A. Nobre et al., 1991; B. Soares-Filho et al., 2010; B. S. Soares-Filho et al., 2006; Werth & Avissar, 2005). It receives high annual

rainfall, on average ~2,200 mm/year (Builes-Jaramillo et al., 2018; Espinoza Villar et al., 2009). This rainfall depends on advected oceanic moisture combined with moisture recycling. ET can contribute up to 30–40% of the atmospheric moisture during the dry season (Eltahir & Bras, 1994; Van Der Ent et al., 2010; Salati et al., 1979; Satyamurty et al., 2013; Staal et al., 2018; D C Zemp et al., 2014) and is important for the initiation of the seasonal monsoon over the southern Amazon (Wright et al., 2017).

The ARB ecosystems host 10–15% of land biodiversity (Hubbell et al., 2008; Lewinsohn & Prado, 2005) and the basin stores an estimated 150 billion to 200 billion tons of carbon (Cerri et al., 2007; Malhi et al., 2006; Saatchi et al., 2011) and surface waters in the basin are a major source and sink of carbon dioxide (Abril et al., 2014; Amaral-Zettler et al., 2020; Guilhen et al., 2020; Raymond et al., 2013; Richey et al., 2002) and the largest natural geographic source of methane in the tropics (Kirschke et al., 2013; Melack et al., 2004; Pangala et al., 2017; Pison et al., 2013). Importantly, the ARB is one of the top fifteen tipping elements of the Earth system (L. E. O. C. Aragão et al., 2014; W. F. Laurance et al., 2001; Lenton et al., 2008; Schellnhuber, 2009; Weng et al., 2018). The population of the ARB is estimated at ~10 million, mostly concentrated in urban areas along the river and its main tributaries. The basin is home of the local, including some indigenous, people that rely on rivers as transportation corridors and utilize these environments for their subsistence (Anderson & Ioris, 1992; Campos-Silva et al., 2021; Endo et al., 2016). Amazon also serves the broader South American population in terms of energy, food, and other forest products.

1.1.2 Water cycle and climate variability in the ARB

The ARB is primarily characterized by lowlands with a warm and rainy climate; however, the upper basin, encompassing the eastern slope of the Andes, exhibits a diverse range

of mountain climates. The climate across the ARB varies from a wet northwest with minimal dry spells to a dry southeast marked by an extended dry season. Notably, alterations in precipitation, particularly during the dry season, play a pivotal role in determining the climatic trajectory of the ARB (Malhi et al., 2008). The hydroclimate system of the ARB operates across various spatial and temporal scales, and major climatic patterns are predominantly driven by large-scale processes. For instance, interdecadal and interannual variabilities (e.g., extreme events) in the ARB's climate are primarily modulated by persistent sea surface temperature (SST) patterns in both the Atlantic and Pacific oceans. Specifically, those linked to El Niño/Southern Oscillation (ENSO). Concurrently, mesoscale processes (e.g., topography and land-atmosphere interactions) modulate localized circulations. Typically, ENSO is accompanied by droughts in the ARB, resulting in low river water levels, a heightened risk of forest fires, and impacts on river ecosystems (Malhi et al., 2008).

Variations in Pacific SST, primarily influenced by ENSO, play a significant role in shaping wet-season rainfall patterns. This influence leads to the suppression of convection in the northern and eastern regions of the ARB during ENSO events. In contrast, the variability in dry-season rainfall is strongly tied to the north-south SST gradient in the tropical Atlantic. The intensification of this gradient results in a northward shift of the Intertropical Convergence Zone at interannual time scales, while also strengthening the circulation of the Hadley Cell over longer periods. Such intensification contributes to prolonged and more intense dry seasons, particularly affecting the southern and eastern regions of the ARB, as evidenced in 2005 (Malhi et al., 2008). The interannual variability of the Atlantic gradient is influenced by distant factors like ENSO and the North Atlantic Oscillation, along with variations in evaporation triggered by the strengthening or weakening of local trade winds. Over extended time scales, alterations in the

North Atlantic, such as changes in thermohaline circulation due to subpolar melting or a warmer North Atlantic associated with the warming of northern hemisphere continents, have the potential to enhance the Atlantic SST gradient. Dry-season rainfall, crucial for vegetation patterns, is often driven by locally generated convection and can be significantly impacted by deforestation (Malhi et al., 2008).

Water in the ARB primarily originates from ocean evaporation, undergoing multiple moisture recycling processes before ultimately returning to the ocean through surface or aerial rivers. The region experiences abundant rainfall, averaging ~2,200 mm/year (Builes-Jaramillo et al., 2018; Espinoza Villar et al., 2009). This substantial precipitation is a result of various factors, including intense radiative heating, low-level convergence of oceanic water vapor, continuous infusion of water vapor into the atmosphere by the rainforest itself, aided by the mechanical uplifting of air by the Andes. Land surface processes play a pivotal role in distributing precipitation into ET (averaging ~1,220 mm/year), surface runoff, and changes in surface and subsurface storage (Malhi et al., 2008). The Amazon River exhibits a highly seasonal flow, with seasonal imbalances between rainfall and downstream river discharge leading to substantial flooding across a vast floodplain area. These flooding events have beneficial ecological and biogeochemical implications. The occurrence of extreme flood and drought events is linked to intense interannual precipitation variability, influencing forest fires and biogeochemical cycles (Malhi et al., 2008). Microclimate control at the forest edges, including temperature and humidity regulation, constitute fundamental aspects of the coupled biosphere-atmosphere system in the ARB. These mechanisms shape the climate not only within the rainforest but also in the surrounding regions. Moreover, these processes contribute to the resilience of the coupled system during the dry season along its southern borders. They ensure a consistent source of water vapor

to the ARB's atmosphere, particularly crucial when Atlantic oceanic inputs weaken (Malhi et al., 2008).

The recent acceleration of the hydrological cycle in the ARB can be attributed to the increased interannual variability (Bagheri et al., 2024; Barichivich et al., 2018; Chagas et al., 2022). In recent years, the ARB has faced numerous climate extremes, including droughts and floods, some classified as "once-in-a-century" events, underscoring the region's susceptibility to climatic shifts (Barichivich et al., 2018; José Antonio Marengo & Espinoza, 2016). Historical records of similar droughts and floods indicate a reduction in the flood return period from 20 years to 4 years since 2000, signifying an increased frequency of extreme flooding events (Barichivich et al., 2018; José Antonio Marengo & Espinoza, 2016). Additionally, regional discharges have shown a rise in high flow in the northwestern regions of the ARB and a decrease in low flow in the southwestern regions during the 1974-2009 period. The dry season has expanded by approximately one month in the southern regions of the ARB since the mid-1970s. Warming is evident over the ARB, with the warming trend varying across different datasets. The warming trend becomes particularly pronounced from 1980 onwards, intensifying since 2000, with years like 2015-16 and 2020 ranking among the warmest in the last three decades (Almeida et al., 2017; Marengo et al., 2018). Determining the climate change fingerprint remains challenging due to the relatively short duration of climate records. However, climate modeling studies simulating the ARB's deforestation predict significant reductions in rainfall over the ARB, impacting regional hydrology and increasing the vulnerability of ecosystem services for the local and regional population within and beyond the ARB.

1.1.3 Land use/land cover change in the ARB

Deforestation, the complete removal of an area's forest cover; and forest degradation, the significant loss of forest structure, functions, and processes; are the result of the interaction between various direct drivers, often operating in tandem (Barreto et al., 2021; Berenguer et al., 2014; Longo et al., 2020; Parrotta et al., 2012; Putz & Redford, 2010). Approximately 16% of the forest is deforested (Mapbiomas_Amazonia, 2022) with a concentration in Brazil where forest degradation has reached 17% (Bullock et al., 2020; Matricardi et al., 2020; Souza Jr et al., 2020). Deforestation in the Brazilian Amazon was less than 1% before 1975 but increased exponentially between 1975 and 1987 (Moran, 1993). The degraded forests are a persistent part of the landscape, as only 14% of them were later deforested (Bullock et al., 2020). Forest loss affects local temperature and precipitation, with increases in land surface temperatures and reductions in precipitation of up to 1.8% across the ARB. The deforestation is primarily a result of cattle ranching and replacement of forests with pasture and croplands at the agriculture frontier ("arc of deforestation") in the southern subbasins (Bagley et al., 2014; Marcos H. Costa et al., 2007; Marcos Heil Costa & Pires, 2010a; Davidson et al., 2012; Guan et al., 2015; Mercedes & Montenegro, 2005; Moore et al., 2007; Morton et al., 2006). In addition, rapid population growth, timber extraction, mining, forest fires, construction of hydroelectric dams, urbanization and road network expansion are among other sources of land use/land cover (LULC) change in the ARB (Foley et al., 2005; B. S. Soares-Filho et al., 2006). In the past four decades, LULC changes occurred across the ARB, however, Tapajos (~31%), Xingu (~30%), Madeira (~21%), and Tocantins (~19%) are the four sub-basins of the ARB with big pockets of LULC change (Mapbiomas_Amazonia, 2022). Substantial LULC change happened around 1995, 1999 and 2004 (Mapbiomas_Amazonia, 2022; Smith et al., 2021). These changes in LULC in

conjunction with ongoing climate change impacted the terrestrial water cycle in recent decades (Sterling et al., 2013). Deforestation leads to local (e.g., changes in landscape configuration, climate change, and biodiversity loss), regional (e.g., impacts on hydrological cycle), and global impacts (e.g., increase of greenhouse gas emissions).

Various anthropogenic drivers, including forest fires, edge effects, selective logging, hunting, and anthropogenic climate change can cause forest degradation (Andrade-Filho et al., 2017; Barlow et al., 2016; Bustamante et al., 2016; Phillips & Derryberry, 2017). Degraded forests have significantly different structure, microclimate, and biodiversity as compared to undisturbed ones. The degraded forests tend to have higher tree mortality, lower carbon stocks, more canopy gaps, higher temperatures, lower humidity, higher wind exposure, and exhibit compositional and functional shifts in both fauna and flora. Degraded forests can come to resemble their undisturbed counterparts, but this depends on the type, duration, intensity, and frequency of the disturbance event. In some cases, this may prohibit the return to a historic baseline. Deforestation and forest degradation are responsible for enormous quantities of CO₂ emissions. The duration of the impacts of anthropogenic disturbances on Amazonian forests varies depending on the nature, frequency, and intensity of the disturbance; while logged forests may return to baseline carbon stocks within a few decades (Rutishauser et al., 2015), burned forests may never recover their original stocks (Silva et al., 2018). Recovery of degraded forests is also dependent on their landscape context, i.e., whether there are forests nearby that can act as sources of seeds and animals, thus speeding up recovery. Avoiding further loss and degradation of Amazonian forests is crucial to ensure they continue to provide valuable and life-supporting ecosystem services.

1.1.4 Process-based analysis of climate variability and LULC change impacts

Over the past few decades, the global terrestrial water cycle has undergone unprecedented changes (Bosmans et al., 2017; Sterling et al., 2013), driven primarily by internal variability in the climate system, anthropogenic climate change (i.e., emission-driven) and direct human disturbances (Bosmans et al., 2017; Wohl et al., 2012). Human activities modulate the climate system at different scales through changes in LULC and components of water cycle to satisfy the growing need for food, fiber, water, and shelter for more than 7.8 billion people (Foley et al., 2005). Humans have changed more than 41% of natural landscape by anthropogenic land cover such as crop fields or pasture which impacts the evaporation-to-runoff ratio which, in general, has increased discharge and decreased evapotranspiration (ET) globally (Bosmans et al., 2017). Extensive LULC changes in watersheds has dramatic short- and long-term impacts on terrestrial hydrology and alters the occurrence and severity of extreme hydrological events (e.g. floods and droughts) which are the causes of the most human suffering among all climate-related events (Sterling et al., 2013). A significant portion of the changes in LULC are essential for agricultural and industrial development and the majority of other human interventions in the terrestrial hydrological cycle such as flow regulation and land development are requirements for ever-growing populations. Therefore, for sustainable development and for avoiding unintended consequences on land and water resources it is of crucial importance to understand the impacts of deforestation, afforestation and the collective LULC changes on terrestrial hydrological cycle.

The system services in the ARB are altered due to climate variability and human disturbances with dominant form of deforestation as a result of replacing forests with pasture and agriculture specially across the “Arc of Deforestation” in the southern subbasins which is the

primary cause of LULC change (Marcos Heil Costa & Pires, 2010b; Davidson et al., 2012; Mercedes & Montenegro, 2005; Moore et al., 2007; Tropek et al., 2014). These changes in LULC in conjunction with ongoing climate change have impacted the terrestrial water cycle in recent decades (Sterling et al., 2013). Dependence of the hydro-ecological systems in the ARB on plentiful rainfall and the range of climatology across the basin highlights the importance of investigating the impacts of climate variability and LULC change on terrestrial hydrological cycle in ARB (Cook et al., 2012; Espinoza et al., 2015, 2016; Espinoza Villar et al., 2009; Nepstad et al., 2008). Previous interannual and interdecadal studies on hydrological alteration in ARB showed an overall long-term increasing trend in terrestrial water storage (TWS), however, the southern and southeastern sub-basins are experiencing significant decreasing trends in TWS, and LULC is known as the primary component contributing to the trend (Chaudhari et al., 2019). However, the processes which led to this alteration in the hydrological cycle of the ARB are not crystal clear yet.

Impacts of human interventions in terms of LULC changes on terrestrial hydrological cycle are complex and depend on the initial LULC. The direct effects of the human induced LULC changes include the morphological and physiological variations in the landscape as reflected by altered aerodynamic roughness, leaf area index (LAI), stem area, surface resistance, albedo, and rooting depth (Bala & Nag, 2012; Bäse et al., 2012). The indirect effects of LULC changes on the soil and atmospheric boundary layer include the altered infiltration capacity and hydraulic conductivity in the shallow soil layer (Bonell et al., 2010; Ghimire et al., 2014; Hassler et al., 2011; Lanckriet et al., 2012; Muma et al., 2011; Neill et al., 2013), as well as varied net radiation, sensible and latent heat flux, and wind speed (Mishra et al., 2010). Both the direct and the indirect effects of LULC changes have strong implications particularly for energy,

momentum, and water balance in the atmospheric boundary layer and could affect hydrologic cycles and climate systems at different scales (e.g., locally, regionally, and globally) (Bala & Nag, 2012; Kumagai et al., 2013; Poveda et al., 2014; Dominick V Spracklen et al., 2012).

The interaction of LULC in climate and land system, being scale-dependent, in addition to lack of comprehensive simulations of the system which include water cycle, ecology, abiotic-biotic linkages, and human interventions make study of impact of LULC change on terrestrial hydrological cycle a cumbersome task. Meanwhile, the study of the impacts of climate variability and LULC change on key hydrological variables (e.g., river discharge, ET, WTD and TWS) and quantification of their effects is currently feasible due to recent advances in fully-physics based hydrological models and emerging remotely sensed data and observations (Bosmans et al., 2017; Foley et al., 2005; Sterling et al., 2013; Wohl et al., 2012). Characterizing and understanding the dynamics of the ARB water cycle is of primary importance for climate and ecological research and for the management of water resources. Consequently, there is a need for comprehensive monitoring of the spatial-temporal dynamics of the ARB water cycle components and how they interact with climate variability and anthropogenic pressure. The region is now facing risks under climate and anthropogenic changes, and changes in Amazon hydrology could have substantial impacts globally (Jimenez et al., 2019). In the past decades, the basin experienced several intense climatic events, such as extreme droughts and floods, with no equivalent in the last 100 years (Barichivich et al., 2018; Marengo & Espinoza, 2016). Severe droughts can lead to environmental disturbances, from increased fire occurrence (Zeng et al., 2008) to abrupt shifts in fish assemblages (Röpke et al., 2017). Moreover, the accumulated negative impacts of increased human interventions across the region, such as damming (Forsberg et al., 2017; Latrubesse et al., 2017), deforestation (Arias et al., 2020; Coe et al., 2009; Gutierrez-

Cori et al., 2021; Leite-Filho et al., 2020; Leite et al., 2012), fires (Aragão et al., 2008; Libonati et al., 2021; Xu et al., 2020; Zeng et al., 2008), and mining (Abe et al., 2019; Lobo et al., 2015), will possibly trigger major modifications that could affect the ARB's water cycle.

1.1.5 Separating the LULC change impacts from CV impacts

Hydrological impacts of LULC change are difficult to discern at large-scale basins with gradual changes and difficult to isolate from climate variability impacts either through observations or experiments (Arias et al., 2018; Dey & Mishra, 2017; Levy et al., 2018; Davidson et al., 2012; Cavalcante et al., 2019). Having a variety of LULC types in various stages of protection and regeneration and possibility of occurring positive feedback adds to the difficulty level (Nepstad et al., 2001; Nobre et al., 2016; Lima et al., 2013; Costa & Pires, 2010; Knox et al., 2015; Costa et al., 2003; Panday et al., 2015; Rodriguez et al., 2010). Because climate variability is typically high, any underlying changes due either to climate change or LULC changes can be effectively obscured (Kundzewicz & Robson, 2004). This complexity is noted as a potential reason for the disagreement in hydrological response to LULC change among macrocatchment studies in the tropical rainforest (Cavalcante et al., 2019). For instance, Trancoso (2006) reported a predominant decline in runoff within the Xingu, Tapajós, and Madeira subbasins due to reduction in precipitation; Arias et al. (2018) observed a reduced river flow across much of the Tapajós, despite no significant trend in annual precipitation; and by masking the deforestation impacts, Panday et al. (2015) estimated the decrease in river flow in Xingu due to climate variability. Conversely, Marengo et al. (1998) did not observe significant trends in discharge within the ARB and Tocantins. However, Costa et al. (2003) noted an uptick in mean discharge in the upper Tocantins, where savanna was the primary original land cover. In the majority of these subbasins, forest predominantly converted to pasture, except in Tapajós

where forest converted to soybean croplands which might explain the reduced river flows in Tapajos (Cavalcante et al., 2019).

Global climate change affects the ARB through temperature increase and alters precipitation patterns and climate extremes, leading to increased tree mortality and terrestrial and aquatic biodiversity loss. Coupled with land-use change through deforestation and degradation, this reduces ET, changes carbon cycling dynamics, decreases the resilience of the ecosystems, and leads to further biodiversity loss and tree mortality, emitting greenhouse gases that impact not only regional, but the global climate. In this way, deforestation in the ARB enhances climate change.

Because major drivers of the hydrological system are not stationary in time, isolating the hydrological impacts of human activities from climate variability is challenging. Separating the impacts of climate variability and anthropogenic impacts on the water cycle of the ARB is important for several reasons, and a large number of methods and theories have been widely used. First, the impacts of climate variability and LULC can be accumulative, subtractive, intensifying, and mitigating, therefore, there is a need for separating the impacts to identify the drivers of the change. Second, separating the impacts of climate change and anthropogenic impacts can help us develop more effective strategies for managing the ARB. For example, if the drivers behind the changes in water availability are primarily due to climate change, prioritizing strategies such as water conservation, drought-resistant crops, and water storage to adapt to those changes might be effective. On the other hand, if changes in water availability are primarily due to human activities, prioritizing strategies such as land use planning, water use efficiency, and pollution control to mitigate those impacts might be effective. Overall, understanding the interplay between climate variability and land cover is fundamental to the conservation and

sustainable management of tropical river basins, where forests play an important role in regional hydrological alterations at regional, continental, and global scales (Coe et al., 2013; Davidson et al., 2012; Malhi et al., 2008).

Various techniques have been employed to disentangle the influences of climate variability and human activities on hydrological processes. These methods include hydrological modeling, conceptual, analytical, and experimental approaches (Cavalcante et al., 2019; Dey & Mishra, 2017; Wang, 2014; Tomer & Schilling, 2009; Schaake, 1990; Wang & Hejazi, 2011). Specific methodologies dedicated to isolating the impacts of climate variability and human activities on streamflow have been devised, such as the Tomer and Schilling framework (Tomer & Schilling, 2009), the elasticity-based method (Schaake, 1990), and the decomposition of the Budyko-type curve method (Wang & Hejazi, 2011), among others (Dey & Mishra, 2017; Wang, 2014; Wei et al., 2013). Acknowledging that each method/technique possesses its unique strengths and weaknesses, Wei et al. (2013) proposed that employing a combination of methods would constitute a more robust research strategy than relying on any single method alone. They also emphasized the need for additional case studies. Paired catchment studies, commonly utilized to assess the impact of vegetation changes on water yield, typically involve small catchments and can be cost-prohibitive (Brown et al., 2005). Alternatively, model simulations are often used, necessitating time-consuming calibration and validation processes, large datasets dependent on model assumptions, and statistical methods like time series analysis (Zégre et al., 2010; Zhao et al., 2010). However, the need for calibration is obviated in physics-based hydrological models, and advancements in remote sensing and computational systems have alleviated many associated limitations.

1.1.6 The ARB tipping points

Tipping points (unstable equilibrium states) are defined as phenomena that, beyond a certain threshold, runaway change propels a system to a new state (van Nes et al., 2016; Scheffer et al., 2001). For example, due to deforestation and replacement of forest with pasture ET decreases and water table becomes shallower owing to extra recharge. Then, groundwater causes a positive feedback mechanism (DeAngelis et al., 2012) in further decreasing ET and recharging groundwater and propelling the forest system to an alternative tree species system. Therefore, once a threshold is passed, the dynamics of the system can accelerate dramatically to cause a ‘runaway change’. Two fundamental different ways in which a system can move to another stable state: (i) a change in external conditions (disturbance; e.g., climate change) which in models are represented by parameters, or (ii) a change in the state of the system itself (perturbations; e.g., human activities) which in models is represented by state variables (van Nes et al., 2016). The first type of tipping points are detected by warning signals or resilience indicators because of the gradual erosion of the resilience of the previous state of the system (van Nes et al., 2016).

The ongoing changes in the ARB’s forest system may result in a loss of resilience and surpassing tipping points, triggering a persistent shift to an alternative state within the ecosystem. Five systemic tipping points are inferred over the ARB including four associated with climate and one associated with human-induced changes (Science Panel for the Amazon, 2021). These tipping points include (1) receiving annual precipitation below 1,000 mm/yr, as inferred from satellite observations of tree cover distributions (Hirota et al., 2011; Staver et al., 2011) or 1,500 mm/yr, as inferred from global climate models (Malhi et al., 2009), (2) a dry season lasting more than seven months, determined from satellite observations of tree cover distributions (Staver et

al. 2011), (3) maximum cumulative water deficit values exceeding than 200 mm/yr (Malhi et al. 2009) or 350 mm/yr (Zelazowski et al., 2011) over the ARB lowlands, inferred from various analyses with global climate models, (4) a 2°C increase in the Earth’s equilibrium temperature, identified through a coupled climate–vegetation model (Jones et al., 2009), and (5) 20-25% accumulated deforestation of the entire basin, determined through a combination of environmental changes (e.g., increased dry season length), climate projections aligned with the most pessimistic pathway of the Intergovernmental Panel on Climate Change (IPCC), and human-induced degradation via deforestation (Lovejoy & Nobre, 2019; Carlos A. Nobre et al., 2016). Existing evidence indicates that, depending on diverse combinations of stressing conditions, disturbances, and feedback mechanisms, the current forest configurations at the local scale, could be replaced by: (i) a seasonally dry, closed-canopy tropical forest with an increasing abundance of deciduous tree species (Dexter et al., 2018; Malhi et al., 2009); (ii) a tropical savanna state dominated by native grass and tree species (Cox et al. 2004; Jones et al. 2009; Hirota et al. 2011; Staver et al. 2011; Lovejoy and Nobre 2019); (iii) an open-canopy degraded state, dominated by invasive alien grasses and native fire-tolerant tree species (Barlow & Peres, 2008; Brando et al., 2012; Flores et al., 2016); and (iv) a closed-canopy secondary forest, dominated by native early successional tree and other plant species (Poorter et al., 2016; Rozendaal et al., 2019). Local-scale forest collapses could initiate cascading effects on rainfall recycling, intensifying dry seasons and wildfire occurrence, potentially leading to massive forest loss at continental scales, particularly in the southwest of the basin. The probability of crossing these tipping points largely depends on heterogeneities across the system, including geological, physical, chemical, and cultural processes that influence connectivity and the likelihood of contagious disturbances. The primary concern is that beyond these potential tipping points, the

system might enter a loop of reduced rainfall, increased fire, and heightened forest mortality. Over the past six decades, the temperature in the ARB has risen by 1-1.5°C (Nobre et al., 2016), approximately 18% of the forest area has been deforested (Mapbiomas_Amazonia, 2022), forest degradation has reached 17% (Bullock et al., 2020; Matricardi et al., 2020), forest fires have significantly increased (Aragão et al., 2018), dry season lengths (measured as the number of consecutive days with less than 50mm rainfall) are three to four weeks longer compared to six decades ago (Fu et al., 2013), and dry season water storage deficit is on a divergent trend (Chaudhari et al., 2019). Some studies suggest that the escalating frequency of unprecedented droughts, such as those in 2005, 2010, 2015-16, and 2020, could be signaling the imminent arrival of a tipping point (Bagley et al., 2014; Lovejoy & Nobre, 2019; Walker, 2020). Consequently, there is an imperative need to curtail deforestation in the ARB, rehabilitate the lost forest in its southern and eastern regions, and provide science-based guidelines to inform forest management policies (Lovejoy and Nobre, 2019; Walker, 2020).

1.2 Research Goal, Objectives, and Science Questions

As discussed above, the hydrology of the ARB has been extensively studied; however, critical scientific gaps remain regarding key processes that govern hydrologic dynamics and the resilience of the rainforest. This inhibits the understanding of hydrological considerations needed for sustainable forest management under climatic change and growing human stressors. This dissertation aims to examine the changes in basin-wide water and energy balances under large-scale climate variability and LULC changes and the resulting shifts in system thresholds toward a new equilibrium. The goal is to quantify the impact of climate variability and LULC change in the past four decades, identifying the dominant hydrological processes at the basin and subbasin scales, and identifying the tipping point associated with the dominant hydrological processes

using a multi-scale assessment of the basin based on the results of high-resolution simulations using LEAF-Hydro-Flood (LHF). This dissertation is driven by the following overarching scientific questions: (1) How have the major components of water and energy balances in the ARB evolved due to changes in hydrological drivers? (2) What dominates terrestrial hydrological processes at the basin and subbasin scales in the ARB? (3) What are the impacts of climate variability and LULC change in the ARB over the past four decades? (4) Are there tipping points in the ARB associated with WTD dynamics? These overarching questions are addressed by answering the following specific science questions under different chapters.

Chapter 2. Analysis of the hydrologic dynamics of the ARB and governing processes

Q1. How did the fundamental hydrological processes in the ARB evolve over the past three decades?

Q2. What key factors govern the seasonality of the ARB at the basin and subbasin scales?

Chapter 3. Quantifying the contribution of climate variability and LULC change in shifting the ARB to the current equilibrium at basin and subbasin scales

Q3. What are the contributions of climate variability and LULC change in shifting the hydrology of the ARB to the current equilibrium at the basin and subbasin scale?

Q4. At what temporal and spatial scale should the impacts of climate variability and LULC change be assessed?

Chapter 4. Investigating tipping points associated with dominant hydrological processes in the ARB

Q5. Are there tipping points associated with dominant hydrological processes in the ARB?

Q6. How resilient is the hydrological system of the ARB against the tipping points?

To investigate the dominant hydrological processes over the ARB at the basins and subbasin scale, the hydrology of the ARB is simulated over the past four decades using the LHF model. Then, the contribution of climate variability and LULC change in shifting the ARB to the new equilibrium is isolated through two sets of separate simulations with static and dynamics LULC. Further, area fraction analysis of water table depth (WTD) and theory of dynamics systems are used to investigate the tipping points associated with WTD in the ARB.

1.3 Dissertation Outline

The research questions are tackled in separate chapters (Chapters 2 through 4), and the key findings are summarized in Chapter 5. The following provides a summary of the remaining chapters.

Chapter 2. Groundwater Dominates Terrestrial Hydrological Processes in the Amazon at the Basin and Subbasin Scales.

Chapter 3. Impacts of climate variability and LULC change on hydrological cycle of the Amazon River basin.

Chapter 4. Tipping points associated with water table depth in the Amazon River basin.

Chapter 5. Summary and Conclusion.

Chapter 2 Groundwater Dominates Terrestrial Hydrological Processes in the Amazon at the Basin and Subbasin Scales

Based on: Bagheri, O., Pokhrel, Y., Moore, N., Mantha, S.P., (2024). Groundwater Dominates Terrestrial Hydrological Processes in the Amazon at the Basin and Subbasin Scales. *Journal of Hydrology*, 628, p.130312.

2.1 Introduction

The Amazon River basin (ARB) is home to the most extensive tropical forest biome on the planet (e.g., 40% of the global tropical forest area) and is also one of the tipping elements of the Earth system (L. E. O. C. Aragão et al., 2014; W. F. Laurance et al., 2001; Lenton et al., 2008; Schellnhuber, 2009; Weng et al., 2018) The basin is an important component of global biodiversity as well as global water, energy, and carbon cycles, and plays a key role in the global climate system through precipitation recycling and atmospheric moisture transport (Arvor et al., 2017; Y. Fan & Miguez-Macho, 2010; Fassoni-Andrade et al., 2021; William F. Laurance et al., 2002; Malhi et al., 2008; B. S. Soares-Filho et al., 2006; Werth & Avissar, 2005). The basin functioning (e.g., carbon storage, maintenance of biodiversity, and climate regulation) in the ARB has been altered substantially over the past few decades due to climate variability and human disturbances with deforestation as the dominant form; the deforestation is primarily a result of cattle ranching and replacement of forests with pasture at the agriculture frontier (“arc of deforestation”) in the southern subbasins (Bagley et al., 2014; Marcos H. Costa et al., 2007; Marcos Heil Costa & Pires, 2010b; Davidson et al., 2012; Guan et al., 2015; Mercedes & Montenegro, 2005; Moore et al., 2007; Morton et al., 2006). In addition, rapid population growth, timber extraction, mining, forest fires, and road network expansion are among other sources of land use and land cover (LULC) change in the ARB (Foley et al., 2005; B. S. Soares-Filho et al., 2006).

The hydrological cycle in the ARB is strongly modulated by evapotranspiration (ET) and frequent (up to 7 recycling per water molecule) (Salati et al., 1979; Staal et al., 2018; Weng et al., 2018) and substantial (25-50% of total Amazonian rainfall) moisture recycling (L. C. E. O. Aragão, 2012; Eltahir & Bras, 1994; Van Der Ent et al., 2010; D. V. Spracklen et al., 2012; Staal et al., 2018; Delphine Clara Zemp et al., 2017). Therefore, the basin's hydrologic system is highly susceptible to widespread deforestation and forest degradation because it can substantially reduce moisture availability for recycling by increasing surface runoff (Lovejoy & Nobre, 2019; Malhi et al., 2008; Schellnhuber, 2009; Delphine Clara Zemp et al., 2017). In addition, the possibility of having positive feedback due to tree loss might exacerbate deforestation impacts (Delphine Clara Zemp et al., 2017); tree loss reduces both ET and rainfall, lengthening dry season, reducing humidity, and potentially increasing forest fire (Delphine Clara Zemp et al., 2017). Over most of the deforested areas in the ARB, land use is beyond moderate intensity and the hydrologic system has evolved under climate variability and anthropogenic disturbances, especially land use change (Chagas et al., 2022). For example, wet (dry) season is becoming wetter (drier) during the past decades in around one-third of the ARB (mainly in southern and eastern regions of the basin) (Leite-Filho et al., 2019) and the seasonal storage deficit has increased over time (Chaudhari et al., 2019). In addition, vapor pressure deficit (VPD) is increasing over South America (Barkhordarian et al., 2019) and mortality rate of wet-climate tree species where dry season is becoming longer is increasing (Esquivel-Muelbert et al., 2019). Moreover, due to the increase in the frequency of extreme droughts, higher temperatures and increased forest degradation, the rainforest is becoming more vulnerable to fires (L. E. O. C. Aragão et al., 2018). Therefore, over many of the deforested regions, especially in southern and

eastern ARB, the hydrological system is likely being transformed with some changes being potentially irreversible (Lovejoy & Nobre, 2019).

Several studies have predicted that with the current rate of deforestation and biodiversity loss, the ARB may have two tipping points, which could lead to savannization of the bistable regions of the tropical forest through loss of moisture recycling as a result of crossing the 40% deforestation threshold (change in internal state of the system due to anthropogenic impacts) or a 4°C increase in temperature (global/regional climatic drivers) (Cox et al., 2004; van Nes et al., 2016; Carlos A. Nobre et al., 2016; Carlos Afonso Nobre & Borma, 2009; Sampaio et al., 2007; Schellnhuber, 2009; B. S. Soares-Filho et al., 2006; Staver et al., 2011; Walker, 2020; Zak & Nippert, 2012). However, based on the Assessment Report 5 of the Intergovernmental Panel on Climate Change (IPCC) and by going beyond a single-factor in explaining the forest degradation and considering the combined roles of global warming, deforestations and wildfires, the threshold for deforestation has been suggested to be as low as 20-25% instead of 40%, which could push the ARB toward an open-canopy degraded state, a very likely near future scenario (Lovejoy & Nobre, 2019; Carlos A. Nobre et al., 2016; Walker, 2020). Other studies have shown that temperatures in the region rose by 1-1.5°C over past six decades (Carlos A. Nobre et al., 2016), ~18% of the forest area is deforested (Mapbiomas_Amazonia, 2022), forest degradation reached 17% (Bullock et al., 2020; Matricardi et al., 2020), forest fires significantly increased (L. E. O. C. Aragão et al., 2018), dry season lengths (number of consecutive days with less than 50mm rainfall) are three to four weeks longer in comparison to six decades ago (Fu et al., 2013), and dry season water storage deficit is on a divergent trend (Chaudhari et al., 2019). Some studies suggest that the increasing frequency of unprecedented droughts such as those of 2005, 2010, 2015-16 and 2020 could be signaling that the tipping point is at hand (Bagley et al., 2014;

Lovejoy & Nobre, 2019; Walker, 2020). Therefore, there is a need to reduce deforestation in the ARB, rebuild the lost forest in its southern and eastern regions and to provide science-based guidelines to assist forest management policies (Lovejoy & Nobre, 2019; Walker, 2020).

Globally, passive and active approaches have been used to alleviate environmental stressors and to restore the forest through a secondary succession (Morrison & Lindell, 2011; Poorter et al., 2021). To measure the success of forest restoration, typical characteristics such as forest structure and diversity and ecosystem functioning are compared between the old-growth forest and the secondary forest where hydrological functioning is often neglected (Poorter et al., 2021). While tree restoration has been recognized as an effective way to store carbon and mitigate the impacts of climate change, not many studies have considered the hydrological effects of tree restoration (Hoek van Dijke et al., 2022). A recent study on the impacts of large-scale tree restoration showed that restoration can significantly alter terrestrial water cycle at different spatial scales and the impacts are non-linear and complex (Hoek van Dijke et al., 2022). Traditional management policies in the ARB were commonly developed focusing on maximizing economic benefits and neglecting hydrological roles of the forest (Carlos A. Nobre et al., 2016). Such omission of the hydrological roles arises partly from the lack of a comprehensive understanding of the short- and long-term impacts of management practices over varying temporal and spatial scales. As such, it is imperative that we better understand the dominant hydrological processes across the ARB that govern forest resilience and are crucial for improved management practices. In addition, since forest management can have long-term implications on the future of the ARB, it is important that such studies investigate the decadal evolution of the dominant processes under climate variability and human disturbances. Lastly,

identifying warning signals can help better monitor the impacts of management policies on the terrestrial hydrological cycle.

However, observational data—even those based on remote sensing—for such long-time scales and all relevant hydrological variables are lacking, especially for the entire ARB, or are available at short temporal scales, which make hydrological modeling the only viable option to study the terrestrial hydrology of the ARB. Early hydrological modeling studies in the ARB were conducted to uncover the underlying processes involved in moisture recycling and to study the impact of land use/land cover change on the water cycle (Marcos Heil Costa & Foley, 1999; Eltahir & Bras, 1994; Carlos A. Nobre et al., 1991; Shukla et al., 1990; Zeng, 1999; Zeng et al., 1996). These studies have emphasized the importance of land-atmosphere feedback in hydrological modeling to reduce the uncertainty in the results as some earlier studies found contradictory outcomes associated with neglecting the feedback (Eltahir & Bras, 1994). The limitations in required data and computational resources to run distributed hydrological land surface models in the past lead to significant growth of lumped hydrological models and data-based studies in the ARB. Lumped models are valuable tools to understand the big picture of hydrology in the ARB and to address wide range of research questions, however, they do not fully account for the heterogeneity in biomes and are simplistic in parameterizing various storage and fluxes, making them inappropriate for studies on process characterization (Heerspink et al., 2020; Maeda et al., 2017).

Advances in process-based hydrological modeling and remote sensing methods have provided new opportunities to simulate basin hydrology and study the dominant terrestrial hydrological processes (Clark et al., 2015; Frappart et al., 2019; Getirana et al., 2012; De Paiva et al., 2013; Pfeffer et al., 2014). Such models have been used to simulate groundwater dynamics

across the ARB, leading to fundamental advances in the understanding of the role of groundwater and providing opportunities to disentangle research questions that were not possible to address before (Chaudhari et al., 2021; Miguez-Macho and Fan, 2012a, 2012b; Pokhrel et al., 2014, 2013). For example, Miguez-Macho and Fan (2012a) investigated the role of groundwater on the surface water dynamics of the ARB and the buffering role of groundwater during the dry season based on the results of LEAF-Hydro-Flood (LHF) simulations. They found that the dynamics of WTD dominates streamflow in the headwater catchments and the two-way exchanges of surface and subsurface water over the large floodplains. In addition, shallow WTD supports large areas of waterlogged wetlands that are rarely flooded. In a following study, Miguez-Macho and Fan (2012b) investigated the role of groundwater in mitigating water stress on related processes to soil moisture and ET. Further, Pokhrel et al. (2013), studied the influence of groundwater on terrestrial water storage (TWS) using LHF model, finding that subsurface storage dominates the dynamics of TWS over a major part of the ARB; however, they reported that where WTD is shallow, the dynamics of TWS is governed by floodwater. In another study and based on the results of the LHF model, Chaudhari et al. (2019) investigated the dominant mechanisms modulating the dynamics of TWS and droughts over the ARB. They suggested that the ARB is getting wetter overall, but the southern and southeastern subbasins are getting drier with the dry season water storage deficit on a divergent trend. A recent study suggests that the double stress of waterlogging and drought is the primary driver of forest-savanna coexistence with alternating drought and waterlogging at the seasonal scale favoring savanna over forests (Mattos et al., 2023). Despite the findings in recent studies, to the best of our knowledge, there are no comprehensive studies that investigated the key processes governing the hydrologic

dynamics at the basin and subbasin scales across the ARB, the linkages therein, and their historical evolution.

The present study addresses the aforementioned research and knowledge gaps by answering the following science questions. (1) How did the fundamental hydrological processes in the ARB evolve over the past three decades? (2) What key factors govern the seasonality of the ARB at the basin and subbasin scales? (3) To what extent can hydrological variables in the ARB serve as viable early or late warning signals of alterations in the terrestrial water cycle during secondary succession? (4) What are the implications for forest management that can be derived from the findings of studies such as ours? We hypothesize that the shallow water table depth (WTD<5m) was a key attribute that supported the ARB's hydrologic regime during the past three decades against climate variability and anthropogenic disturbances. As such, shallow groundwater fraction area could be taken as a proxy to monitor the impacts of human activities on the basin's hydrology and ecosystem functioning. Our second hypothesis is that the changes in the spatial distribution of ET serve as a direct measure of the hydrological impact of large-scale LULC changes in the basin. In addressing these questions and hypotheses, we first identify the dominant hydrological mechanisms by using the results from a basin-scale, fully process-based hydrological model. Then, we investigate how the key hydrological processes have evolved over the last three decades. Finally, we examine the role of the governing hydrological processes for sustainable forest management in the ARB.

2.2 Methods

2.2.1 Model Description

The model used in this study is LHF (Miguez-Macho and Fan, 2012a, 2012b; Pielke et al., 1992; Pokhrel et al., 2014, 2013; Walko et al., 2000). As described in detail in Miguez-

Macho and Fan (2012a), LHF is a fully process-based hydrology model capable of resolving coupled surface and subsurface hydrological processes at the continental-scale. The model was developed at two stages building on the Land-Ecosystem-Atmosphere Feedback (LEAF), the land-surface component of Regional Atmosphere Modeling System (RAMS) (Walko et al., 2000). The physics in the original LEAF model is described in detail in Walko et al. (2000). Turbulent and radiative exchange of the atmosphere with multilayer soil and snow water and thermal energy, surface storage, vegetation canopy, canopy air are inherited features of LEAF in LHF (Miguez-Macho and Fan, 2012a, 2012b). These include the parameterizations for simulating ET, which are similar to those used in state-of-the-art land surface models (e.g., Lawrence et al., 2019); details are available in Walko et al. (2000). However, LEAF parameterizations including representation of sub-grid hydrologic heterogeneity, lateral soil water movement based on TOPMODEL (Beven & Kirkby, 1979) and groundwater flow processes have been replaced with new schemes or largely improved. The new developments and enhancements have been particularly tested over the ARB as described in the following.

At the first stage of LHF development over North America (Miguez-Macho et al., 2007, 2007), LEAF-Hydro was adapted from LEAF by adding a prognostic groundwater module to allow (1) the rise and fall of water table or shrinkage and growth of the vadose zone, (2) the recharged water table to reach a new equilibrium following a rain event by discharging into rivers within a grid cell and convergence and divergence of lateral flow among adjacent cells, (3) two-way exchange between surface water and groundwater to represent both gaining and losing streams, (4) river routing to the ocean using the kinematic wave method and (5) sea level to influence coastal drainage by assigning the sea level as the groundwater head boundary condition. During the second stage over the ARB (Miguez-Macho and Fan, 2012a, 2012b), LHF

was developed through further enhancement of LEAF-Hydro by incorporating a river-floodplain routing scheme to estimate streamflow more realistically by solving the full momentum equations of open channel flow, also considering back water effect and the inertia of deep flow, which are both significant in the ARB (Bates et al., 2010; Miguez-Macho and Fan, 2012a, 2012b; Yamazaki et al., 2011). The incorporation of flood dynamics also enabled an explicit simulation of floodwater-groundwater interactions, a dominant process in the ARB. The initial LHF studies over the ARB provided an extensive evaluation of many hydrologic variables across the basin (Miguez-Macho and Fan, 2012a, 2012b). The model was subsequently used in numerous studies that presented further evaluations using observational and satellite-based data on various hydrologic fluxes and stores, and by using different atmospheric forcing datasets demonstrating robust model performance over the ARB (Brown et al., 2022; Chaudhari et al., 2021, 2019; Chaudhari and Pokhrel, 2022; Miguez-Macho and Fan, 2012a, 2012b; Pokhrel et al., 2014, 2013).

2.2.2 Atmospheric Forcing

LHF model in this study is forced with ERA5 reanalysis (Hersbach et al., 2020) available from 1950 to present at the spatial resolution of 0.25 degree and hourly time steps. The availability period and the spatial resolution were the main reasons for using ERA5 data. In previous studies, LHF results forced by WATCH Forcing Data methodology applied to ERA-Interim (WFDEI) reanalysis were successfully validated over ARB, however, the dataset is not available after 2019 (Chaudhari et al., 2019). Staal et al. (2020) used ERA5 over the ARB to conduct hydrological and atmospheric moisture tracking simulations and their results showed that ERA5 performs better than ERA-Interim in estimating wind fields and rainfall, especially in tropics (Staal et al., 2020). A total of eight variables from ERA5 dataset are used: precipitation,

surface pressure, surface solar (i.e., shortwave) radiation downwards, surface thermal (i.e., longwave) radiation downwards, air temperature, dewpoint temperature, u- and v-components of wind speed. Specific humidity is calculated from dewpoint temperature and surface pressure. The 3-hourly data at the coarser resolution noted above are spatially interpolated within LHF to the model grid resolution (~2km) using a bilinear interpolation (Chaudhari et al., 2021; Miguez-Macho & Fan, 2012, 2012; Pokhrel et al., 2013, 2014).

2.2.3 Land Use/Land Cover and Leaf Area Index

The annual land use/land cover (LULC) maps are derived from the European Space Agency (ESA) Climate Change Initiative's Land Cover project; the original data are reclassified and aggregated to match the land use categories used in LHF, following our previous study (Chaudhari et al., 2019). Specifically, the 22 classes from the ESA land cover maps are reclassified into the 30 classes of LHF (Table S3). The datasets comprise an annual time series land cover maps with 300-meter spatial resolution for the 1992 to 2020 period. The baseline maps in the ESA dataset are generated using the Medium-spectral Resolution Imaging Spectrometer (MERIS) instrument based on the UN Land Cover Classification System (LCCS) and the maps were further modified based on the detected changes in land use and land cover by AVHRR (1992-1999), SPOT-Vegetation (1999-2012), and PROBAV (2013-2020) instruments. The LHF model updates LULC on an annual basis to account for year-to-year LULC changes; in the ARB, these annual changes are largely caused by human activities. The lookup table for leaf area index (LAI) is derived by overlaying the ESA land use map over the LAI maps from Moderate Resolution Imaging Spectroradiometer (MODIS) for the period of 2000 to 2020 and using a pixel-by-pixel analysis and the monthly values (Table S4) are calculated from the long-term 4-day mode of LAI for each LHF land cover class.

Table 2-1. Reclassification of ESA land use/land cover classes into LHF classes.

LHF Classes	ESA Classes
Evergreen needleleaf forest	Tree cover, needleleaved, evergreen, closed to open (>15%) Tree cover, needleleaved, evergreen, closed (>40%) Tree cover, needleleaved, evergreen, open (15-40%)
Evergreen broadleaf forest	Tree cover, broadleaved, evergreen, closed to open (>15%) Tree cover, mixed leaf type (broadleaved and needleleaved) Tree cover, flooded, fresh or brakish water Tree cover, flooded, saline water
Deciduous needleleaf forest	Tree cover, needleleaved, deciduous, closed to open (>15%) Tree cover, needleleaved, deciduous, closed (>40%) Tree cover, needleleaved, deciduous, open (15-40%)
Deciduous broadleaf forest	Tree cover, broadleaved, deciduous, closed to open (>15%) Tree cover, broadleaved, deciduous, closed (>40%) Tree cover, broadleaved, deciduous, open (15-40%)
Mixed woodland	Mosaic natural vegetation (tree, shrub, herbaceous cover) (>50%) / cropland (<50%)
Woodland	Mosaic tree and shrub (>50%) / herbaceous cover (<50%) Tree or shrub cover
Wooded grassland	Mosaic herbaceous cover (>50%) / tree and shrub (<50%)
Closed shrubland	Shrubland Shrubland evergreen Shrubland deciduous Shrub or herbaceous cover, flooded, fresh/saline/brakish water
Open shrubland	Sparse vegetation (tree, shrub, herbaceous cover) (<15%) Sparse tree (<15%) Sparse shrub (<15%) Sparse herbaceous cover (<15%) Lichens and mosses
Grassland	Grassland
Crop/mixed farming	Mosaic cropland (>50%) / natural vegetation (tree, shrub, herbaceous cover) (<50%)
Irrigated crop	Cropland, irrigated or post-flooding
Cropland	Cropland, rainfed Herbaceous cover
Bare ground	Bare areas Consolidated bare areas Permanent snow and ice
Urban and built up	Urban areas
Lakes, rivers, streams (inland water)	Water bodies

Table 2-2. Reclassification of ESA land use/land cover classes into LHF classes.

LHF Land Cover Classes	Jan	Feb	Mar	Apr	May	Jun	Jul	Aug	Sept	Oct	Nov	Dec
Lakes, rivers, streams	0.01	0.01	0.01	0.01	0.01	0.01	0.01	0.01	0.01	0.01	0.01	0.01
Mixed woodland	1.29	1.23	1.20	1.23	1.29	1.26	1.20	1.17	1.17	1.17	1.19	1.33
Crop/mixed farming	1.24	1.20	1.28	1.71	2.11	2.12	1.66	1.28	1.29	1.26	1.24	1.25
Irrigated crop	1.10	0.76	0.75	0.75	0.75	1.17	1.26	1.33	1.33	1.20	1.18	1.18
Evergreen needleleaf forest	1.15	1.05	0.74	0.69	0.70	0.82	1.18	1.21	1.23	1.21	1.17	1.14
Evergreen broadleaf forest	3.20	1.60	2.15	4.10	5.05	5.61	5.69	6.00	6.16	5.70	5.06	4.19
Deciduous broadleaf forest	1.74	1.71	1.88	2.18	1.81	1.69	1.39	1.24	1.21	1.23	1.57	1.71
Woodland	1.21	1.18	1.24	1.58	1.57	1.57	1.27	1.21	1.21	1.20	1.21	1.20
Wooded grassland	0.66	0.64	0.65	0.68	0.73	0.85	0.85	0.84	0.82	0.77	0.75	0.71
Closed shrubland	1.20	1.21	1.29	1.63	1.58	1.26	1.18	1.13	1.13	1.14	1.15	1.20
Open shrubland	0.20	0.20	0.22	0.22	0.20	0.18	0.17	0.18	0.20	0.20	0.20	0.20
Grassland	0.71	0.69	0.69	0.71	0.71	0.71	0.69	0.72	0.74	0.69	0.69	0.71
Cropland	1.60	1.61	1.62	1.68	1.60	1.20	1.05	0.76	0.76	0.85	1.14	1.30
Bare ground	0.20	0.20	0.22	0.21	0.20	0.20	0.19	0.19	0.20	0.20	0.20	0.20
Urban and built up	0.69	0.69	0.70	0.73	0.73	0.72	0.70	0.68	0.68	0.67	0.67	0.68

2.2.4 Simulation Setup

The LHF model is set up for the entire ARB (~7.1 million km²) including the Tocantins River basin (Figure 2-1). Simulations are conducted for the 1979–2020 period at a spatial resolution of 1 arcmin (~2 km) with a time step of 4 minutes as in previous studies (Chaudhari et al., 2019; Miguez-Macho & Fan, 2012; Pokhrel et al., 2013, 2014), and the output is saved at daily time steps. To capture the hillslope processes at up to the first-order stream valleys, very fine spatial scale for the simulations is desired, however, due to the computational costs and the coarse resolution of input data (such as soil characteristics) the spatial resolution of 1 arcmin is chosen as a tradeoff, as in previous studies. Reservoirs are not considered in the simulation, however, based on previous studies the impact of the reservoirs in the ARB are not substantial in the downstream reaches (Chaudhari & Pokhrel, 2022). As the focus of this study is to investigate the terrestrial hydrological processes at basin and subbasin scales, the impacts of reservoirs would not alter the findings. Starting with the equilibrium water table (Y. Fan et al., 2013) for

1979, the model is spun up for ~200 times for the year 1979 to stabilize WTD and the results for the 1992–2020 period (28 years) are analyzed. As the primary goal of this study is to examine the dominant processes in the ARB on a decadal scale and since the land cover and LAI datasets are available after 1992, simulations for 1979 to 1992 are discarded as additional spin-up. Moreover, as the model simulates land surface, hydrologic, and groundwater processes on a full physical basis, no calibration was performed (Chaudhari et al., 2019).

2.2.5 Trend Analysis

The Mann-Kendall (MK) test (Kendall, 1948; Mann, 1945) which serves as a prevalent method for detecting alterations in time-series data (Li et al., 2014) is used to detect the long-term trend. In this study, the detected trend is deemed statistically significant when the p value is less than 0.05 (i.e., 95% confidence level). Moreover, we employ the Theil-Sen slope estimator (Sen, 1968; Theil, 1950) to calculate the slope of change which computes the median slopes of lines fitted through pairs of data points in the dataset. Importantly, it exhibits greater robustness against outliers compared to simple linear regression methods (Lavagnini et al., 2011). The outcomes of the MK test are interpreted utilizing the z-score metric, wherein the sign of the z-score denotes the direction and magnitude of the trend. To comprehensively address the heterogeneity observed in the changes across key hydrological variables in our study, we separately calculate the mean slope separately for areas exhibiting negative and positive slopes. Additionally, we compute the basin-averaged slope to provide a more intricate understanding of the transformations occurring over the past three decades within the ARB.

2.3 Results and Discussion

2.3.1 Validation

The simulated streamflow from LHF is compared with observations obtained from the Agência Nacional de Águas (ANA) in Brazil (<http://hidroweb.ana.gov.br>, last accessed: 10 September 2022). In this regard, 55 stream gauging stations from a wide range of river discharge magnitudes with at least 30 years of record are considered across the ARB. Figure 2-1 presents the results of three performance metrics, namely the Pearson correlation coefficient (PCC), modified Kling–Gupta efficiency (KGE) and Nash–Sutcliffe efficiency (NSE) (Siqueira et al., 2018). High values for PCC, KGE and NSE metrics can be observed for most stations, indicating overall good performance for various topographic locations and river discharge values. However, there are some stations with relatively lower PCC, KGE and NSE, which are situated mostly in streams with low annual mean flow and steep slopes, including the headwaters across the Tapajos and Madeira subbasins and along the streams in the northeastern regions of the ARB. The lower accuracy at those stations is likely related to high topographic gradient, where precipitation drains quickly, causing rather erratic patterns of seasonal streamflow, which adds challenges to resolving hillslope processes for low order streams at 2km resolution. In addition to the above statistical measures, the long-term seasonality of streamflow for 12 major gauge stations is compared (Figure 2-1). R-squared and RSR (a standardized version of the root mean square error (RMSE) that takes the standard deviation of the observed data at different stations into account (Legates & McCabe, 1999)) indicate good model performance in predicting the streamflow seasonality.

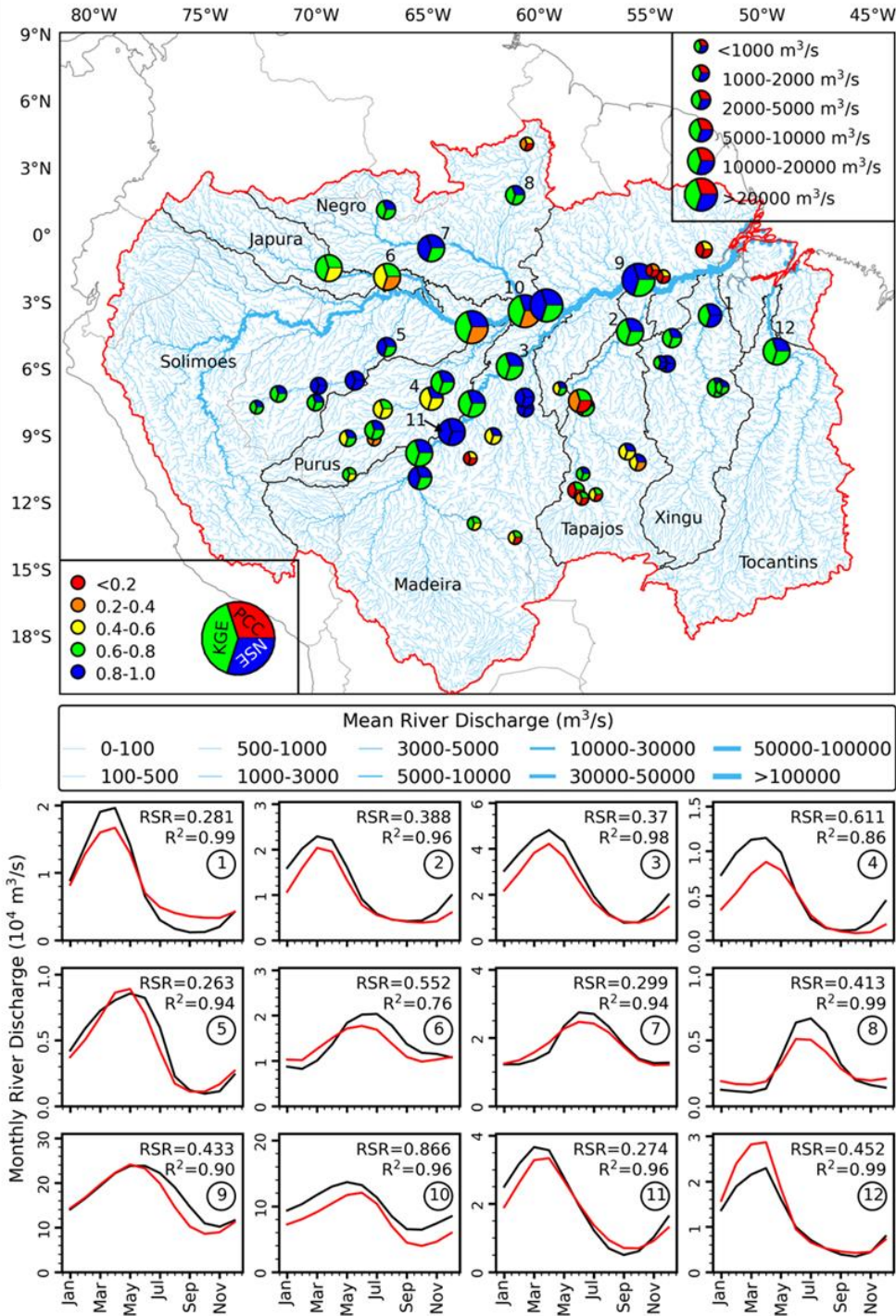


Figure 2-1. River discharge validation based on monthly average values derived from daily river discharges at 55 gauge stations across the ARB. The size of the circles in the top panel indicates flow magnitude with each of the three portions of the circles showing a model performance metric: PCC (red), KGE (green), and NSE (blue). The background image shows simulated river discharge indicated by line thickness (~2km grids). The grid panels at the bottom depict the long-term seasonal cycle of monthly river discharge for 12 major gauge stations indicated on the top panel.

As shown in previous studies (Chaudhari et al., 2019; Felfelani et al., 2017; Pokhrel et al., 2013) and corroborated in this study (Section 3.2), groundwater is the major component of TWS in the ARB because over most parts of the basin the water table is relatively shallow. Therefore, given the lack of systematic water level observations in the ARB, TWS validation can be used as a proxy for groundwater validation. Comparison of TWS anomalies between LHF simulations and GRACE data (Figure 2-2) shows a high level of agreement for the basin-averaged anomalies and for most of the eight subbasin-averaged anomalies. However, at some of the subbasins there are some differences which are likely caused by the biases in forcing data, imperfect model parameterizations, and potential biases in GRACE data for small subbasins (Chaudhari et al., 2018, 2019; Felfelani et al., 2017; Longuevergne et al., 2010) such as Tocantins. However, in all subbasins the simulated TWS follows the patterns of precipitation anomalies (grey bars in Figure 2-2), further suggesting that some of the discrepancies could be attributed to precipitation biases. The model performs better in the first half of the simulation period in comparison to the second half, especially in the western subbasins including Solimoes and Japura, which could be partially attributed to the decreasing trend in precipitation in the first half of the simulation period (Figure 2-3).

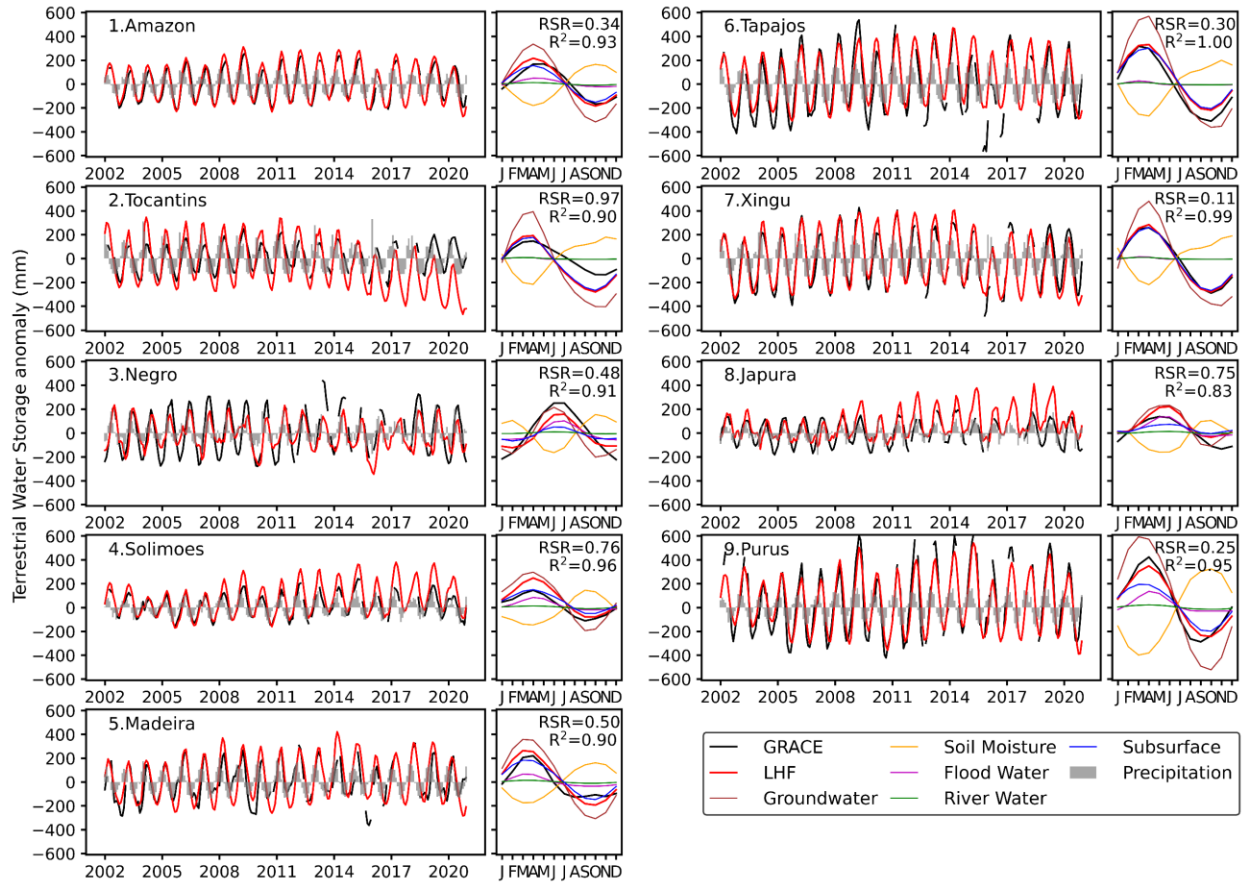


Figure 2-2. Validation of TWS anomalies obtained from LHF simulations against GRACE anomalies (CSR Mascons) for the entire ARB and its eight subbasins for the period of 2002-2020. Basin and subbasin-averaged precipitation anomalies are obtained from ERA5 dataset (grey bars). Seasonal cycles of GRACE and simulated TWS and its components are shown in the right panel of each time series. GRACE results are shown as the mean of mascon solutions and simulated TWS anomalies are calculated with respect to the anomaly window of 2004-2009 for consistency with GRACE.

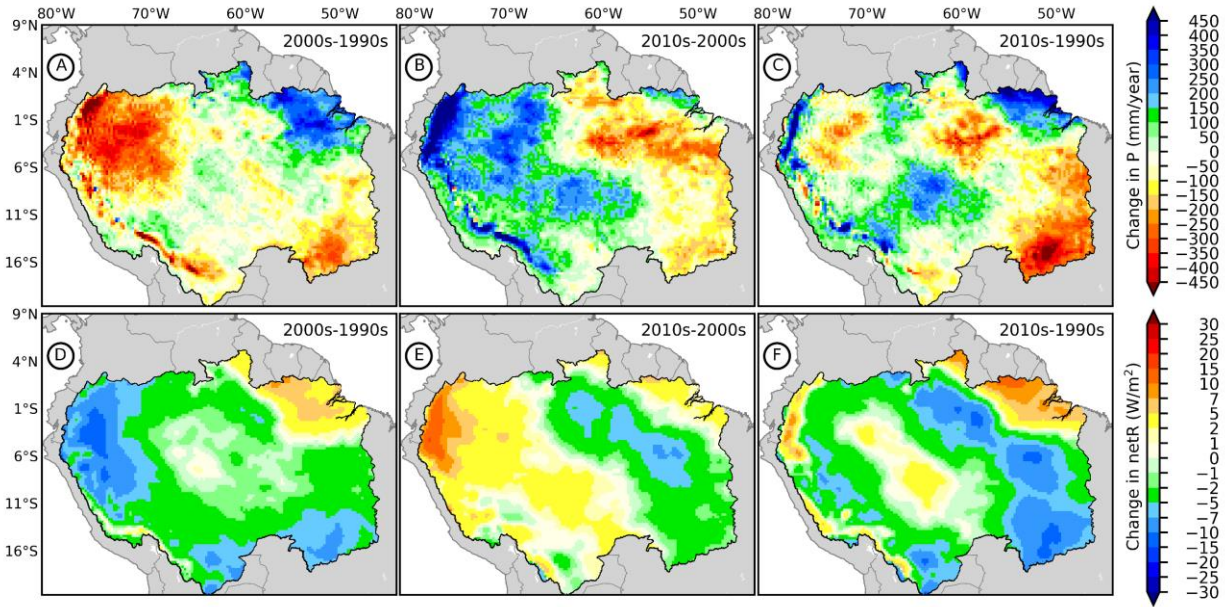


Figure 2-3. The absolute change in decadal mean of the spatial distribution of annual precipitation (Panels A to C) and net radiation (Panels D to F) over the preceding three decades (Hersbach et al., 2020). The absolute changes in decadal mean in the 2000s (2001 to 2010) from the 1990s (1992 to 2000) and in 2010s (2011 to 2020) from 2000s are showcased in the respective panels.

The model simulates the seasonality of TWS very well in comparison to GRACE (low RSR and high R^2 ; Figure 2-2), which adds more confidence to the results of this study as the seasonality is a key focus area in this study (Figure 2-2). The seasonal cycle of TWS components shows the dominant role of groundwater storage in governing TWS changes in the majority of the subbasins, especially in the subbasins with relatively deep groundwater ($WTD > 2m$) such as Tocantins, Tapajos, and Xingu. However, in the subbasins where the groundwater is relatively shallow, flood water storage plays an equally prominent role in modulating TWS anomalies (e.g., Solimoes, Purus, and Negro). We note that because soil moisture storage in LHF is defined as the moisture above WTD, the seasonal cycles of groundwater and soil moisture storage have an inverse relationship.

Decadal mean of the spatial distribution of ET is validated against MODIS MOD16A3GF Version 6.1 (Running et al., 2021) product, a year-end and gap-filled yearly composite dataset

produced at 500m resolution for the period of 2000-present (Figure 2-4A). The comparison of long-term annual mean of ET between the LHF simulation results (Figure 2-4B) and MODIS data shows a good agreement (Figure 2-4D). However, there are notable differences over certain areas which include flood-dominated regions, grasslands, and shrublands (Figure 2-5). These differences could be attributed to the differences in the way ET is estimated. The annual MODIS ET was derived based on the Penman-Monteith equation (Monteith, 1965), which includes inputs of daily meteorological reanalysis data along with MODIS remotely sensed data products such as dynamic vegetation properties, albedo, and land cover (Running et al., 2021). ET in LHF is, however, calculated based on energy balance approach (Miguez-Macho et al., 2007; Walko et al., 2000). Another source of discrepancy is the different in spatial resolution between the two products; model results could have higher uncertainties in regions within waterbodies including, river channels, lakes, and wetlands, where MODIS product might have accurately captured the ET dynamics. In addition to MODIS ET, the long-term annual mean of ET is compared with The Global Land Evaporation Amsterdam Model (GLEAM; Figure 2-4C) V3.8a (Martens et al., 2017; Miralles et al., 2011) product, a set of algorithms to estimate daily components of land evaporation at 0.25 degree grid cell from satellite and reanalysis data for the period of 1980-present based on the Priestly and Tylor equation (Priestley & Taylor, 1972) and Gash's analytical model (Gash, 1979). The comparison of long-term annual mean of ET between the LHF simulation results and GLEAM data shows a better agreement than MODIS over most of the ARB (Figure 2-4E). However, along the northern boundary of the ARB, the comparison shows more discrepancy in comparison to MODIS. A further investigation by comparing MODIS and GLEAM datasets shows that there are notable discrepancies even between the two datasets (Figure 2-4F), making it difficult to draw a clear conclusion on model performance. In

general, given that MODIS and GLEAM ET are also estimates—not true observations—that is known to include uncertainties (Xu et al., 2019), these comparisons demonstrate that the simulated ET is not out of bounds (Figure 2-4) and add further confidence to the results of this study.

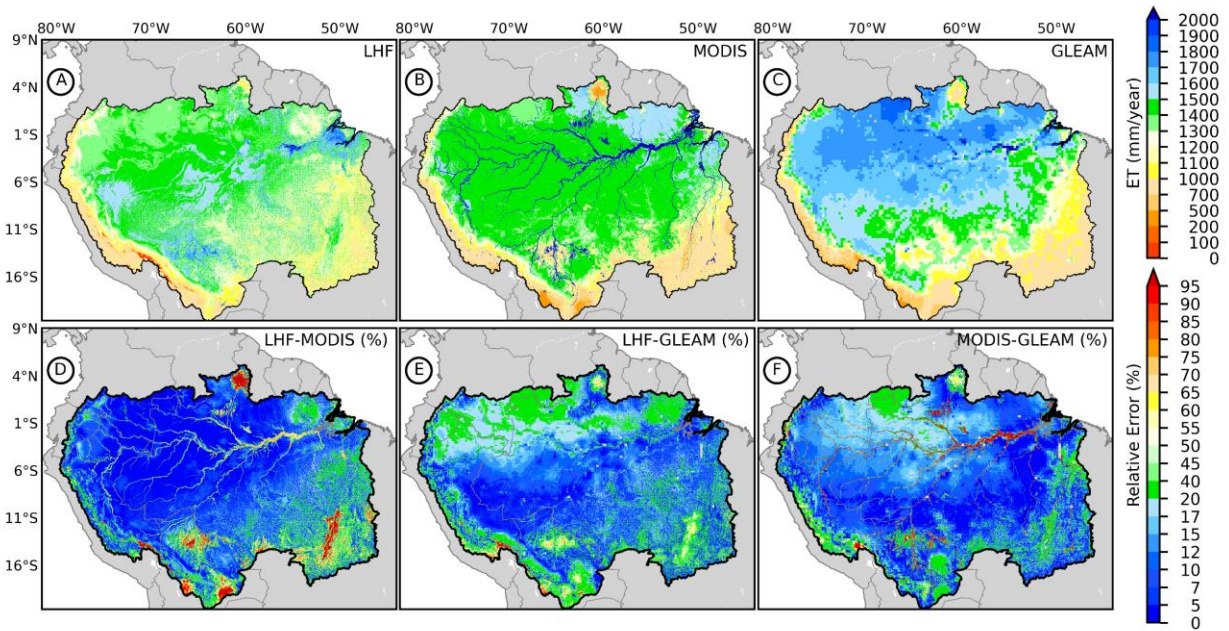


Figure 2-4. Decadal mean of the spatial distribution of annual ET in the past two decades from LHF model (A), MODIS (Running et al., 2021) dataset (B), and GLEAM (Martens et al., 2017) (Miralles et al., 2011) dataset (C). The relative errors (%) in LHF results compared to MODIS and GLEAM are shown in panels D and E, respectively. Panel F shows the relative difference between MODIS and GLEAM.

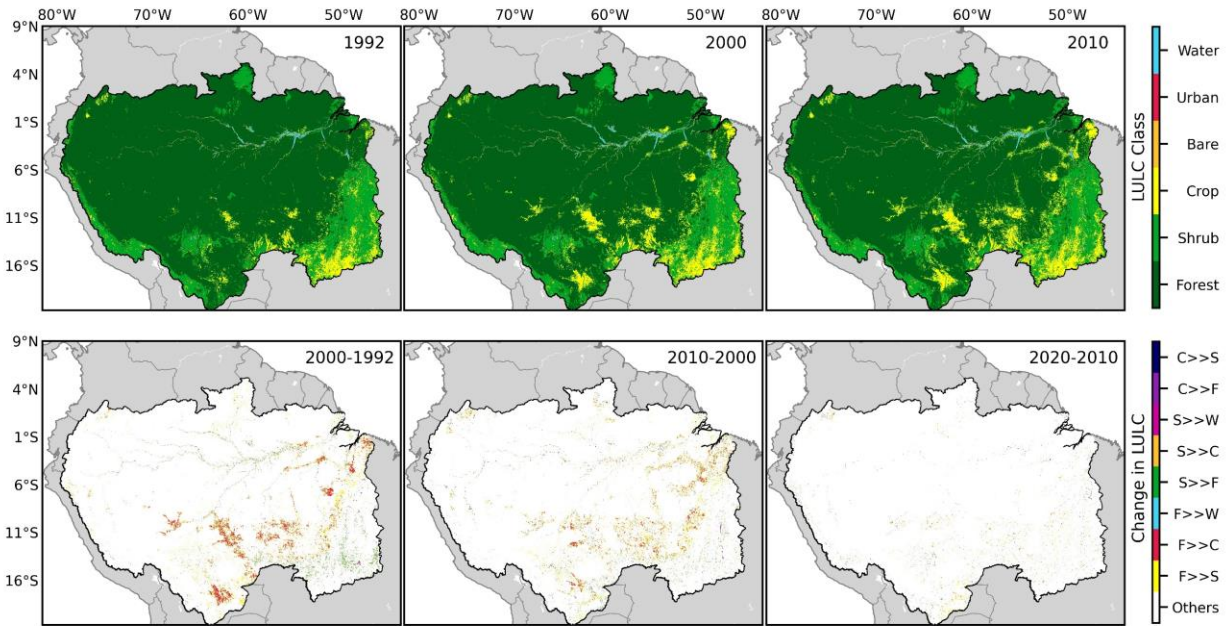


Figure 2-5. Land use and land cover (LULC) maps for 1992, 2000 and 2010 are shown in the top panels (Santoro et al., 2017). The changes in LULC in the 1990s (1992 to 2000), 2010s (2001 to 2010) and 2010s (2011 to 2020) are shown in bottom panels. The lower colorbar shows the initial and final LULC type and in the colorbar. F, S, C, and W stands for Forest, Shrubland, Cropland and Water, respectively.

Overall, the evaluation of river discharge, TWS, and ET with multiple independent products, in addition to a substantial validation presented in multiple previous studies (Chaudhari et al., 2019; Miguez-Macho & Fan, 2012; Pokhrel et al., 2013, 2014), presents sufficient basis on the usefulness of the model to study the dominant hydrological processes and their spatial and temporal variability across the ARB. Further, given that the model is fully physically based, not calibrated with observations, and applied over a large domain of the ARB, we consider the model performance to be satisfactory for our application.

2.3.2 Dynamics of Key Hydrological Processes

In this section we address the first research question by presenting an in-depth analysis of the dynamics of key hydrological processes within the ARB over the last three decades with a focus on various water and energy balance components and associating the changes in these

components with major hydrologic drivers. The dynamics of the hydrological functioning of the basin, driven by climatic and anthropogenic factors, have substantial implications for forest and ecosystem management of the ARB. Exploring the shifts in these processes provides insights into the basin's sensitivity to climatic change, the impacts of human activities, and overall forest resilience. The subsequent sub-sections unravel the details of each hydrological component, shedding light on the interplay among them and implications for forest management.

2.3.2.1 Dynamics of Groundwater Mechanisms

The hydrological dynamics within the ARB have undergone substantial changes over the past three decades (Figure 2-6). The variations in WTD across the ARB exhibit a remarkable spatial heterogeneity from east to west, serving diverse functions and roles (Figure 2-6F). The WTD varies, with shallow water tables ($WTD < 5m$) found predominantly in the central and northwestern regions, and deeper water tables ($5m < WTD < 20m$) in the southeastern parts. This spatial pattern, consistent with earlier studies (Miguez-Macho and Fan, 2012; Fan et al., 2013; De Graff et al., 2015), underscores the prevalence of deep groundwater in the headwater catchments of the basin, notably influencing headwater streamflow (Frappart et al., 2019; Miguez-Macho & Fan, 2012). In the low-lying floodplains, groundwater-surface water interactions regulate seasonal hydrologic dynamics, converting groundwater storage into a sink during the wet season and a source during the dry season—a key mechanism that sustains baseflow (Miguez-Macho and Fan, 2012).

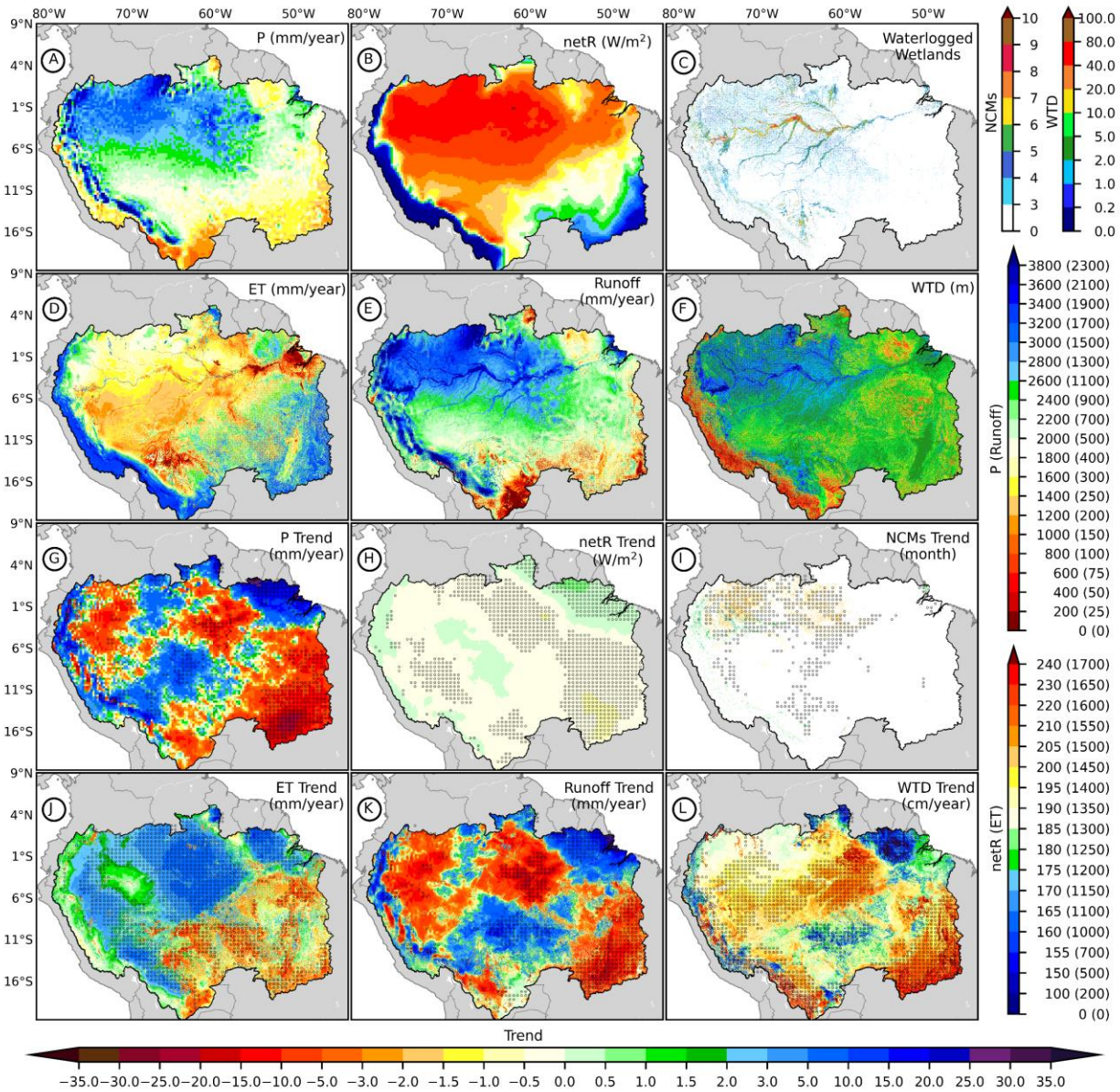


Figure 2-6. The long-term (1992-2020) trends in the major drivers and major components of water and energy balances in the ARB over the past three decades. The long-term mean of annual precipitation, net radiation, ET, runoff, and WTD are shown in panels A, B, D, E, and F, respectively. Panel C shows waterlogged wetlands based on the number of consecutive months with WTD < 0.25m. The Mann-Kendall trends and significance (markers) at 95% confidence level for precipitation, net radiation, waterlogged wetlands, ET, runoff, and WTD are shown in panels G to L, respectively.

The basin-averaged WTD over the ARB changed with a heterogeneous pattern ($\pm 19\%$) during the past three decades. A notable decline in WTD over the past three decades with an average slope of 69 mm/year over these regions is apparent (Figure 2-6L), with the trend being statistically significant (Mann-Kendall test; 95% confidence level; markers in Figure 2-6L). Examining the ARB at the basin scale, conspicuous indications of a diminishing trend are discernible across its southeastern, southern, western, and central portions which are dominantly driven by precipitation and influenced by net radiation (Figures 2-6A and 2-6B). It is worth noting that the magnitude of this declining trend varies in correspondence with the prevailing trends in precipitation (Figure 2-6G) and net radiation (Figure 2-6H). In situations where precipitation has undergone a decrease and net radiation a concurrent increase, the decline in TWD level is more pronounced relative to other regions where a decreasing (increasing) trend in precipitation (net radiation) can be seen. In contrast, some portions within the basin exhibit an upward trend in WTD with an average slope of 44 mm/year over these regions. This ascending trend, notably observed in the northeastern extremity of the basin, can be attributed to an increase in precipitation. The expansion in negative trend in the “arc of deforestation” areas can predominantly be attributed to the reduction in ET stemming from deforestation practices (Panels D and L in Figure 2-7). These actions lead to a reduction in the available evaporative surfaces (substantial reduction in LAI) within these localized zones where increase in ground evaporation could not compensate for sharp reduction in transpiration (Figure 2-7).

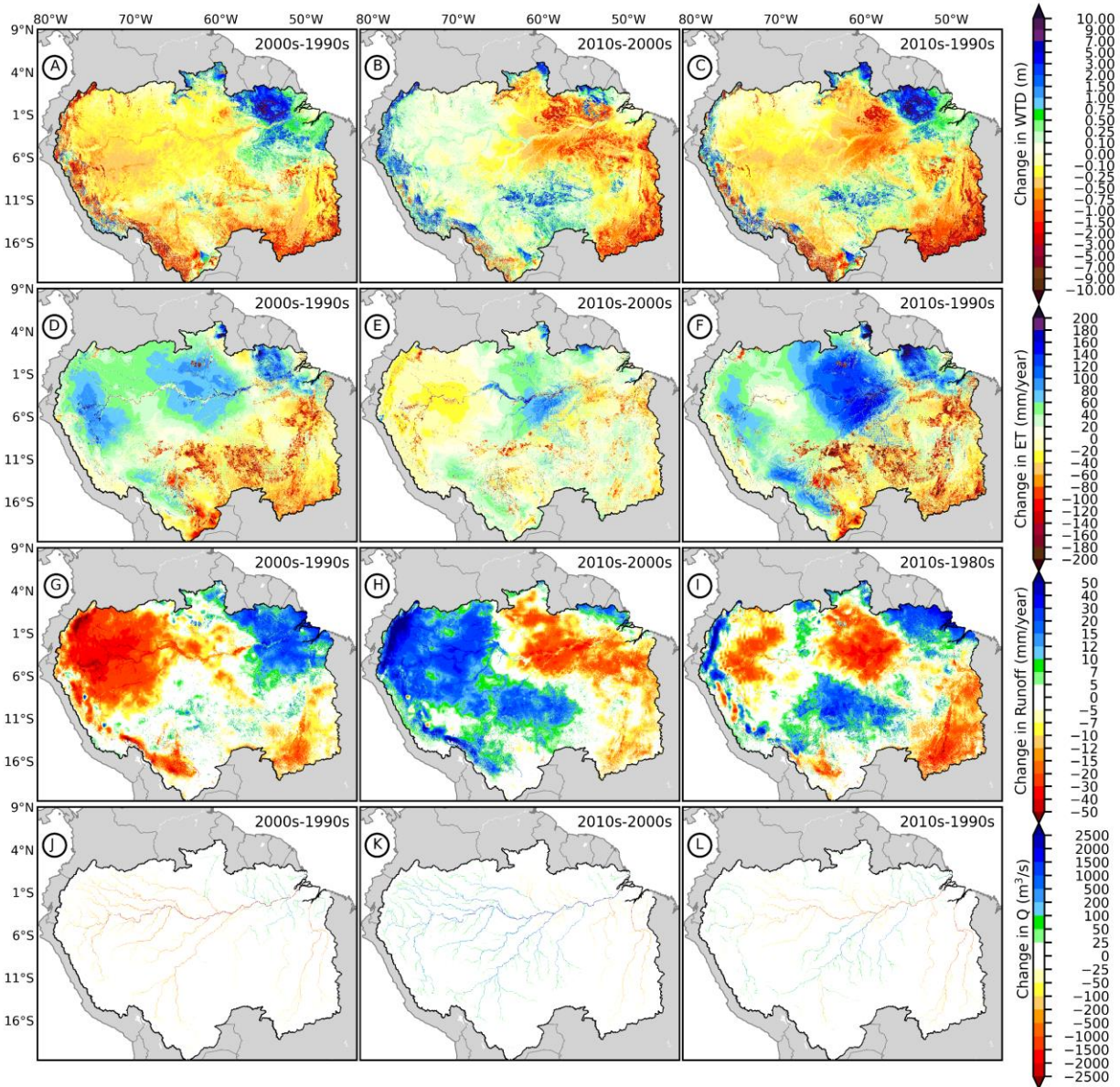


Figure 2-7. The mean decadal changes in key hydrological variables, including annual WTD (Panels A to C), annual ET changes, (Panels D to F), annual Runoff changes (Panels G to I), and annual River Discharge variations (Panels J to L).

A closer examination of decadal trends in WTD reveals the dominant role of precipitation while also underscoring the prominent role of net radiation in governing the dynamics of WTD at larger temporal and spatial scales (Figures 2-6A, B, and F). The decadal analyses offer further insights into the aforementioned observation, particularly in light of divergent changes in

precipitation and net radiation during the 2000s and 2010s (Figure 2-3). This phenomenon is pronounced in the northwest and northeast areas of the basin, where relatively limited deforestation has occurred. During the 2000s, groundwater storage experienced a general decline, manifesting as deeper water tables in many regions (Figure 2-7). A decrease in precipitation within the northwestern region of the basin was accompanied by a concurrent decline in WTD within that same geographical area (Figure 2-7). Further, contrasting outcomes are observed in the northeastern ARB, where increased precipitation resulted in a notably shallower WTD, where the augmenting net radiation played a key role in regulating this mechanism. Analyzing the alterations in precipitation, net radiation, and WTD throughout the 2010s reveals a pattern that runs in contrary to the changes detailed earlier. Groundwater depth is another major modifier for WTD dynamics at large temporal and spatial scales (Figures 2-6F and L). The southeastern subbasins exhibited an accelerated WTD decline in the 2000s due to reduced moisture transport into these areas (Figure 2-3). Here, the “dry gets drier” paradigm is evident, with regions with deeper water tables experiencing greater declines (e.g., Feng and Zhang, 2015). This trend can be attributed to reduced precipitation and infiltration, exacerbated by deforestation in certain regions (Figures 2-3 and 2-5).

The contribution of decadal changes in WTD (Figures 2-7:A-C) to the long-term trend (Figures 2-6L) exhibits considerable spatial variations. While the decadal changes from the 1990s to the 2000s dominate the long-term trends in the northeastern ARB, the changes from the 2000s to the 2010s dictate the long-term trends more strongly along the Andes and the central-southern portions of the basin. In the southeastern ARB, the strong and significant long-term trend is a result of persistent decline in WTD during the three decades (Figures 2-6L and 2-7:A-

C), which can be further linked to a notable decline in precipitation in this region (Figures 2-3A-C).

The area fraction (the proportion of the basin/subbasin area that is occupied by a particular range of WTD) of varying WTDs indicates that WTD of less than 2m is dominant across the ARB (~34% area), whereas WTD between 2-5m is common in ~30% of the basin (Figure 2-6F and Table 2-1). This implies that at least 34% of the forest over the ARB is supported by groundwater during the dry season, which underscores the importance of shallow groundwater for forest resilience in the ARB. At the subbasin scale, in over 50% of the Solimoes, Japura and Negro basins WTD is shallower than 2m, suggesting an even greater groundwater role in these subbasins. In Madeira and Purus, WTD is shallower than 2m in ~30% of areas, whereas in Tocantins, Xingu, and Tapajos, such shallow groundwater is not commonly observed. Further, in Purus, Solimoes, Japura and Negro subbasins, areas with WTD within the top 5m accounts for ~70% while the WTD is between 2-5m in ~30% of areas. Lastly, WTD is between 5-10m in 10% of areas in Solimoes, Japura and Negro and 20-30% in the other subbasins.

In terms of the temporal evolution, during the 1990s, WTD was shallower than 0.25m in over 4.5% of ARB which supports water-logged wetlands (Table S2). At the subbasin scale, such shallow WTD is observed in ~10% of the Solimoes, Japura, and Negro subbasins. In the Tocantins, Xingu and Purus, WTD is mostly deeper than 0.25m. The decadal analysis shows that the area fraction of WTD shallower than 0.25m decreased by ~42% from the 1990s to the 2000s; however, it recovered by ~7% in the 2010s (Table S2). Over the past three decades, the area fraction of WTD<0.25m decreased by ~38%, which likely caused significant biodiversity and ecosystem loss if it passed the functional thresholds for these systems. The area fraction of

WTD<2m also decreased over the ARB by ~17% from the 1990s to the 2000s, with an additional decline in the 2010s by ~4%. This amounts to a total decline in areas with WTD<2m by ~19% during the past three decades. Most of this reduction occurred in regions with WTD less than 1m. As a result, the areas with WTD less than 2m and greater than 1m increased by ~5% and most of this increase occurred in the Solimoes and Negro subbasins. The areas with WTD between 5-20m increased at the expense of decline in areas with shallower WTDs.

Table 2-3. The annual mean of shallow groundwater percentage in the past three decades at the basin and subbasin scales over ARB.

Basin/ Subbasin (m)	1990s						2000s						2010s					
	<0.25	0~1	1~2	2~5	5~10	10~20	<0.25	0~1	1~2	2~5	5~10	10~20	<0.25	0~1	1~2	2~5	5~10	10~20
Amazon	4.44	19.62	14.55	30.05	18.55	11.40	2.59	15.85	14.94	33.27	18.64	11.48	2.76	14.85	15.26	33.53	18.90	11.61
Tocantins	0.02	1.75	12.91	41.28	21.10	17.25	0.01	0.90	9.16	43.25	21.98	17.90	0.01	0.72	7.98	41.12	23.42	18.96
Xingu	0.00	0.27	8.65	37.63	27.44	17.47	0.00	0.13	6.66	40.12	26.99	17.75	0.00	0.11	4.95	40.71	28.00	17.66
Tapajos	0.03	3.64	13.98	33.77	26.94	17.31	0.01	2.05	11.17	36.93	26.79	18.09	0.00	1.20	12.36	38.59	27.58	16.35
Madeira	5.15	16.03	15.83	25.81	19.65	13.36	3.92	12.02	16.10	28.97	19.86	13.74	3.81	11.58	16.37	30.29	19.46	13.69
Purus	0.28	7.96	25.76	38.86	19.13	8.15	0.01	3.16	25.47	43.14	19.82	8.26	0.02	2.14	23.31	46.82	19.57	8.05
Solimoes	10.00	37.11	13.55	24.10	12.57	5.19	4.68	30.04	16.22	26.52	13.95	5.59	5.56	31.18	16.95	26.08	13.14	5.17
Japura	9.26	46.96	15.27	26.64	7.57	2.15	5.48	43.17	15.00	29.42	8.15	2.45	7.49	44.75	15.88	27.96	7.68	2.30
Negro	9.53	42.75	18.62	23.41	8.02	4.84	6.42	38.91	20.54	25.42	8.03	4.86	5.96	36.37	22.31	25.53	8.33	4.97

Table 2-4. The percentage change in annual mean of shallow groundwater area fraction in the past three decades at the basin and subbasin scale over.

Basin/ Subbasin (m)	2000s-1990s						2010s-2000s						2010s-1990s					
	<0.25	0~1	1~2	2~5	5~10	10~20	<0.25	0~1	1~2	2~5	5~10	10~20	<0.25	0~1	1~2	2~5	5~10	10~20
Amazon	-41.81	-19.22	2.64	10.72	0.49	0.63	6.77	-6.35	2.15	0.78	1.42	1.20	-37.87	-24.35	4.85	11.59	1.91	1.84
Tocantins	-60.70	-48.29	-29.05	4.77	4.18	3.76	-14.81	-20.64	-12.92	-4.93	6.55	5.93	-66.52	-58.96	-38.22	-0.40	11.00	9.91
Xingu	0.00	-51.04	-22.99	6.61	-1.65	1.59	0.00	-14.64	-25.75	1.46	3.75	-0.53	0.00	-58.21	-42.82	8.17	2.04	1.05
Tapajos	-80.00	-43.76	-20.13	9.37	-0.57	4.46	-12.53	-41.27	10.71	4.49	2.96	-9.58	-82.50	-66.97	-11.58	14.28	2.37	-5.55
Madeira	-23.95	-25.02	1.70	12.23	1.07	2.84	-2.75	-3.65	1.69	4.55	-2.04	-0.35	-26.03	-27.76	3.41	17.34	-0.99	2.48
Purus	-95.27	-60.30	-1.12	11.01	3.62	1.45	66.66	-32.43	-8.47	8.53	-1.26	-2.58	-92.11	-73.18	-9.49	20.48	2.31	-1.16
Solimoes	-53.18	-19.06	19.69	10.02	10.96	7.79	18.81	3.80	4.47	-1.64	-5.80	-7.44	-44.37	-15.98	25.04	8.21	4.52	-0.23
Japura	-40.78	-8.06	-1.77	10.44	7.65	14.08	36.59	3.65	5.91	-4.95	-5.73	-6.04	-19.11	-4.71	4.04	4.98	1.49	7.18
Negro	-32.59	-8.97	10.36	8.57	0.07	0.45	-7.19	-6.53	8.61	0.43	3.79	2.36	-37.44	-14.92	19.86	9.04	3.87	2.82

The analysis of the consecutive months with shallow groundwater (<0.25 m; following Miguez-Macho and Fan, 2012) shows the role of groundwater in supporting waterlogged wetlands (Figure 2-6C). The following key observations can be made from this figure. First, waterlogged wetlands exhibit a predominant presence alongside the main river channels within the Amazon River, displaying notable prevalence within the Madeira, Solimoes, Japura, and Negro subbasins. Second, the waterlogged wetlands are highly dependent on high precipitation since groundwater is very shallow in these regions and groundwater buffer impact is relatively small. Third, a detailed temporal analysis reveals that regions experiencing continuous waterlogging for 6 to 9 months, particularly within the central and northern reaches of the basin, have witnessed a reduction of over 2 months during the past three decades (Figure 2-6I). Conversely, certain waterlogged regions along the mainstem Amazon, the extended Andes region, and the Madeira subbasin, have undergone an increase of at least one additional month of waterlogging as compared to the trends three decades ago. Fourth, the decadal analysis suggests that the waterlogged wetlands decreased by over 37% in the past three decades (Figure 2-6 and Table 2-2). The highest decline occurred in the Solimoes, Negro, Madeira and Japura, in a descending order. Fifth, these types of wetlands do not recover in a short timeframe (Figure 2-6). Although annual precipitation increased in the 2010s, the extent of wetlands did not change significantly. Overall, the extent of waterlogged wetlands decreased substantially across the ARB.

2.3.2.2 Dynamics of ET Processes

The long-term basin-averaged ET changed with a split pattern of $\pm 9\%$ during the past three decades. ET is more homogeneously distributed within the basin's boundaries in 1990s in comparison to 2010s (Table 2-5), with some areas exhibiting lower ET attributable to limited net

radiation (e.g., Andes; Figure 2-4B) or water availability (e.g., Tocantins subbasin; Figure 2-6A). Results indicate that ET exhibits strong positive (significant) trend with an average slope of ~3 mm/year over majority of the central and western ARB with a mixed signal in the eastern and southeastern regions (Figure 2-6J). Again, the spatial patterns of trends are a result of spatially heterogeneous changes in ET during the three decades (Figures 2-7:D-F) which has been noted in the previous studies as well (Heerspink et al., 2020). Over the past two decades (2000s and 2010s), the spatial distribution of ET has undergone a noticeable shift from a relatively homogenous pattern to a distribution that is more pronounced in the central regions of the ARB (Figure 2-6D). The findings suggest that the primary driver for this shift is a significant increase (decrease) in transpiration (Figure 2-8) resulting from climate variability (LULC change). Analyzing the longterm-mean of ET over the past three decades (Figure 2-6D) reveals three distinct major regions within the ARB, each characterized by different ET characteristics. The central region of the ARB, known for its high rainfall (Figure 2-6A) and dense forest cover (Figure 2-5), exhibits the highest rates of ET among the identified regions. In contrast, the northwestern region of the ARB displays relatively lower ET values compared to the central region, primarily due to reduced surface radiation (Figure 2-3) despite receiving greater precipitation than the central region (Figure 2-3). The southeastern region of the ARB stands out with substantially lower ET rates compared to the other regions, which can be attributed to the combined effects of deforestation and a lower rate of precipitation in this specific area (Figures 2-6D, 2-5, and 2-3).

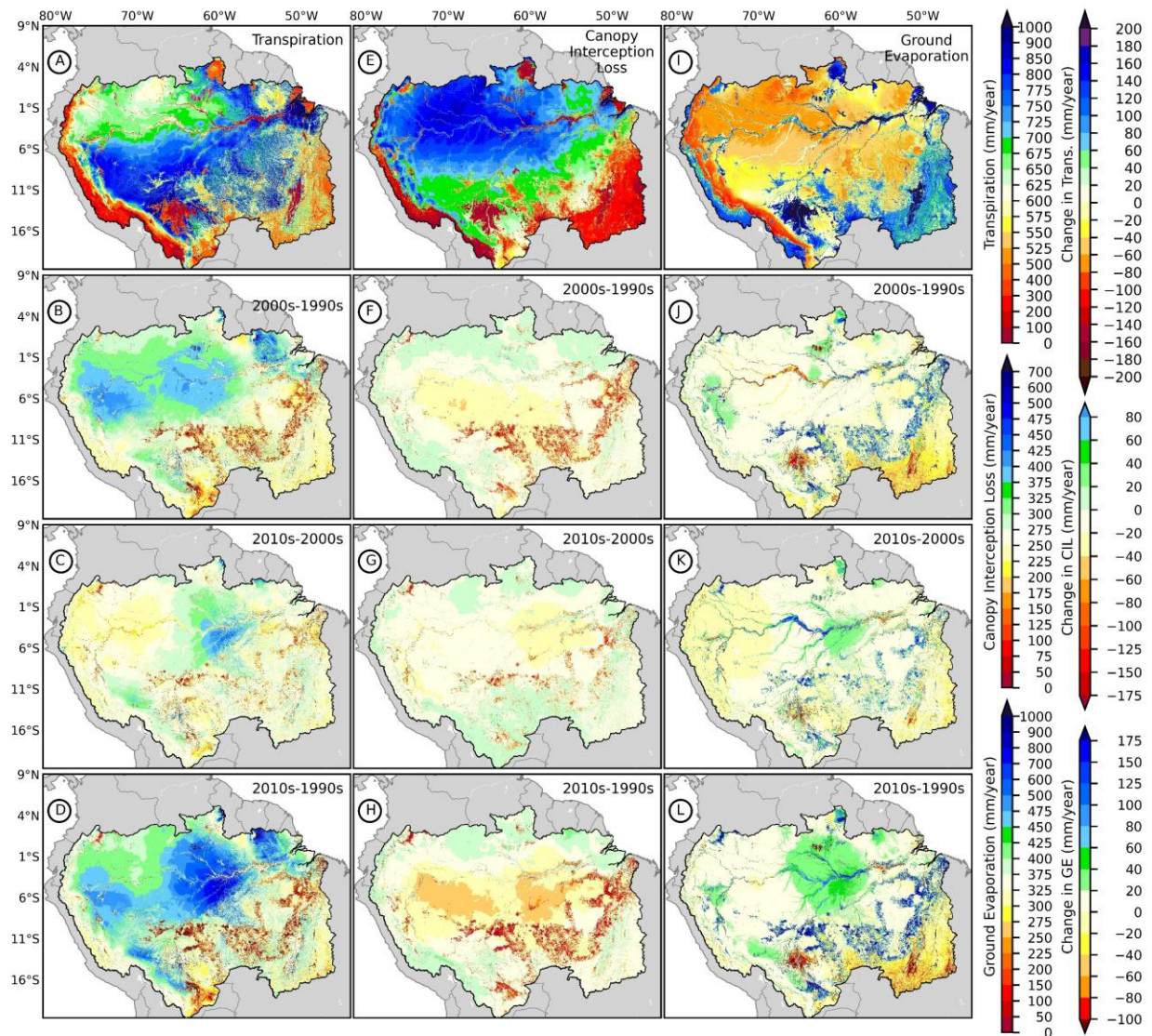


Figure 2-8. Long-term average (1992~2020) depicting the spatial distribution of annual transpiration (Panel A), canopy interception loss (Panel E), and ground evaporation (Panel I). Panel B displays the absolute changes in the decade-mean annual transpiration during the 2000s (2001 to 2010) relative to the 1990s (1992 to 2000). Panel C illustrates the equivalent changes during the 2010s (2010 to 2020) compared to the 2000s, while Panel D exhibits the same for the 2010s in relation to the 1990s. Likewise, the absolute changes in the decade-mean annual canopy interception loss during the 2000s versus the 1990s, the 2010s versus the 2000s, and the 2010s versus the 1990s are presented in Panels F, G, and H, respectively. The corresponding variations in ground evaporation during these periods are portrayed in Panels J, K, and L.

Over the northwestern region of the ARB transpiration and canopy interception loss are the dominant components of ET (Figures 2-8), whereas transpiration is the dominant component over the central regions. Over major parts of Madeira, the majority of Tocantins and the boundaries of the southern subbasins ground evaporation is the most dominant component of total ET. The change in ET in the 2000s is caused primarily by the change in transpiration rather than the other components (Figure 2-8). However, for the decrease in ET in the southern regions in 2000s, the change in ET partitioning is more complex. Over the agricultural lands in these regions ground evaporation increased, however, transpiration and canopy interception loss decreased, resulting in an overall decrease in ET with an average slope of ~ 3.2 mm/year. Among the southern subbasins, Tocantins is different from others in that the decrease is mostly a result of decrease in ground evaporation. The changes from the 1990s to the 2000s are far more pronounced than the changes in ET from the 1990s to the 2010s. Overall, the results indicate that ground evaporation in the ARB is more sensitive to climate variability than transpiration.

Transpiration is the dominant component of ET in the ARB and canopy interception loss and ground evaporation contribute almost equally to the total ET (Table 1). A comparison of total ET over the ARB during the 1990s, 2000s and 2010s indicates that the total ET increased, likely driven by the increase in net radiation. Moreover, transpiration contribution to total ET increased over the past three decades by $\sim 4.6\%$, owing to a combination of climate variability (increased due to increase in surface radiation) and human impacts (decreased due to deforestation). At the subbasin scale transpiration is the dominant component of total ET, but canopy interception loss and ground evaporation do not contribute equally to total ET as on the entire ARB scale. Canopy interception loss in Purus, Solimoes, Japura and Negro is the dominant contributor to ET after

transpiration, but in Tocantins, Tapajos and Madeira ground evaporation contributes most dominantly to ET after transpiration.

Table 2-5. The decadal mean of basin-averaged annual ET and its components (transpiration (Trans), canopy interception loss (CIL), and ground evaporation (GE) over the ARB and its subbasins (in mm/year).

Basin/ Subbasin	1990s				2000s				2010s			
	ET	Trans	CIL	GE	ET	Trans	CIL	GE	ET	Trans	CIL	GE
Amazon	1322	623	329	370	1335	643	312	380	1343	652	302	389
Tocantins	1373	701	309	363	1337	688	273	376	1345	698	259	388
Xingu	1322	709	299	314	1299	699	271	329	1300	700	255	344
Tapajos	1323	612	279	432	1314	614	256	443	1328	624	248	456
Madeira	1211	542	124	544	1171	530	108	533	1172	536	104	532
Purus	1451	740	417	293	1472	777	388	307	1491	796	376	319
Solimoes	1334	600	444	290	1379	641	440	298	1372	636	428	308
Japura	1269	582	383	304	1316	627	371	317	1303	626	360	317
Negro	1325	596	416	313	1380	640	417	323	1408	660	414	335

2.3.2.3 Dynamics of Runoff and River discharge

The ARB displays two distinct regions characterized by high and low runoff, related primarily to precipitation patterns (Figures 2-6A and E). The high runoff regions encompass the central, northern, western, and southwestern parts of the basin. In these areas, runoff dynamics are primarily governed by precipitation, as in these regions, the water table is relatively shallow (e.g., within 2m from the surface) (Figure 2-6F). Analysis of the long-term trend of runoff over the past three decades reveals a complex interplay of increased and decreased runoff in these regions (Figure 2-6K). However, the majority of these areas have experienced a decreased or relatively stable runoff and the trend in precipitation primarily explains the trend in runoff (Figures 2-6G and 2-6K). Conversely, the low runoff regions comprise the northeastern, eastern, southern, southeastern, and certain central and western sections of the basin. In most of these regions, runoff has increased due to deforestation and cropland expansion (Figures 2-6K and 2-5). Nevertheless, the effects of decrease in precipitation and increase in net radiation in the southeast and sought of this region counterbalance the runoff increase resulting from

deforestation (Levy et al., 2018). As a result, these regions have experienced a decrease or marginal increase in runoff.

The long-term basin-averaged runoff changed with a heterogenous pattern ($\pm 29\%$) over the past three decades across the ARB. Investigating the decadal analysis of the change in runoff offers more details about the long-term trend observed in runoff (Figure 2-7:G-I). Overall, runoff has decreased over some regions of the ARB by an average slope of ~ 8 mm/year in the past three decades. The majority of this decrease occurred in the 2000s due to multiple major droughts during this period (Figures 2-3 and 2-7G). In the 2010s, the runoff experienced an increase due to a rise in precipitation, but it could not reach the runoff levels observed in the 1990s over majority of the regions (Figures 2-7H and 2-7I). At the subbasin scale, the Solimoes subbasin did not experience substantial changes in runoff. On the other hand, the Tocantins, Xingu, and Madeira subbasins witnessed significant runoff decreases of approximately 47.8%, 18.0%, and 1.7%, respectively, with climate variability being the primary driver, mainly attributed to the reduction in precipitation (Figure 2-3). Conversely, the runoff in the Purus, Japura, Negro, and Tapajos subbasins increased by approximately 15.3%, 4.5%, 2.5%, and 1.4%, respectively. LULC change played a substantial role in these subbasins (Figure 2-5). Tapajos and Xingu subbasins stand out with the highest impact of LULC change, showing runoff increases of more than 5% over the past three decades. These results emphasize the combined influence of climate variability and LULC change in shaping the variability of runoff across different subbasins within the ARB.

In the 2000s river discharge in Xingu, Tapajos and major parts of Madeira remained relatively stable (Figure 2-7J). Over the northeastern regions of the ARB, river discharge increased in some river portions such as in the Negro. However, over other areas of the basin,

river discharge decreased substantially, especially in the downstream reaches. In the 2010s, river discharge in areas that had experienced a decrease in the 2000s increased substantially (Figure 2-7K). However, over the northeastern regions of the basin the areas that experienced an increase during the 2000s, river discharge decreased or remained unchanged. The only consistent decreasing trend over the past three decades is in the Tocantins, which can be observed primarily in the main river channels (Figure 2-7L). These results indicate that river discharge in the ARB has a delayed response compared to ET and WTD. The analysis of TWS presented in the following will further corroborate this finding.

The decadal analysis of river discharge seasonality indicates that the lowest monthly river discharge (in October) decreased by ~23% during the past three decades while the highest monthly discharge (in May) increased by ~3% (Figure 2-9). Most of the reduction in the low flow occurred during the 2000s due to frequent droughts. In addition, the high flow in the 2000s occurred one month earlier (in April) than in the 1990s. The results imply that while the high flow recovered from the droughts during the 2000s, the low flow did not, even after a decade. Overall, this means that the dry season in the ARB is getting drier and the wet season is getting wetter. This finding complements the findings from previous studies pointing to an accelerating Amazonian hydrologic cycle (Barichivich et al., 2018; Chagas et al., 2022).

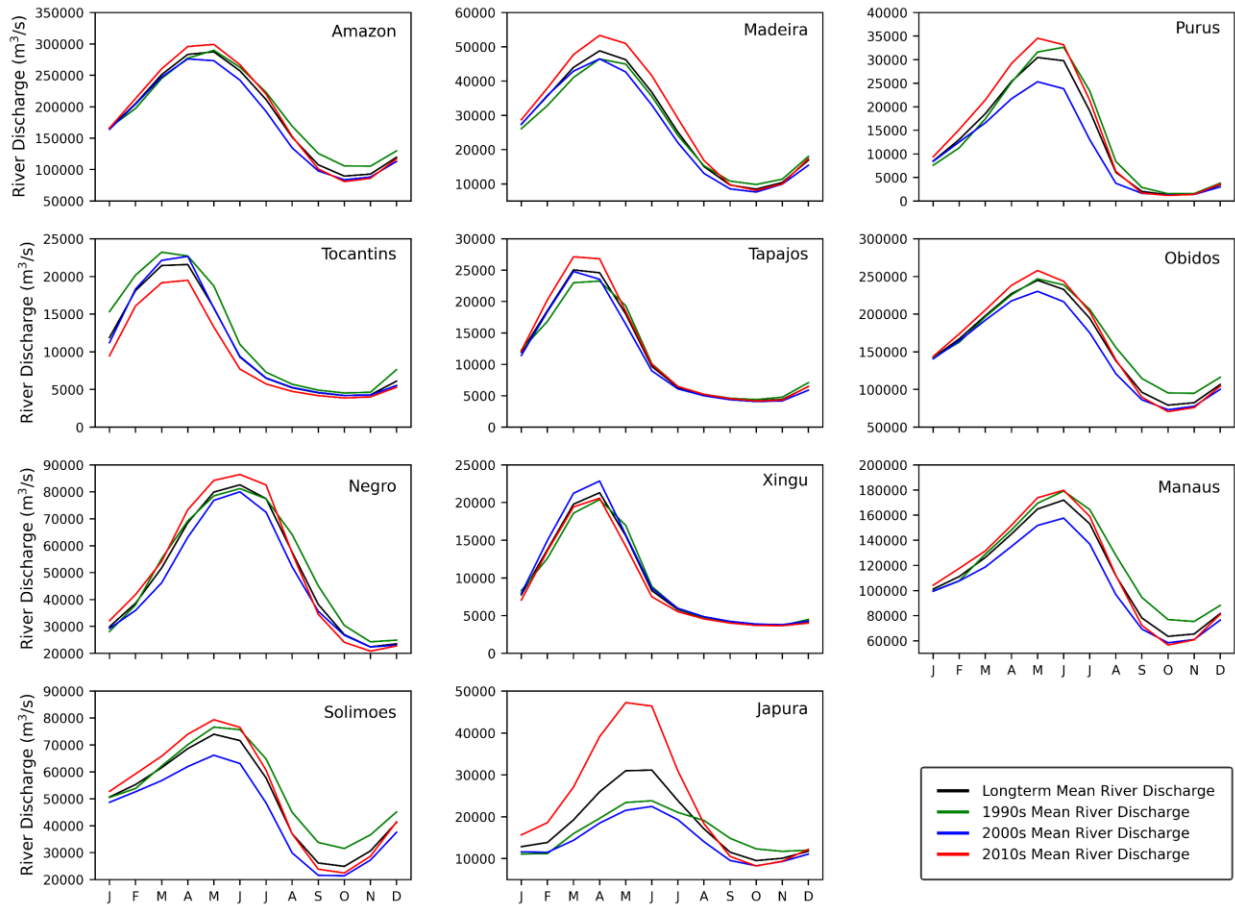


Figure 2-9. Analysis of seasonality and decadal variations of river discharge at the outlets of major subbasins in the ARB.

The decadal analysis at the subbasin scale indicates that Solimoes has a dominant impact on the high discharge in the mainstream of the ARB, while Tocantins and Tapajos have the least impact (Figure 2-9). However, none of the subbasins play a dominant role in governing the low discharge in the ARB. The timing of high flow has not changed over the past three decades and it occurs in March in Tocantins and Tapajos, in April in Madeira and Xingu, in May in Solimoes and Purus, in June in Negro and Japura.

The analysis of the change in high discharge at the subbasin scales indicates that at all the subbasins and during the past three decades, river discharge at the outlet increased except for the Tocantins where it decreased by ~16% (Figure 2-9). The other change worth mentioning in

discharge is the ~98% increase in the peak in Japura due to the increase in precipitation in the 2010s (Figure 2-3). The elongated shape of Japura and shallow groundwater level over the majority of the subbasin makes river discharge more responsive to the changes in precipitation than in other subbasins. Over the past three decades, river discharge in Tapajos and Madeira increased by ~17% and ~15%, respectively, due to a combination of increase in precipitation and deforestation (Figure 2-3 and 2-5). In the other subbasins, the changes in high discharge are well below 10% in comparison to the 1990s. Despite the increasing trend in high discharge among the majority of the subbasins, the low discharge decreased in all subbasins.

2.3.2.4 Dynamics of TWS

Results show that the spatial patterns of TWS remained relatively stable, but its magnitude changed substantially during the past decades (Figures 2-10A and 2-11). The spatial distribution of the trends in TWS anomalies closely parallels the trend observed in WTD (Figures 2-10A and 2-6L). Nonetheless, it is noteworthy that the spatial pattern of the trend in floodwater anomalies governs the spatial pattern of TWS trend along the mainstem of the Amazon (Figure 2-10D) which was reported by Pokhrel et al., (2013) as well; the contribution of water in river channels is less prominent (Figure 2-10C). Overall, a decreasing trend in TWS anomalies is observed across the ARB which is largely associated with a decline in precipitation and increase in net radiation. However, some regions with an increasing trend over the "arc of deforestation", the Andes, and the northeastern areas of the basin can be observed. The increasing trend in TWS over the "arc of deforestation" is associated with decrease in ET and over the other regions with increase in precipitation and net radiation.

The decrease (increase) in the 2000s (2010s) along the mainstem of the Amazon River is associated with the fluctuations in flood water due to drought or wet periods, and as a result, no

substantial trend is observed in the long-term trend (Figure 2-10A) (Pokhrel et al., 2013).

Tocantins subbasin experienced a decreasing trend in TWS over the past three decades due to the decline in groundwater storage which could be attributed to the reduced moisture transport into the eastern margins of ARB (Walker, 2020). Over other southern subbasins including the Xingu, Tapajos and Maderia subbasins, TWS decreased from the 1900s to the 2000s and it increased from the 2000s to the 2010s. The changes in TWS over the southern subbasins are dominantly associated with the changes in groundwater storage (Figures 2-10B and 2-11). Negro, Japura and Solimoes subbasins experienced a decrease in TWS from the 1990s to the 2000s; however, in the 2010s TWS increased in comparison to the 2000s. While flood water is the dominant component of the variations in TWS in these subbasins, groundwater component is the dominant contributor to TWS. Over the northeast region of the ARB, TWS increased substantially during the 2000s due to a large drop in WTD in comparison to the 1990s. The same region experienced a decrease in TWS from the 2000s to the 2010s. Again, groundwater is the dominant portion of TWS in this region and the variations in WTD lead to changes in TWS there. As depicted in Figure 2-11, the changes in TWS for the majority of regions across the ARB are governed by groundwater which confirms our hypothesis regarding the mediating role of shallow groundwater. It should be noted that in the LHF model soil moisture and groundwater compete for the same subsurface store (Pokhrel et al., 2013), thus an increase in groundwater storage would lead to a decrease in soil moisture, and vice versa.

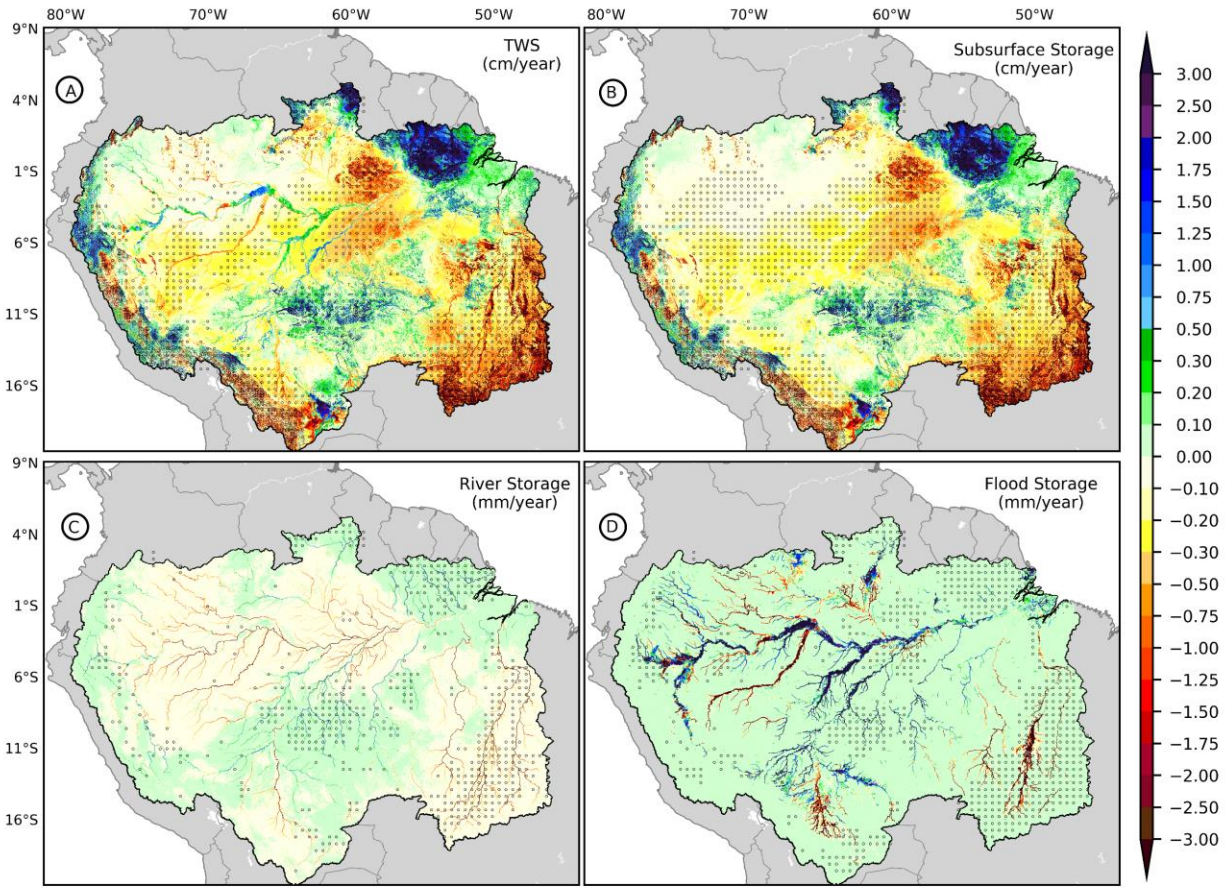


Figure 2-10. Temporal (1992-2020) trend in simulated TWS anomalies (panel A) and the anomalies of its components, namely subsurface (B), river (C), and floodwater (D) stores, across the ARB. Markers indicate significant trends from Mann-Kendall test at 95% confidence level.

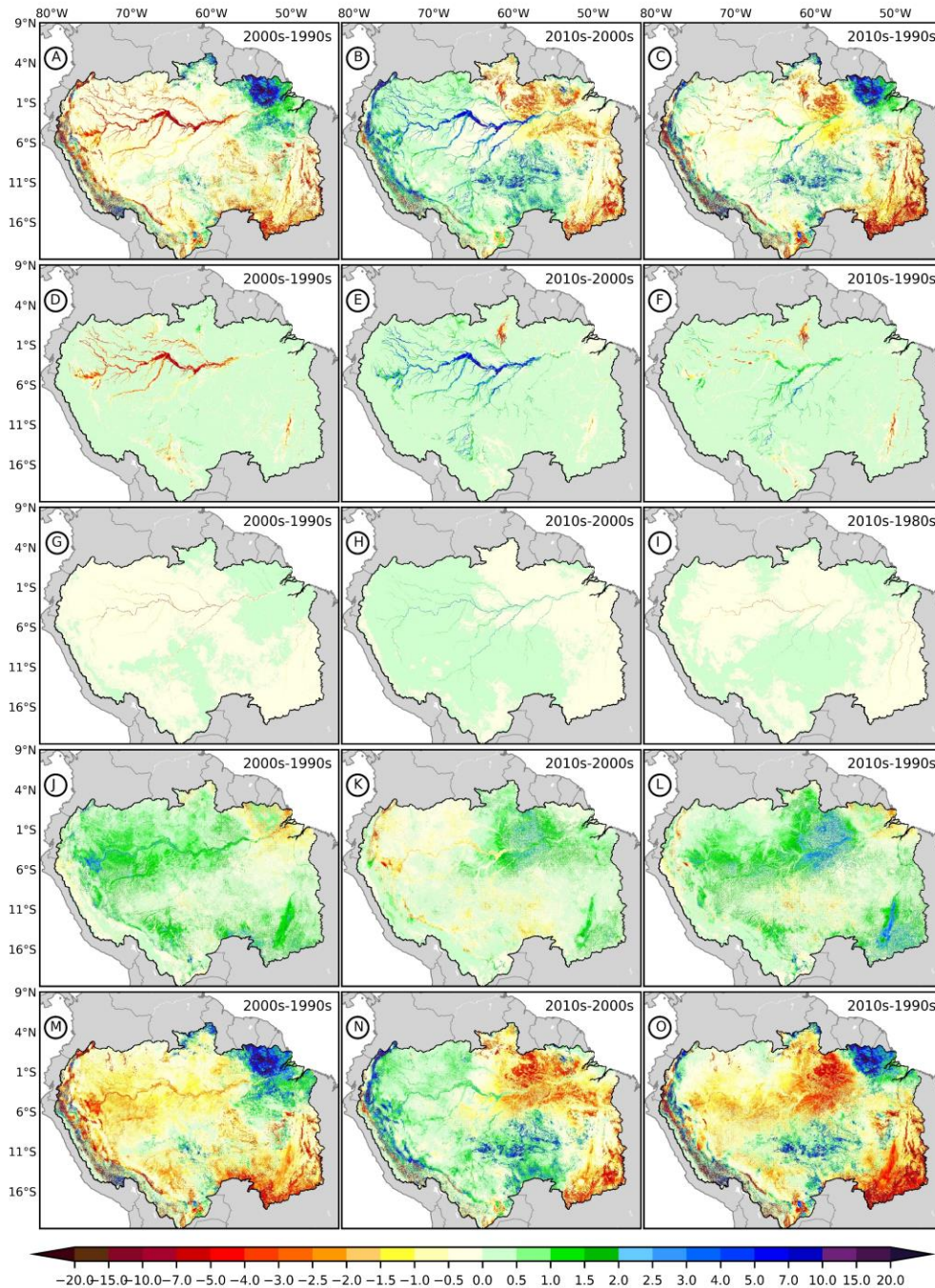


Figure 2-11. Decadal averages illustrating the change in TWS (Panels A, B, and C) and its components, namely, floodwater (Panels D, E, and F), river water (Panels G, H, and I), soil moisture storage (Panels J, K, and L), and groundwater storage (Panels M, N, and O). Panels A, D, G, J, and M depict alterations during the 2000s (2000 to 2010) relative to the 1990s (1992 to 2000). Similarly, panels B, E, H, K, and N showcase changes observed during the 2010s (2010 to 2020) compared to the 2000s. Lastly, panels C, F, I, L, and O present changes that transpired in the 2010s in contrast to the 1990s. All values the values in the figure are in meters.

2.3.3 Governing Hydrological Processes

Here, we address the second research question regarding the key factors that are governing the seasonality of the ARB at the basin and subbasin scales. In addition to many other roles, groundwater in the ARB supports streamflow and ET during the dry season. The comprehensive groundwater area fraction analysis unravels the dynamics of surface-subsurface fluxes (Figure 2-12), indicating that in general $WTD < 5m$ dominantly supports river discharge (Q) and ET across the ARB. The lag time between the peaks of streamflow and ET is about one month and June–November is the driest season. During April–June groundwater (with $WTD < 1m$) supports Q, but after June it becomes deeper with $WTD < 2m$ being the more dominant condition until early September when the hydraulic gradient decreases. As seen in the Amazon panel (Figure 2-12), the increase in area fraction of $1m < WTD < 2m$ is a result of depletion in $WTD < 1m$ that occurs around June. During the past three decades (Figure 2-12), the role of groundwater to support stream discharge and ET during the dry season increased at the peak of the dry season by ~7% and ~30%, respectively. The dry season is longer (~1 month) and more pronounced in the 2010s than two decades ago. Subsurface, river, and flood storages, on average, contribute to 68.8%, 26.4%, 4.8% of total TWS variability in the ARB, respectively. A previous study showed that groundwater storage contributed to 20~35% of the TWS seasonal volume variation (Frappart et al., 2019). Subsurface storage fluctuates by ~15.6% seasonally to mitigate surface water and ET deficits. Contribution of subsurface storage increased in the 2010s, contributing by more than 21% to the total storage variability than it did in the 1990s. The impacts of frequent droughts in the 2000s are evident in the surface and subsurface storages through substantial decadal changes in the timing and magnitude of peak subsurface, river and flood storages contributions in TWS variability (Figure 2-12). From the 1990s to the 2000s, annual mean of floodwater contribution

in TWS variability decreased by ~38%, and as a result, the ratio of Q to precipitation (Q/P) decreased by ~5%. The timing and seasonality of Q/P in the Solimoes, Madeira, Tapajos, and Purus is similar to that in the entire ARB. The substantial difference between these subbasins comes from the difference in the contribution of subsurface storages to the TWS variability. The share of subsurface storage in total TWS variability in Solimoes, Tapajos, and Purus is more pronounced than Madeira. This implies that Solimoes, Madeira, Tapajos, and Purus have a dominant impact on the seasonality of surface and subsurface fluxes in the ARB.

The seasonal cycle of ET over precipitation ratio (ET/P) and Q/P in the Tocantins overlaps almost perfectly without any noticeable lag between their peaks. This is because the Tocantins receives the lowest amount of precipitation among the ARB subbasins. Moreover, shrubland is the dominant form of the land use/land cover in the subbasin (Figure 2-3) and ground evaporation contributes to total ET almost equally as transpiration (Table 2-5). In terms of timing, Q/P peak occurs in August, one month later than in the ARB, however, Q/P peak occurs at the same time as in the ARB (in August). Therefore, the terrestrial hydrological cycle in the Tocantins is more strongly governed by groundwater than over the entire ARB. In addition, Q seasonality in the Tocantins contributes to the high flows in the ARB and ET seasonality in Tocantins causes a longer dry period in the ARB. In the Tocantins, groundwater contribution to surface fluxes (Q and ET) begins one month earlier than in the ARB; during March-June WTD<1m supports the surface fluxes, leading to a substantial reduction in shallow groundwater storage. During June-July, 1m<WTD<2m dominantly supports the surface fluxes, and the contribution from 2m<WTD<5m begins in early August. In the Tocantins, subsurface, flood, and river storages, on average, contribute to 91.5%, 6.3%, 2.2% of total TWS variability, respectively. Subsurface storage fluctuates by ~5.4% seasonally to mitigate Q and ET deficits,

experiencing an overall decadal decreasing trend. Xingu follow similar timings as in the Tocantins.

In the Negro sub-basin over 88% of the area is covered by forest, and it receives an average annual precipitation of ~3,000 mm (Figures 2-6A and 2-5). As a result, groundwater only compensates for the Q deficit during the dry season. The dry season in the Negro (May-October) is the second shortest after Japura. The Q/P and ET/P peaks (in September and October, respectively) occur two months later in the Negro than in the ARB (Figure 2-12). Therefore, Q seasonality in the Negro contributes to the amplitude of high flows in the ARB, but ET seasonality in the Negro does not contribute to the dry period in the ARB. WTD<1m supports Q during June-September. In addition, at the northern region of Negro that is covered with shrublands (Figure 2-5), groundwater is deeper than in the other areas in the subbasin (Figure 2-12F), and it also receives 1,500 mm/year of precipitation which is substantially less than the average precipitation over the ARB (Figure 2-12A). In the northern region WTD<5m from February to October supports Q and ET (Figure 2-12). In Negro, subsurface, flood, and river storages, on average, contribute to 74.7%, 22.0%, and 3.2% of total TWS variability, respectively. The seasonality of Q and ET and dynamics of groundwater in Japura is similar to that in Negro. However, since it is partially located in the two hemispheres, ET/P has two peaks. The first peak occurs around January and the second around September.

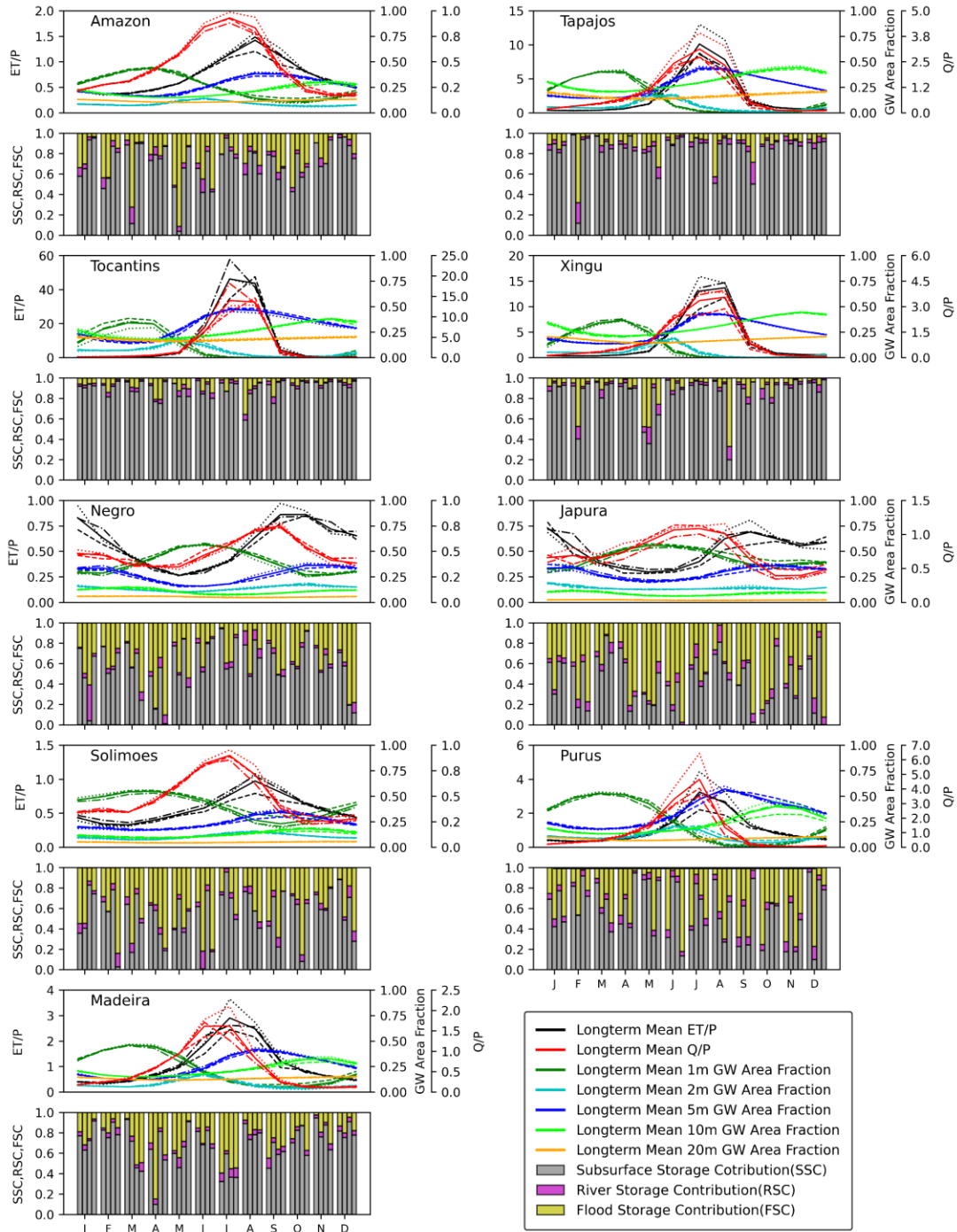


Figure 2-12. Ratio of monthly ET (left axis) and Q (far right axis) to precipitation, and groundwater area fraction for different water table depths (right axis) for the entire ARB and its major subbasins (top panels). Solid, dashed, dotted-dashed, and dotted lines indicate the long-term mean, 1990s mean, 2000s mean, 2010s mean, respectively. Contribution of subsurface (SSC), river (RSC), and floodwater (FSC) storage components to the monthly TWS anomaly for the ARB and its subbasins (bottom panels). The first, second, third, and fourth bars for each month represent the averages for 1992-2020 (long-term), 1990s, 2000s, and 2010s, respectively.

The ARB is dominantly energy limited where solar radiation governs ET (Figure 2-6B and D). Precipitation and net radiation seasonality across the ARB are out of phase from July to October, but net radiation and ET are in phase throughout the year. During March-August, precipitation decreases; however, groundwater buffer prevents substantial drop in ET. These results imply that in the absence of groundwater support, and with less than ~125 mm/month of precipitation (Amazon panel in Figure 2-13), the ARB could have become a water-limited region.

On average, the share of transpiration, canopy and ground evaporation to total ET are ~48%, ~24% and ~28%, respectively (Table 1). June-September is the driest period, during which groundwater storage supports ET, leading to decrease (increase) in groundwater (soil moisture) storage (Figure 2-13). Transpiration increases during this period while ground evaporation remains largely stable, which highlights groundwater support for ET. The decadal analysis shows that P, ET, and net radiation decreased by ~11.5%, ~0.2% and ~3.4% respectively during June-September from the 1990s to the 2000s. Therefore, ET did not decrease substantially despite the large decline in precipitation. This again confirms the role of shallow groundwater (<5m deep) in mitigating ET deficit. The decadal analysis on ET components in the 2000s indicates that the decadal average of annual transpiration and ground evaporation increased by ~3.3% and ~2.7% respectively in comparison to the 1990s. However, the decadal average of annual canopy interception loss decreased by ~5% which is due to the substantial deforestation that happened in this decade (Figure 2-5). A similar trend is found in the 2010s in comparison to the 1990s; annual ET, transpiration and ground evaporation increased by ~1.6%, ~4.7%, ~5.0%, respectively, whereas canopy interception loss decreased by ~8.1%.

At the subbasin scale, the seasonality of ET and its components exhibits similar hydrological behavior within three distinct subbasin groups: i) Solimoes, Madeira and Purus; ii) Tocantins, Tapajos and Xingu; and iii) Negro and Japura. The hydrological behavior observed in the first group closely mirrors that of the ARB. On average, the components, transpiration, canopy interception loss, and ground evaporation, contribute approximately 47%, 24%, and 29% to the total ET, respectively (Table 1). A decadal analysis within this group reveals substantial changes from the 1990s to the 2000s, with relatively minor fluctuations from the 2000s to the 2010s. The increase in ET within this subgroup is primarily attributed to climatic variability; however, deforestation in the Madeira has masked these increases due to climate variability, resulting in a reduced ET rate in comparison to the 1990s. In summary, over the course of the 2000s and 2010s, the decadal averaged annual ET in Solimoes and Purus subbasins exhibited an increase of ~2.8%, while Madeira experienced a decrease of ~3.2%. The increase in transpiration predominantly influenced the interdecadal variability of ET in Solimoes and Purus, whereas canopy interception loss played a dominant role in the changes observed in the Madeira subbasin.

In the second group, the share of transpiration, canopy loss transpiration and ground evaporation to total ET is ~50%, ~18% and ~31%, respectively (Table 1). Consequently, ground evaporation plays a more prominent role in governing the seasonal dynamics of ET in this group compared to the first group (Figure 2-13). A decadal analysis of this group elucidates the factors contributing to the decrease in ET during the 2000s and 2010s when contrasted with the 1990s. On average, ET in Tocantins, Tapajos and Xingu decreased by over 10% in August (driest month) from the 2010s to the 1990s. While all components of ET contribute to this decrease, the majority of it is due to over 34% decrease in canopy interception loss. It is noteworthy that

canopy interception loss evaporation in these subbasins is primarily driven by the evaporation from croplands and shrublands. Specifically, croplands cover approximately 28%, 21%, and 13% of the respective areas in Tocantins, Tapajos, and Xingu, while shrublands encompass around 57%, 7%, and 8% of these regions. In contrast, in the third group of subbasins, Negro and Japura, the contributions of transpiration, canopy interception loss, and ground evaporation to the total ET are approximately 46%, 32%, and 22%, respectively. Over the 2000s and 2010s, ET increased by ~6.3% and ~2.7% in Negro and Japura, respectively, with the change in transpiration exerting a dominant influence on this direction of change.

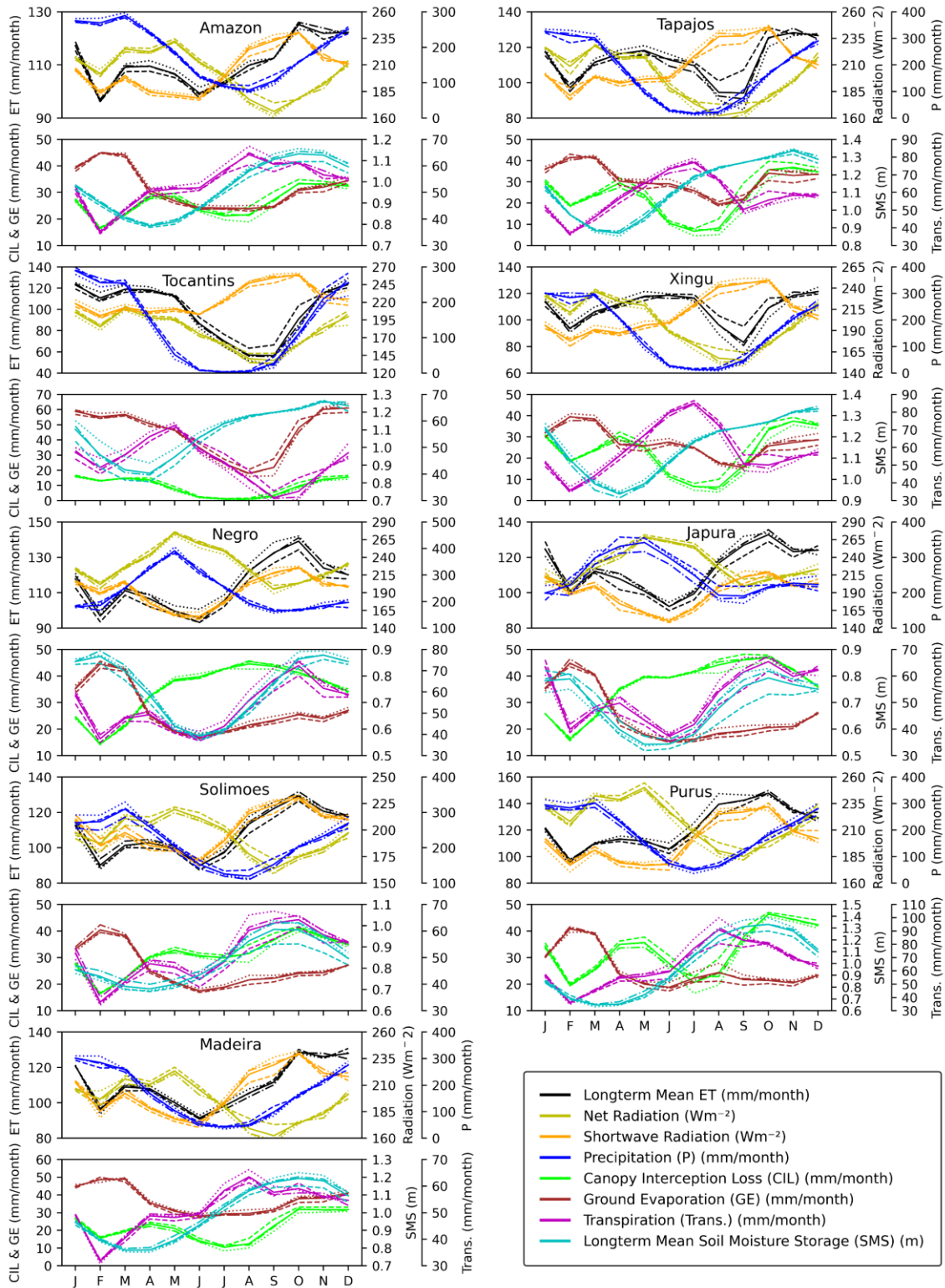


Figure 2-13. Seasonality of ET over the ARB and its major subbasins. Solid, dashed, dotted-dashed, and dotted lines indicate the mean during 1992-2020 (long-term), 1990s, 2000s, and 2010s, respectively.

2.3.4 Early/Late Warning Signals

Early and late warning signals play a pivotal role in monitoring and responding to hydrological changes within the ARB. This section addresses the third research question, providing insights into the implications of these signals, emphasizing their importance in understanding hydrological dynamics and enabling effective management strategies. As shown in section 3.3, WTD<5m has a dominant impact on the seasonality of surface fluxes at the basin and subbasin scale and it largely mitigates the impacts of climate variability and LULC change on ET and river discharge (Figure 2-6). However, the mitigation impact of groundwater for ET is more limited than river discharge.

Assessing hydrological changes within the ARB requires a nuanced understanding that extends beyond standard hydrologic indicators such as river discharge. Our findings underscore the limited utility of river discharge as a standalone indicator, given its strong dependence on groundwater dynamics (Figure 2-12). Providing a more nuanced perspective, alterations in ET distribution serve as valuable precursors of hydrological shifts (Table 1). While groundwater largely supports ET during the dry season, shifts in ET patterns provide valuable early indications of hydrological changes. Notably, in the deforested regions, increased ground evaporation partially compensates for reduced transpiration due to diminished LAI. Integrating remote sensing data and harnessing computational advancements can enhance the monitoring of ET dynamics, reducing the latency of distributed hydrological models.

Spatial patterns of shallow groundwater area fractions (Figure 2-6F) offer another layer of early indicators. These indicators spotlight regions undergoing variations in hydrological processes, directing immediate attention, and enabling prompt management interventions. However, observational WTD datasets are notably absent in the ARB, impeding comprehensive

management strategies. While the establishment of a monitoring well network within the top 5 meters of the land surface remains crucial, this study demonstrates (see section 3.2.4) the potential utility of GRACE data as a proxy for WTD. It is, nevertheless, important to acknowledge that while GRACE offers insights, its uncertainties and coarse resolution render it unreliable for local and finer-scale monitoring.

Late warning signals, primarily rooted in TWS changes, intricately reflect alterations in floodwater and groundwater dynamics (Figure 2-10). Understanding how climate variability and human activities influence TWS alterations is pivotal for devising adaptable management strategies. By embracing both early and late warning signals, hydrological monitoring and management strategies can be holistically designed to mitigate the impact of hydrological fluctuations. In essence, the interplay of early and late warning signals significantly contributes to our understanding of hydrological transformations within the ARB. These signals, specifically derived from ET distribution, spatial groundwater patterns, and TWS shifts, could collectively pave pathways for a more comprehensive and effective hydrological monitoring and management framework. This framework, in turn, empowers stakeholders to anticipate, respond to, and alleviate the impacts of hydrological changes in a proactive and informed manner.

2.3.5 Hydrological Implications for Forest Management

The analysis of groundwater area fraction (i.e., areas with $WTD < 0.25\text{m}$) revealed that waterlogged wetlands are located mostly along the main channel of the Amazon River which are not permanently flooded and are supported by rather shallow groundwater as noted by Miguez-Macho and Fan, 2012 as well. The variation in the extent of these wetlands is strongly governed by precipitation because groundwater is very shallow in waterlogged regions. As such, large-scale land cover/land use change in the ARB, which could cause substantial change in

precipitation (through change in moisture recycling or shift in the precipitation pattern) should be avoided (Carlos A. Nobre et al., 2016). The extent of these wetlands should be considered as the first criterion in any management/development practices since any shift in precipitation pattern will impact the water-logged wetlands and they are a rich niche for ARB biodiversity (Duponchelle et al., 2021). The second design criterion could be the area fraction of WTDs of up to 5m. As indicated by the comprehensive analysis of the fractional area of groundwater, groundwater sustains surface fluxes during the dry season. Therefore, the management/development practices could support this process by preserving the extent of WTD area fraction and tree species with rooting depth of more than 5m. In cases where a change in land use is unavoidable, WTD area fraction could be maintained within some thresholds that do not alter various impacted processes discussed in the results section. It is worth noting that the seasonal dynamics of groundwater area fraction beyond the thresholds can cause seasonal drought and waterlogging stress to favor the condition for other alternatives state at least at local scales (Ying Fan et al., 2017; Hirota et al., 2011; Khanna et al., 2017; Lovejoy & Nobre, 2019; Mattos et al., 2023; Staal et al., 2018, 2020; Staver et al., 2011).

The third management criterion could be the lag time between the peak of Q/P and ET/P. As shown in the WTD fraction area analysis at the basin scale (Figure 2-6) the lag time is the key in sustaining the rainforest from tipping into savanna. Therefore, it is crucial to sustain the lag time to Q/P which occurs around two months earlier than ET/P in the subbasins with intensive land use. The fourth management criterion could be the spatial distribution of ET. Management practices that result in a more uniform distribution of ET across the ARB could be beneficial. As shown in the results, the deforestation across the “arc of deforestation” caused a shift in ET pattern, and higher contribution of forested regions will increase the chance of forest degradation

and dieback (Cox et al., 2004; Delphine Clara Zemp et al., 2017). Similar strategies can be applied to the subbasins with similar hydrological behavior. The analysis of groundwater area fraction in conjunction with seasonality of ET/P, Q/P and TWS components showed that Tocantins, Tapajos and Xingu have similar hydrological responses. In addition, Solimoes, Madeira and Purus can be grouped together hydrologically with Negro and Japura.

The trend and decadal analyses showed that ET is the one of the earliest key hydrological variables which responds to climate variability and anthropogenic impacts by shifting from a uniform to a forest concentrated pattern. This is because over tropical forests, transpiration is the dominant contributor to total ET, therefore, forested areas generally compensate for the reduced contribution of transpiration in the deforested areas. Therefore, the substantial change in ET pattern can be taken as an early warning signal. In addition, we showed how WTD area fractions change seasonally and at the interdecadal scale to mitigate the changes in ET and river discharge. The trend analysis on groundwater storage indicates that there is a decreasing trend in the storage, implying that groundwater storage can be taken as another warning signal for hydrological alteration in the ARB.

Overall, the results showed that the status of groundwater shallow area fraction in conjunction with the spatial distribution of ET can be taken as a proxy for assessing the future of management practices. The spatial distribution of ET can be monitored as an early warning signal and the changes in shallow groundwater area fraction as a late warning signal to monitor the hydrologic changes. However, in the deforested areas ET is highly impacted by climate variability since ground evaporation is the dominant contributor to the total ET after transpiration. For example, in the Tocantins, ground evaporation contributes to over 43% of total ET, therefore, ET would indicate the changes that occur locally and under climate variability

rather than due to human disturbances. The comprehensive WTD area fraction analysis of WTD, WTDs of up to 5m are the governing hydrological attributes of the ARB. The WTD<5m fulfills a wide range of functions and supports ET and river discharge across the ARB. However, there is no comprehensive observational dataset of WTD available in the ARB, even though such a dataset is crucial for management, deploying policies and future management practices in the ARB. Therefore, it is important to develop a network of monitoring wells especially in the first 5m from the land surface, however, as shown in this study (see section 3.2) GRACE data could be used as a proxy, but the uncertainties and coarse resolution of GRACE would not provide a reliable monitoring at local and finer scales.

2.4 Conclusions

Dominant terrestrial hydrological processes are investigated at basin and subbasin scales based on three decades of hydrological variability across the ARB. The results of comprehensive groundwater fractional area analysis suggested that shallow groundwater (<5m) is the dominant attribute of the ARB which strongly modulates the dynamics of surface-subsurface fluxes at basin and subbasin scales during the dry season. The results of area fraction of varying WTDs indicate that WTD<2m is prevalent at ~34% of the basin area, whereas WTD between 2-5m is common at ~30% of the basin. This implies that at least 34% of the Amazonian Forest is supported by groundwater during the dry season. The area fraction of WTD<2m decreased by ~19% during the past three decades. Most of this reduction occurred in regions with WTD less than 1m. As a result, the areas with WTD less than 2m and greater than 1m increased by ~5% and most of this increase occurred in the Solimoes and Negro subbasins. The areas with WTD between 5-20m increased at the expense of decline in areas with shallower WTDs. Therefore, forest management practices in the ARB, which may alter WTD, should ensure that the resultant

WTD is able to support ET and river discharge through the processes discussed in the results section.

WTD<0.25m supports waterlogged wetlands at ~4.5% of the ARB area and in up to 10% in Solimoes, Japura, and Negro subbasins. These types of wetlands are not flooded and highly dependent on precipitation to sustain their extent. The trend analysis showed a decreasing trend in the extent of the waterlogged wetlands (by ~37%). The impacts on the wetlands should be considered in the management policies to avoid the unintended consequences which may disrupt the roles of the wetlands. The wetlands are very susceptible to large-scale changes in land use/land cover and are playing an important role in sustaining the biodiversity of the ARB. The lag time between the seasonal peak of ET and river discharge is a key mechanism sustaining the rainforest from tipping into savanna. The management practices should improve the lag time in ways that the peak of discharge occurs around two months earlier than the peak of ET in the dry season. Further, the decadal analysis showed that ecohydrological processes that depend on shallow groundwater are more susceptible to climate and human factors than those dependent on deeper groundwater processes and they lose their functionality due to decrease in precipitation sooner.

The long-term basin-averaged ET changed with a split pattern of $\pm 9\%$ with transpiration being the dominant contributor (~49%) to total ET in the past three decades. The contribution of transpiration (~4% increase), canopy (~2% increase) and ground evaporation (~5.9% increase) evolved dramatically in response to deforestation. As ET increased over the forested regions due to climate variability impacts and it decreased over deforested regions due to a combination of climate variability and deforestation impacts, the spatial distribution of ET shifted from a homogenous distribution to a more intense ET in the central region of the ARB. The shift in ET

intensity distribution can lead to further forest degradation and dieback in the forested areas where the forest contributes more than it used to do three decades ago. WTD ($\pm 19\%$) and runoff ($\pm 29\%$) changed with a heterogeneous patterns across the ARB. Analyzing river discharge confirms the crucial buffering role of groundwater. The results of this analysis imply that while the high flow recovered from the droughts during the 2000s, the low flow did not, even after a decade. Overall, this means that the dry season in the ARB is getting drier and the wet season is getting wetter. The ARB is dominantly energy limited, however, our results imply that in the absence of groundwater support, and with less than ~ 125 mm/month of precipitation, the ARB could have become water-limited, at least in some regions. These results also indicate that river discharge in the ARB has a delayed response to the changes in the basin compared to ET and WTD. The only consistent decreasing trend over the past three decades, which is observed in the main river channels, is in the Tocantins. Terrestrial water storage (TWS) decreased (increased) in the 2000s (2010s) compared to that in the 1990s. The results showed that the dominant role of subsurface storage in contributing into TWS dynamics has intensified in the past three decades. Although groundwater is the dominant contributor to total TWS, the dynamics of TWS over the regions along major river channels are controlled by flood water since groundwater is relatively shallow in these regions. ET is likely to be impacted more by climate change and variability than shallow groundwater (< 5 m deep). Therefore, groundwater storage needs to be monitored as the primary indicator of the system status in forest restoration designs and the spatial distribution of groundwater area fractions and ET as an early warning signal on the changes that are occurring in the terrestrial hydrological cycle in the ARB.

The spatial resolution and temporal period of the simulations are two of the limitations of this study. The improvement of the model resolution might assist in defining some design criteria

in the headwater streams which are rich instream physical habitats. However, due to the coarse input data resolution and high computational costs, it was not possible at the time of conducting the simulations for this research to do the simulations at finer resolution than one arcminute and it is one of the limitations of this study. The ESA land cover/land use data is not available for the entire ARB before 1992. Covering the periods before 1992 could provide more insight into what the natural states of the hydrological system in the ARB were. However, since this study focused on the hydrological processes, the use of such extended simulations would not alter the key findings. Moreover, the thresholds of ET and WTD change need further research using coupled land surface and atmospheric models and by developing a wide range of scenarios which is out of the scope of this study. In sum, this study provided crucial insights on the dominant terrestrial hydrological processes in the ARB to inform forest management practices.

Chapter 3 Climatic and Anthropogenic Impacts on the Hydrology of the Amazon River Basin

Based on: Bagheri, O. and Pokhrel, Y. (202x). Climatic and Anthropogenic Impacts on the Hydrology of the Amazon River Basin. [Under Preparation]

3.1 Introduction

Over the past few decades, substantial changes have occurred in the global terrestrial water cycle (Bosmans et al., 2017; Sterling et al., 2013). These changes have been primarily driven by internal variability in the climate system, anthropogenic climate change (i.e., emission-driven) and direct human disturbances (Bosmans et al., 2017; Wohl et al., 2012). Human activities modulate the climate system at different scales through changes in land use/land cover (LULC) and components of water cycle to satisfy the growing need for food, fiber, water, and shelter for more than 7.8 billion people (Foley et al., 2005). Humans have altered more than 41% of natural landscape through anthropogenic land cover change such as croplands or pasture expansion, impacting evaporation-to-runoff ratio which, in general, increases (decreases) discharge (evapotranspiration) globally (Bosmans et al., 2017). Extensive LULC changes in watersheds can have dramatic short- and long-term impacts on terrestrial hydrology. They can alter the occurrence and severity of extreme hydrological events (e.g. floods and droughts) which are the most prevalent causes of human suffering among all climate-related hazards (Sterling et al., 2013). A significant portion of the changes in LULC are essential for agricultural and industrial development. Therefore, for sustainable development and to avoid unintended consequences on land and water resources, it is of crucial importance to understand the impacts of deforestation, afforestation and the collective LULC changes on terrestrial hydrological cycle.

The impacts of human interventions in terms of LULC changes on terrestrial hydrological cycle are complex and depend on the initial LULC conditions. The direct effects of the human induced LULC changes include the morphological and physiological variations in the landscape as reflected by altered aerodynamic roughness, leaf area index (LAI), stem area, surface resistance, albedo, and rooting depth (Bala and Nag, 2012; Bäse et al., 2012). The indirect effects of LULC changes on the soil and atmospheric boundary layer include the altered infiltration capacity and hydraulic conductivity in the shallow soil layer (Bonell et al., 2010; Muma et al., 2011; Lanckriet et al., 2012; Hassler et al., 2011; Neill et al., 2013; Ghimire et al. 2014a), as well as varied net radiation, sensible and latent heat flux, and wind speed (Mishra et al., 2010; Liu, 2011). Both the direct and the indirect effects of LULC changes have direct implications particularly on energy, momentum, and water transfer in the atmospheric boundary layer and could affect hydrologic cycles and climate systems at varying scales (e.g., locally, regionally, and globally) (Liu, 2011; Bala and Nag, 2012; Kumagai et al., 2013; Spracklen et al., 2012; Poveda et al., 2014).

The interaction of LULC in climate and land system, being scale-dependent, in addition to lack of comprehensive simulations of the system which include water cycle, ecology, abiotic-biotic linkages, and human interventions make study of impact of LULC change on terrestrial hydrological cycle a cumbersome task. Meanwhile, the study of the impacts of LULC change on key hydrological variables (e.g., river discharge, ET, WTD and TWS) and quantification of their effects has become possible due to recent advances in fully-physics based hydrological models and emerging remotely sensed data and observations (Bosmans et al., 2017).

Nevertheless, studies that focus on or include the impact of LULC changes (Bosmans et al., 2017) are still limited, at least at scales such as the entire Amazon River basin (ARB).

Bosmans et al. (2017), studied the hydrological impacts of LULC and human water use and found that the effect of LULC change is of the same order of magnitude as the effect of human water use, hence it needs to be accounted for in studies of anthropogenic impacts on water resources. They also found that LULC changes lead to increase in discharge by reducing evapotranspiration on average from 1850 to 2000, however, there is a large spatial variability in magnitude and sign of change.

The Amazon is the largest river system and home to the most extensive tropical forest on the planet. The importance of Amazonia as a component of the global terrestrial hydrologic cycle and its key role in global atmospheric circulation by precipitation recycling and atmospheric moisture transport is well known (Cox et al., 2004; Nobre et al., 1991; Malhi et al., 2008; Soares-Filho et al., 2010). The ARB contributes to 60% of tropical rainforests in the world, to global biodiversity, to nutrition cycling, and plays a vital role in sustaining climate and ecosystem services (Arvor et al., 2017; William F. Laurance et al., 2002; Jose Antonio Marengo et al., 2012). The climate of the ARB varies from a wet northwest with almost no dry season to a dry southeast with a long dry season. Dependence of the hydro-ecological systems in the ARB on plentiful rainfall and the range of climatology across the Amazon highlights the importance of investigating the impacts of LULC change on terrestrial hydrological cycle in the ARB (Cook et al., 2012; Espinoza et al., 2015, 2016; Espinoza Villar et al., 2009; Nepstad et al., 2008).

The system services in the ARB are altered due to climate variability and human disturbances with dominant form of deforestation as a result of replacing forests with pasture and agriculture, especially across the “Arc of Deforestation” in the southern subbasins which is the primary cause of LULC change (Marcos Heil Costa & Pires, 2010b; Davidson et al., 2012; Mercedes & Montenegro, 2005; Moore et al., 2007; Tropek et al., 2014). In addition, the

growing human population, industrial logging, mining, expanding transportation networks, and human-caused fires are identified as other drivers of LULC change (Bagley et al., 2014; Butt et al., 2011; Marcos Heil Costa & Pires, 2010b; William F. Laurance et al., 2002). In the past three decades, LULC changes occurred across the ARB, however, Madeira, Tapajos, Xingu, and Tocantins are the four sub-basins of the Amazon with big pockets of LULC change (ESA-CCI; <http://maps.elie.ucl.ac.be/CCI/>, last access: 24 June 2020). Significant LULC change happened around 1995, 1999 and 2004. These changes in LULC, in conjunction with ongoing climate change, have impacted the terrestrial water cycle in recent decades (Sterling et al., 2013). Previous interannual and interdecadal studies on hydrological alteration in the ARB showed an overall long-term increasing trend in terrestrial water storage (TWS), however, the southern and southeastern sub-basins are experiencing significant decreasing trends in TWS, and LULC is known as the primary component contributing to the trend (Chaudhari et al., 2019).

The effects of deforestation on terrestrial hydrological cycle are well discussed in previous studies, however, to the best of our knowledge large-scale, interdecadal assessment of the impacts of LULC change are rare due to numerous shortcomings in data and physics-based models, and no quantitative implication for sustainability has been proposed so far. Most previous studies have focused on the changes in annual streamflow instead of flow regime across the basin. Deforestation (afforestation) increases (decreases) annual streamflow but there is no linear relationship between the deforested (afforested) coverage and the relative annual streamflow change. Numerous studies over different watersheds have attempted to provide a comprehensive representation of the terrestrial water cycle and to quantify the response of the system to the changes in key hydrological variables including land use at different temporal scales. Yet, there are many outstanding issues regarding LULC change impacts which include:

(1) terrestrial water cycle feedbacks to LULC changes in large river basins; (2) spatial patterns of LULC change within the basin and the resulting impacts on hydrological processes; and (3) the thresholds/tipping points of LULC change for sustainable practices in large basins. These highlight the need for a deeper understanding of the key underlying processes contributing to the system equilibrium in case of LULC change which is especially important in moving toward more sustainable solutions. Investigating tipping points for ARB are useful since they give a rough estimation in lack of comprehensive simulations of the system which includes water cycle, ecology, and human interventions components.

This study aims to examine the changes in basin water and energy balances under large-scale LULC changes and the resulting shifts in system threshold toward a new equilibrium. In this study, we present the hydrological changes in hydrological variables using a multi-scale assessment of the ARB based on the results of validated high resolution (~2km) simulations using LEAF-Hydro-Flood model and under static and dynamic LULC scenarios by keeping the other parameters of the model constant. Our study is driven by the following overarching research question: What are the impacts of LULC changes on key hydrological variables at the interannual and interdecadal scales, and how did the hydrological regime change in the ARB?

3.2 Methods

3.2.1 Model Description

The hydrology model utilized in this study, referred to as LHF (Miguez-Macho and Fan, 2012a, 2012b; Pielke et al., 1992; Pokhrel et al., 2014, 2013; Walko et al., 2000) is described in detail by Miguez-Macho and Fan (2012a). LHF is a comprehensive process-based hydrology model capable of simulating coupled surface and subsurface hydrological processes at the continental-scale. It was developed in two stages, building upon the Land-Ecosystem-

Atmosphere Feedback (LEAF), which serves as the land-surface component of the Regional Atmosphere Modeling System (RAMS) (Walko et al., 2000). The original LEAF model's physics are thoroughly described in Walko et al. (2000), encompassing turbulent and radiative exchanges between the atmosphere and multiple layers of soil, snow, water, and thermal energy, as well as surface storage, vegetation canopy, and canopy air. LHF inherits these features from LEAF (Miguez-Macho and Fan, 2012a, 2012b). Notably, the parameterizations for simulating evapotranspiration (ET) in LHF are similar to those employed in cutting-edge land surface models, such as Lawrence et al. (2019); further details can be found in Walko et al. (2000). Nevertheless, LEAF's parameterizations, which include the representation of sub-grid hydrologic heterogeneity, lateral movement of soil water based on TOPMODEL (Beven & Kirkby, 1979), and groundwater flow processes, have been replaced or significantly enhanced with new schemes. These advancements have undergone rigorous testing, particularly over the ARB, as described in the subsequent sections.

During the initial phase of LHF development over North America (Miguez-Macho et al., 2007, 2007), LEAF-Hydro was derived from LEAF by incorporating a prognostic groundwater module. This addition allowed for several important features: (1) the dynamic rise and fall of the water table or expansion and contraction of the vadose zone, (2) the equilibrium adjustment of the recharged water table following rainfall through discharge into rivers within a grid cell and the convergence and divergence of lateral flow among neighboring cells, (3) the representation of both gaining and losing streams through the two-way exchange between surface water and groundwater, (4) the routing of river flow to the ocean using the kinematic wave method, and (5) the inclusion of sea level as a boundary condition for coastal drainage. Subsequently, during the second stage focused on the ARB (Miguez-Macho and Fan, 2012a, 2012b), LHF underwent

further improvement by incorporating a river-floodplain routing scheme. This enhancement allowed for a more realistic estimation of streamflow by solving the complete momentum equations of open channel flow, while considering important factors such as backwater effects and the inertia of deep flow, which are particularly significant in the ARB (Bates et al., 2010; Miguez-Macho and Fan, 2012a, 2012b; Yamazaki et al., 2011). The inclusion of flood dynamics also facilitated an explicit simulation of interactions between floodwater and groundwater, a dominant process in the ARB. Initial studies using LHF over the ARB extensively evaluated various hydrologic variables across the basin (Miguez-Macho and Fan, 2012a, 2012b). Subsequently, the model has been employed in numerous studies that further evaluated its performance using observational and satellite-based data for different hydrologic fluxes and storage variables, as well as different atmospheric forcing datasets, demonstrating its robustness in simulating hydrological processes over the ARB (Brown et al., 2022; Chaudhari et al., 2021, 2019; Chaudhari and Pokhrel, 2022; Miguez-Macho and Fan, 2012a, 2012b; Pokhrel et al., 2014, 2013).

3.2.2 Atmospheric Forcing

In this study, the LHF model is forced by ERA5 reanalysis data (Hersbach et al., 2020) covering the period from 1950 to the present, with a spatial resolution of 0.25 degrees and hourly time steps. The availability of data for an extended period and the finer spatial resolution were the primary reasons for selecting ERA5 over WATCH Forcing Data methodology applied to ERA-Interim (WFDEI) as LHF was successfully validated in previous studies using WFDEI (not available beyond 2019) reanalysis over the ARB (Chaudhari et al., 2019). In addition, Staal et al. (2020) utilized ERA5 over the ARB for hydrological and atmospheric moisture tracking simulations, demonstrating that ERA5 outperformed ERA-Interim in estimating wind fields and

rainfall, particularly in tropical regions (Staal et al., 2020). Eight variables from the ERA5 dataset are utilized in this study: precipitation, surface pressure, downward surface solar (shortwave) radiation, downward surface thermal (longwave) radiation, air temperature, dewpoint temperature, u- and v-components of wind speed. Specific humidity is calculated based on dewpoint temperature and surface pressure. The 3-hourly data at the coarser resolution mentioned above are spatially interpolated within LHF to match the model's grid resolution (~2km) using bilinear interpolation (Chaudhari et al., 2021; Miguez-Macho & Fan, 2012, 2012; Pokhrel et al., 2013, 2014).

3.2.3 Land Use/Land Cover and Leaf Area Index

The annual LULC maps are derived from the Amazonia MapBiomes multi-disciplinary network; the original data are reclassified and aggregated to match the land use categories used in LHF, following a previous study (Chaudhari et al., 2019; Souza Jr et al., 2020). Specifically, the 24 classes and sub-classes from the MapBiomas land cover maps are reclassified into the 30 classes of LHF (Table 2-1). The datasets comprise an annual time series land cover maps with 30-meter pixel resolution for the 1985 to 2021 period. The baseline maps in the MapBiomas dataset are generated by applying random forest to Landsat archive using Google Earth Engine to map five major classes: forest, non-forest natural formation, farming, non-vegetated areas, and water (Souza Jr et al., 2020). Due to the absence of data in the MapBiomas dataset prior to the year 1985, a method to generate time series products for the period between 1981 and 1984 is employed. First, to establish a baseline, we utilized the trend in leaf area index (LAI) and the MapBiomas LULC map for the year 1985. Then, through a pixel-by-pixel analysis, pixels with a mean annual LAI greater than 5 are identified and classified into the forest canopy. For all other pixels, the previous year's LULC type are retained. The selection of a threshold LAI value of 5

for facilitating the transition to forest cover was based on LAI classifications found in relevant literature (Asner et al., 2003; Myneni et al., 2007; Xu et al., 2018). The reverse prediction of LULC changes was limited to the forest canopy alone, as it is challenging to predict the LULC type based on LAI values below 5. Furthermore, given that forest cover is the predominant land cover in the Amazon region, it is reasonable to assume that a majority of the LULC changes in the basin are transitions from forest cover. The LHF model updates LULC on an annual basis to account for year-to-year LULC changes; in the ARB, these annual changes are largely caused by cattle ranching and agriculture. The lookup table for leaf area index (LAI) is derived by overlaying the LULC maps over the LAI maps from Moderate Resolution Imaging Spectroradiometer (MODIS) for the period of 2000 to 2020 and using a pixel-by-pixel analysis and the monthly values (Table 2-2) are calculated from the longterm 4-day mode of LAI for each LHF land cover class.

3.2.4 Simulation Setup

The LHF model is configured to cover the entire ARB spanning approximately 7.1 million km², including the Tocantins River basin (Figure 2-1). Simulations are carried out for the period of 1979-2020, using a spatial resolution of 1 arcminute (~2km) and a time step of 4 minutes, consistent with previous studies (Chaudhari et al., 2019; Miguez-Macho & Fan, 2012; Pokhrel et al., 2013, 2014), and the output is stored at daily intervals. While a finer spatial scale is desirable to capture hillslope processes in the first-order stream valleys, the computational expenses, and the coarse resolution of input data (e.g., soil characteristics) justify the use of a 1 arcminute resolution as an optimal choice. The simulations do not consider reservoirs; however, prior investigations indicate that the impact of reservoirs in the downstream regions of the ARB is negligible at the current state (Chaudhari & Pokhrel, 2022). Given that this study's objective is

to isolate the influence of climate variability from the effects of LULC changes at the basin and subbasin scales, the inclusion of reservoirs would not significantly affect the findings. To ensure stable initial WTD, the model is spun up for ~400 years, initializing with the equilibrium water table from 1979 (Fan et al., 2013). The results are subsequently analyzed for the period spanning 1980 to 2020 (41 years). Furthermore, since the model comprehensively simulates land surface, hydrologic, and groundwater processes based on physical principles, no calibration was conducted (Chaudhari et al., 2019). In order to address the research questions, two scenarios are established: static (representing the impacts of climate variability) and dynamic (incorporating the impacts of both climate variability and LULC changes). The sole distinction between the two scenarios is that in the static scenario, LAI and LULC are frozen throughout the entire period, resembling the conditions of the year 1981. All other inputs and parameters are identical between the two sets of simulations. The originality of the LHF model framework, coupled with the integration of dynamic human influences through LULC changes and climate change effects through atmospheric forcing, establishes a cutting-edge framework for assessing the interdecadal impacts of LULC changes on the terrestrial water cycle.

3.3 Results and Discussion

3.3.1 Validation

Key hydrological variables including river discharge, ET, and terrestrial water storage (as a proxy for groundwater) are validated in detail in section 2.3.1.

3.3.2 Impacts on Groundwater

Substantial variation in WTD across the ARB, with differences ranging from east to west (Figure 3-1), serves diverse vital roles and functions. Over the past four decades, the water table in the ARB has undergone changes influenced by both climate variability and anthropogenic

impacts, primarily in forms of land use/land cover (LULC) change. Generally, the water table has become deeper across the basin, but certain areas have seen shallower water tables due to various factors. Notably, the Andes, certain regions of Madeira, Tapajos, and Xingu subbasins, as well as selected areas in the northern and northeastern parts of the basin, have experienced shallower water tables (panel H in Figure 3-1). The dynamics of precipitation patterns are the primary drivers of fluctuations in WTD, while topography and surface radiation contribute to modifying this pattern (Figures 3-1, 3-2, 3-3, and 3-4). The research findings from this and previous studies suggest that the frequent droughts experienced in the past two decades in the ARB (Figure 3-3), coupled with the geographical distribution of deforested regions in the south and southeastern areas, have yet to substantially disrupt primary moisture transport processes in the basin, explaining the dominance of climate variability's impact on WTD dynamics over LULC change despite the substantial extent of deforestation (Staal et al., 2018, 2020; Delphine Clara Zemp et al., 2017). The development of croplands in the southern and southeastern regions of the basin has led to a shallower water table in these regions. This can be attributed to the reduction of ET (Figure 3-1P and Figure 3-2), as well as reduced root water extraction compared to the undisturbed area.

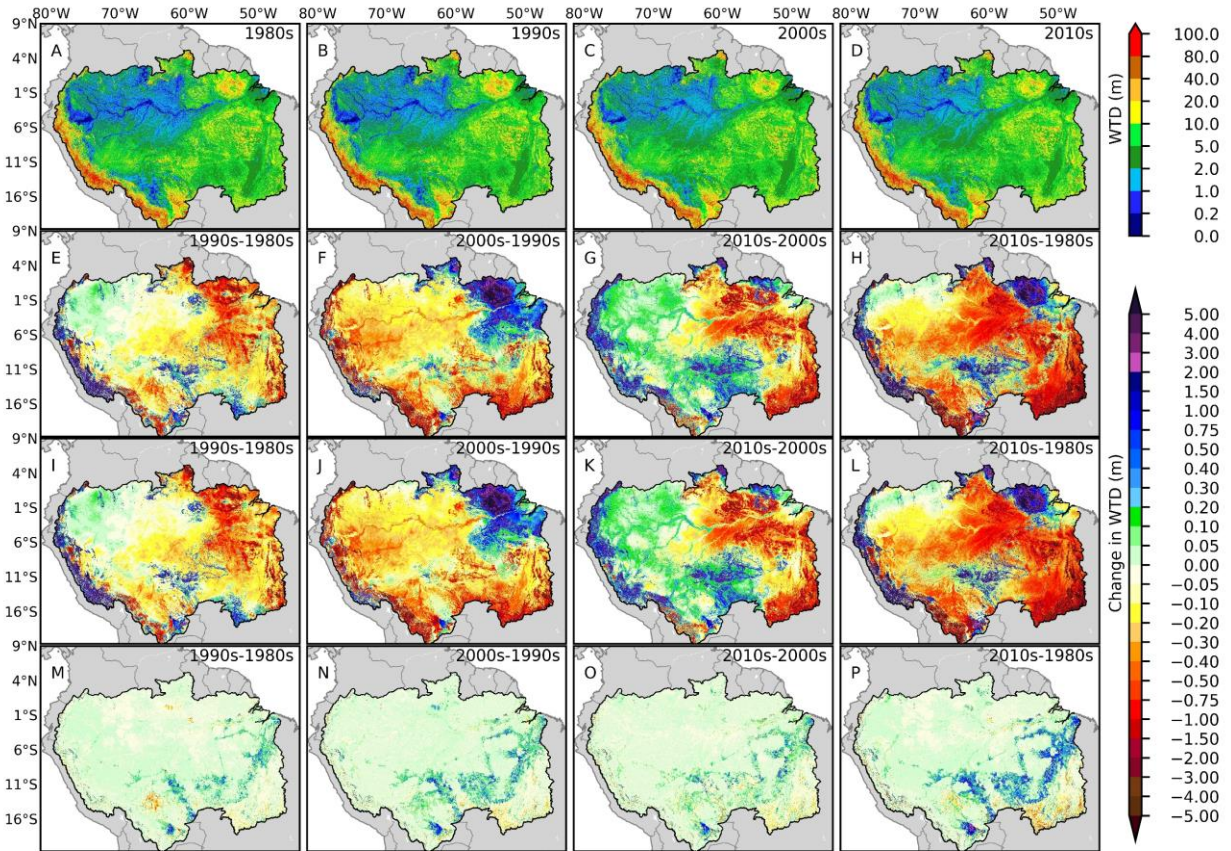


Figure 3-1. Decadal mean of the spatial distribution of WTD in the past four decades (A-D), the decadal changes in WTD due to climate variability and anthropogenic intervention in the 1990s (1991 to 2000) from the 1980s (1981 to 1990), in 2000s (2001 to 2010) from 1990s, in 2010s (2011 to 2020) from 2000s and in 2010s from 1980s (E-H), the decadal changes in WTD due to climate variability in the 1990s from the 1980s, in 2000s from 1990s, in 2010s from 2000s and in 2010s from 1980s (I-L) and the decadal changes in WTD due to deforestation in the 1990s from the 1980s, in 2000s from 1990s, in 2010s from 2000s and in 2010s from 1980s (M-P).

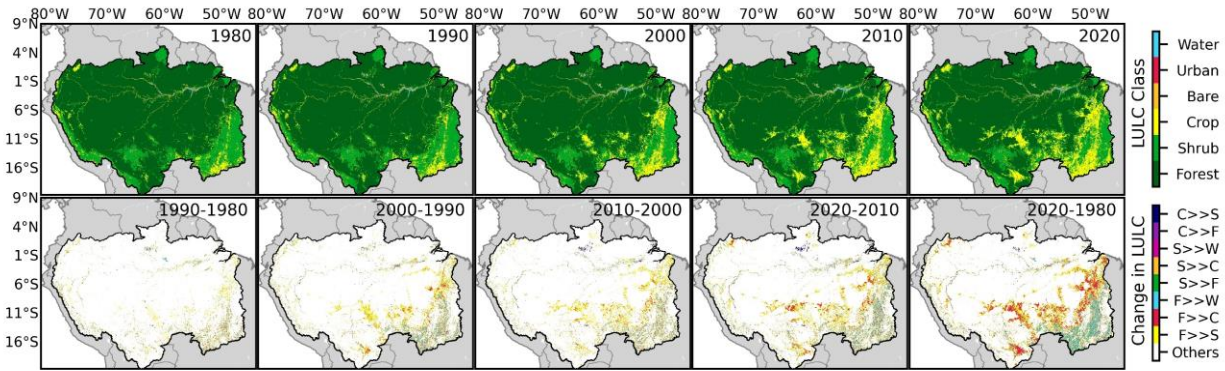


Figure 3-2. Land use and land cover (LULC) maps for 1985, 1990, 2000, 2010 and 2020 (top panels; Santoro et al., 2017), and the changes in LULC in the 1980s (1985 to 1990), 1990s (1991 to 2000), 2000s (2001 to 2010), and 2010s (2011 to 2020) (bottom panels). The lower colorbar shows the initial and final LULC type, where F stands for forest, S stands for Shrubland, C stands for Cropland and W stands for Water.

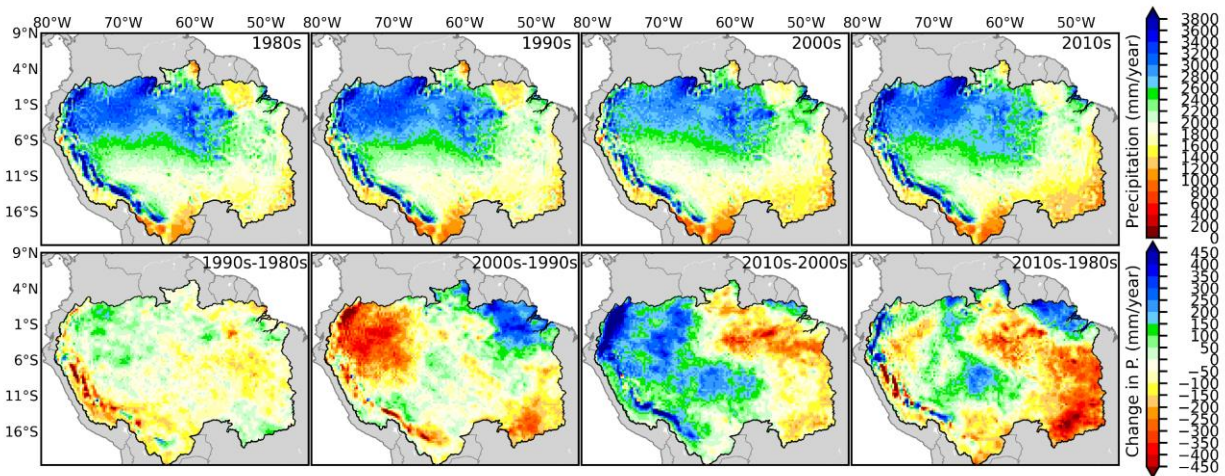


Figure 3-3. The decadal mean of the spatial distribution of precipitation in the past four decades is shown in the top panels (Hersbach et al., 2020). The absolute changes in decadal mean precipitation in the 1990s (1991 to 2000) from the 1980s (1981 to 1990), in the 2000s (2001 to 2010) from 1990s, in 2010s (2011 to 2020) from 2000s and in 2010s from 1990s are shown in bottom panels.

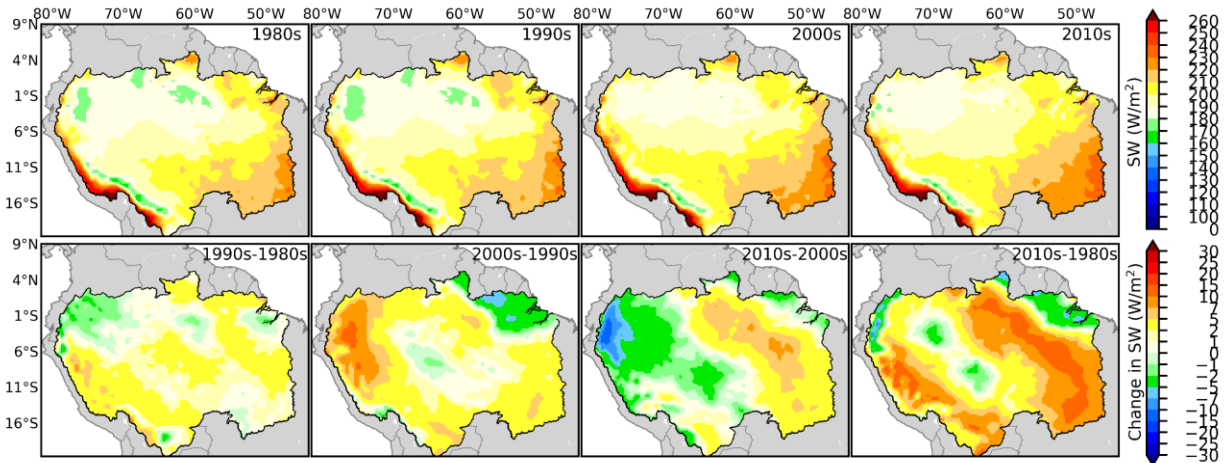


Figure 3-4. The decadal mean of the spatial distribution of short-wave radiation in the past four decades is shown in the top panels (Hersbach et al., 2020). The absolute changes in decadal mean short-wave radiation in the 1990s (1991 to 2000) from the 1980s (1981 to 1990), in the 2000s (2001 to 2010) from 1990s, in 2010s (2011 to 2020) from 2000s and in 2010s from 1990s are shown in bottom panels.

The analysis of WTD spatial maps spanning the past four decades in the ARB (panels A to D in Figure 3-1) reveals five distinct structures across the basin. Firstly, ~4.5% of the ARB is characterized by waterlogged areas with a very shallow water table ($WTD < 0.25\text{m}$), providing crucial support for the biodiversity found in waterlogged wetlands (Duponchelle et al., 2021). These waterlogged wetlands are typically located along the main river channels across the Amazon River and are particularly prevalent in the Solimoes, Japura, Negro, and Madeira subbasins, covering approximately 12%, 7%, 6%, and 4% of the area of these subbasins, respectively. At the basin scale, over the past three decades, waterlogged wetlands have experienced a shrinkage of ~33% due to climate variability, however, they have expanded by ~0.6% due to LULC changes, indicating the dominant role of climate variability in the dynamics of waterlogged regions across the ARB. The majority of the shrinkage in waterlogged areas occurred during the 2000s, accounting for ~39% of the total reduction. Nonetheless, they have experienced a recovery of ~13% during the 2010s, attributed to an increase in precipitation rates

in that decade (Figure 3-3). At the subbasin scale, the Madeira, Negro, Solimoes, and Japura subbasins experienced approximately 35%, 33%, 31%, and 12% shrinkage in waterlogged areas, respectively.

Furthermore, a shallow ($WTD < 2m$) and a transitional water table ($2m < WTD < 5m$) encompasses ~35 % and ~27% of the ARB, respectively. These regions play a critical role in regulating the seasonal dynamics of surface water across floodplains. They facilitate a two-way exchange process, transitioning from a sink during the wet season to a source during the dry season (Miguez-Macho and Fan, 2012). This exchange process effectively mediates interactions between floodwater and groundwater, sustaining the growth and survival of trees during the dry season. The main distinction between the shallow and transitional regions lies in the highly seasonal nature of the WTD in the transitional region. The region characterized by $WTD < 2m$ is primarily located in the northern areas of the ARB, particularly in the central and western parts of the basin, as well as in certain floodplains of the Madeira subbasin. It approximately covers 59%, 57%, 50%, 42%, 33%, 20%, 16%, and 14% of the Japura, Negro, Solimoes, Purus, Madeira, Tapajos, Xingu, and Tocantins subbasins, respectively. The analysis of this fraction of groundwater reveals a dominant control of climate variability, resulting in a ~20% reduction due to climate variability and ~2% growth due to LULC changes. Unlike the region characterized by $WTD < 0.25m$, the shrinkage in the $WTD < 2m$ region occurred more gradually over the past three decades, with reductions of approximately 7%, 9%, and 2% in the 1990s, 2000s, and 2010s, respectively. At the subbasin scale, approximately 1%, 7%, 4%, 27%, 25%, 35%, 67%, and 51% shrinkage occurred in the Japura, Negro, Solimoes, Purus, Madeira, Tapajos, Xingu, and Tocantins subbasins, respectively.

The transitional region emerges with $2\text{m} < \text{WTD} < 5\text{m}$, extending southward from the region with $\text{WTD} < 2\text{m}$ and reaching the northern boundary of Madeira. Groundwater at this level over the floodplains is only accessible to plants with deep roots and since this region receives less precipitation in comparison to the region with $\text{WTD} < 2\text{m}$, it is highly seasonal as it supports the forest and savanna water demand during the longer dry season. This transitional region approximately covers 42%, 33%, 32%, 32%, 28%, 24%, 23%, and 19% of the Tocantins, Tapajos, Xingu, Purus, Japura, Negro, Madeira, and Solimoes subbasins, respectively. Over the past three decades $\sim 18\%$ and $\sim 0.8\%$ growth happened at this area fraction of groundwater due to climate variability and LULC change, respectively. These findings further emphasize the dominant influence of climate variability in modulating the dynamics of WTD. The major growth in this transitional region occurred during the 2000s, a period marked by multiple droughts that affected the ARB. At the subbasin scale, a combination of shrinkage and growth in this transitional region is observed. Specifically, approximately 15% and 7% shrinkage occurred in the Tocantins and Xingu subbasins, respectively. Conversely, the Purus, Negro, Solimoes, Madeira, Tapajos, and Japura subbasins experienced growth of approximately 38%, 37%, 29%, 31%, 8%, and 5%, respectively.

On the other hand, the presence of a deep-water table ($\text{WTD} > 5\text{m}$) in the headwater catchments of the ARB emerges as the primary factor contributing to streamflow in these upstream areas (Miguez-Macho and Fan, 2012). Regions with $5\text{m} < \text{WTD} < 20\text{m}$ are commonly distributed in the southern and southeastern parts of the basin. Previous studies have suggested that active water withdrawal by forest roots in the ARB can reach depths below 10m (Bruno et al., 2006), therefore, the impacts on $5\text{m} < \text{WTD} < 10\text{m}$ separately assessed.

The region with $5\text{m} < \text{WTD} < 10\text{m}$ covers ~17% of the ARB and is primarily distributed on the eastern side of the basin, along with a region on the western side (Figure 3-1). At the basin scale, this area fraction of groundwater has grown by ~36% due to climate variability and has experienced a shrinkage of ~3% due to LULC changes. The most substantial increase occurred during the 1990s and 2000s, and this extent was sustained during the 2010s. This region approximately covers 26%, 26%, 21%, 17%, 16%, 10%, 9%, and 8% of the Tapajos, Xingu, Tocantins, Purus, Madeira, Solimoes, Negro, and Japura subbasins, respectively.

At this level of groundwater, the impact of LULC changes on the dynamics of WTD increases significantly, even surpassing 20% in the Tapajos and Xingu subbasins. However, in subbasins where the region with $5\text{m} < \text{WTD} < 10\text{m}$ covers less than 10% of their area, climate variability remains the dominant factor in governing the dynamics of this area fraction of groundwater. This area fraction has experienced growth throughout the entire ARB over the past three decades, with an increase of approximately 65%, 53%, 45%, 37%, 31%, 26%, 9%, and 8% in the Purus, Madeira, Negro, Xingu, Tapajos, Solimoes, Japura, and Tocantins subbasins, respectively.

The region with water table depths ranging from 10m to 20m is commonly found on the west and northwest of the ARB, covering ~11% of the basin. This region responded differently under the impact of climate variability, experiencing a growth of ~15%, and under LULC changes, undergoing a shrinkage of ~2% over the past three decades. The majority of the growth in this area fraction occurred during the 1990s, after which it slowed down. At the subbasin scale, this region approximately covers 17%, 17%, 16%, 12%, 8%, 5%, 4%, and 2% of the Tocantins, Xingu, Tapajos, Madeira, Purus, Negro, Solimoes, and Japura subbasins, respectively. Similar to the previous cases, the region with $10\text{m} < \text{WTD} < 20\text{m}$ has grown under the impact of

climate variability, while it has shrunk under LULC changes. Climate variability dominates in some subbasins more than others, and the impact of LULC exceeds 20% in the Tapajos and Xingu subbasins. Over the past three decades, this region has experienced growth of approximately 24%, 16%, 13%, 15%, 9%, and 5% in the Tocantins, Solimoes, Xingu, Madeira, Tapajos, and Negro subbasins, respectively. However, in the Japura subbasin, there has been a shrinkage of approximately 4% in the area fraction of groundwater.

Lastly, a distinct region with WTD values exceeding 20m is prevalent beneath the Andes and in high-elevation areas in the northeast and eastern sections of the basin, covering ~6% of the ARB. Under the impact of climate variability, this region has grown by ~6%, but it has experienced a shrinkage of ~3% due to LULC changes, indicating that LULC changes contributed to more than 30% of the variability in this area fraction. At the subbasin scale, this region approximately covers 9%, 8%, 5%, 4%, 3%, 2%, and 0.1% of the Tocantins, Xingu, Negro, Tapajos, Madeira, Japura, and Purus subbasins, respectively. Despite the impact of LULC changes, climate variability still dominates the variability of WTD at this level. It has grown by approximately 93%, 14%, and 2% in the Tocantins, Xingu, and Solimoes subbasins, respectively, under the influence of climate variability. However, it has experienced shrinkage of approximately 105%, 23%, 12%, 79%, and 4% in the Purus, Tapajos, Japura, Negro, and Madeira subbasins, respectively, due to the impact of climate variability.

3.3.3 Impacts on Evapotranspiration

Examining the decadal mean of ET during the 1980s (Figure 3-5) and considering this period as one with minimal human impacts, certain patterns in the spatial distribution of ET over the ARB can be inferred. ET is observed to be more homogeneously distributed within the basin's boundaries, with some areas exhibiting lower ET values attributed to limitations in surface

radiation (e.g., Andes) or limited water availability (e.g., Tocantins subbasin). Additionally, certain regions within the ARB display higher ET values compared to the uniform average due to sparse vegetation cover (e.g., Madeira subbasin) or the presence of vast floodplains (e.g., river mouth region). However, over the past three decades (1990s, 2000s, and 2010s), the spatial distribution of ET has undergone a noticeable shift from a relatively homogenous pattern to a distribution that is more pronounced in the central regions of the ARB (Figure 3-5). The findings suggest that the primary driver for this shift is a significant increase (decrease) in transpiration resulting from climate variability (LULC change). Analyzing the data for the past three decades reveals three distinct major regions within the ARB, each characterized by different ET characteristics. The central region of the ARB, known for its high rainfall (Figure 3-3) and dense forest cover (Figure 3-2), exhibits the highest rates of ET among the identified regions. In contrast, the northwestern region of the ARB displays relatively lower ET values compared to the central region, primarily due to reduced surface radiation (Figure 3-4) despite receiving greater precipitation than the central region (Figure 3-3). The southeastern region of the ARB stands out with substantially lower ET rates compared to the other regions, which can be attributed to the combined effects of deforestation and a lower rate of precipitation in this specific area (Figures 3-5, 3-2, and 3-3).

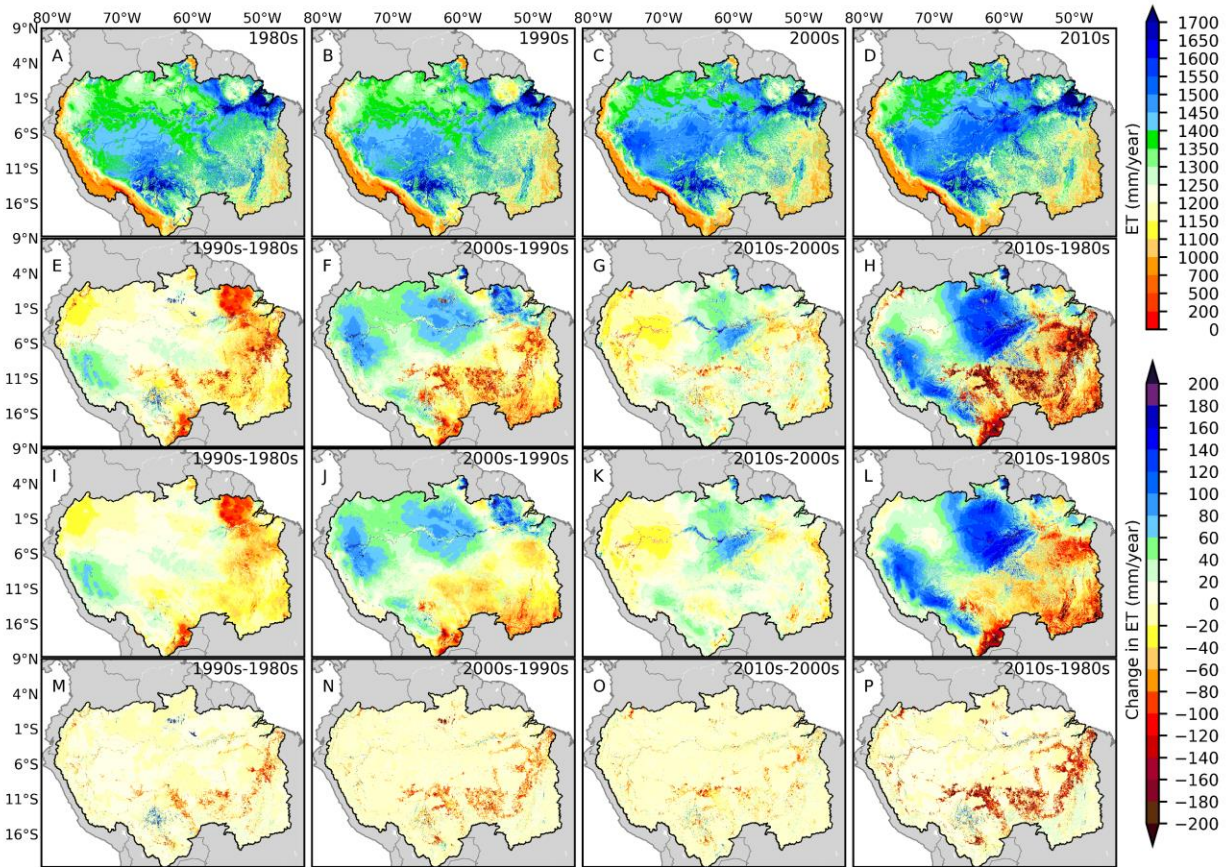


Figure 3-5. Decadal mean of the spatial distribution of ET in the past four decades (A-D), the decadal changes in ET due to climate variability and anthropogenic intervention in the 1990s (1991 to 2000) from the 1980s (1981 to 1990), in 2000s (2001 to 2010) from 1990s, in 2010s (2011 to 2020) from 2000s and in 2010s from 1980s (E-H), the decadal changes in ET due to climate variability in the 1990s from the 1980s, in 2000s from 1990s, in 2010s from 2000s and in 2010s from 1980s (I-L) and the decadal changes in ET due to deforestation in the 1990s from the 1980s, in 2000s from 1990s, in 2010s from 2000s and in 2010s from 1980s (M-P).

It is important to note that ET in this study encompasses three primary components: transpiration, canopy interception loss, and ground evaporation. The analysis of the past four decades reveals two distinct spatial patterns in the changes of ET over the ARB, influenced by the combined impact of climate variability and deforestation (Panels E to H in Figure 3-5). Firstly, in the central, northern, and a broad region along the Andes (energy limited regions), ET has increased during the specified period due to the dominant influence of climate variability,

manifested as climatological drought characterized by reduced precipitation and enhanced surface radiation (Figures 3-5, 3-3, and 3-4). The results indicate that the transpiration component of ET serves as the main driver behind the observed increase (~80% of the increase) in these regions. Additionally, the decline in WTD suggests that, in the absence of sufficient precipitation, groundwater contribution to ET has increased. This groundwater utilization compensates not only for the decrease in precipitation but also responds to the augmented water demand resulting from increased surface radiation. Furthermore, the ground evaporation component of ET contributed ~20% to the overall increase in ET within this region. Conversely, in the northwestern corner of the ARB, ET has experienced a decrease primarily due to deforestation, which has resulted in a significant reduction in transpiration, along with the expansion of croplands.

Secondly, in the southern and southeastern regions of the ARB, a decrease in ET has been observed, which can be attributed to the combined influence of deforestation (~80% of the reduction) and climate variability (~20% of the reduction). It is noteworthy that the levels of precipitation and surface radiation in these regions have not undergone significant changes during the analyzed period, highlighting the amplifying role of climate factors in the impact of deforestation on the water cycle within these specific areas (Figure 3-3 and 3-2). In the deforested areas, there has been an increase of ~40% in the contribution of ground evaporation to the overall ET. However, this increase is offset by a ~28% decrease in the contribution of transpiration and a ~43% decrease in canopy interception loss, resulting in an overall ~13% decrease in ET over the southern croplands. This highlights the substantial influence of deforestation on the reduction in ET in these regions, with climate variability further amplifying the overall impact.

The investigation of the impacts of climate variability and LULC change on basin average ET reveals that ET has increased by ~1% during the past three decades. Climate variability contributed to this increase by ~2%, while LULC change led to a decrease of ~1% in ET. This indicates that LULC change accounted for ~32% of the overall ET alteration during the past three decades. At the subbasin scale, ET in the northern and western subbasins increased, while in the southern and eastern subbasins, it decreased. In Negro, Solimoes, Purus, and Japura subbasins, ET approximately increased by 6%, 4%, 4%, and 2%, respectively, primarily due to an increase in surface radiation. However, in Tocantins, Xingu, and Tapajos subbasins, ET decreased by approximately 6%, 5%, and 3%, respectively, primarily due to deforestation and the reduction in transpiration. ET in Madeira remained relatively unchanged. These findings emphasize the complex interplay between climate variability and LULC change in shaping ET patterns across different subbasins within the ARB.

Transpiration emerges as the major component of ET in the ARB, both at the basin and subbasin scales. The contribution of canopy interception loss and ground evaporation depends on the ratio of open canopy in the basin or subbasin, a higher open canopy ratio results in a higher contribution of ground evaporation. At the basin scale, climate variability is responsible for 74% of the alteration in transpiration, with LULC change accounting for 26% of the change. Similarly, for canopy interception loss, climate variability contributes to approximately 63% of the alteration, while LULC change contributes to 37%. However, ground evaporation is more heavily influenced by LULC change, accounting for approximately 78% of the alteration, with climate variability contributing to only 22%. At the subbasin scale, the impact of climate variability and LULC change on transpiration varies across different subbasins. For instance, climate variability has a profound impact on transpiration in the Negro subbasin, leading to an

increase of ~12%, while LULC change has a minimal impact with a decrease of only 0.1%. On the other hand, in the Purus subbasin, both climate variability and LULC change result in a decrease in transpiration, with climate variability leading to a reduction by 2% and LULC change contributing to a decrease by 11%. Similarly, for canopy interception loss, climate variability and LULC change have led to alterations in different directions across subbasins. Climate variability has decreased canopy interception loss in all subbasins, with reductions ranging from 2% to 14%. On the other hand, LULC change has led to both decreases and increases in canopy interception loss, with reductions ranging from 0.5% to 13% and increases ranging from 2% to 10% across different subbasins. The alteration in the ground evaporation component of ET is mainly dominated by LULC change, unless there have been substantial variations in precipitation. LULC change has led to increases in ground evaporation in some subbasins, ranging from 2% to 11%, while climate variability has resulted in decreases ranging from 0.1% to 8%. These findings highlight the complex and region-specific interplay between climate variability and LULC change in shaping the components of ET in the ARB and its subbasins.

3.3.4 Impacts on Runoff

The ARB displays two distinct regions characterized by high and low runoff, primarily driven by precipitation pattern (Figure 3-6 and 3-3). The high runoff regions encompass the central, northern, western, and southwestern parts of the basin. In these areas, runoff dynamics are primarily governed by precipitation, as in these regions, the water table is generally within 2m from the surface. Analysis of climate variability over the past four decades reveals a complex interplay of increased and decreased runoff in these regions. However, the majority of these areas have experienced a declining or relatively stable runoff. Conversely, the low runoff regions

comprise the northeastern, eastern, southern, southeastern, and certain central and western sections of the basin. In most of these regions, runoff has increased due to deforestation and the expansion of croplands. Nevertheless, the effects of climatological drought in these areas counterbalance the runoff increase resulting from deforestation. As a result, these regions observe a decrease in runoff or exhibit negligible changes in overall runoff patterns.

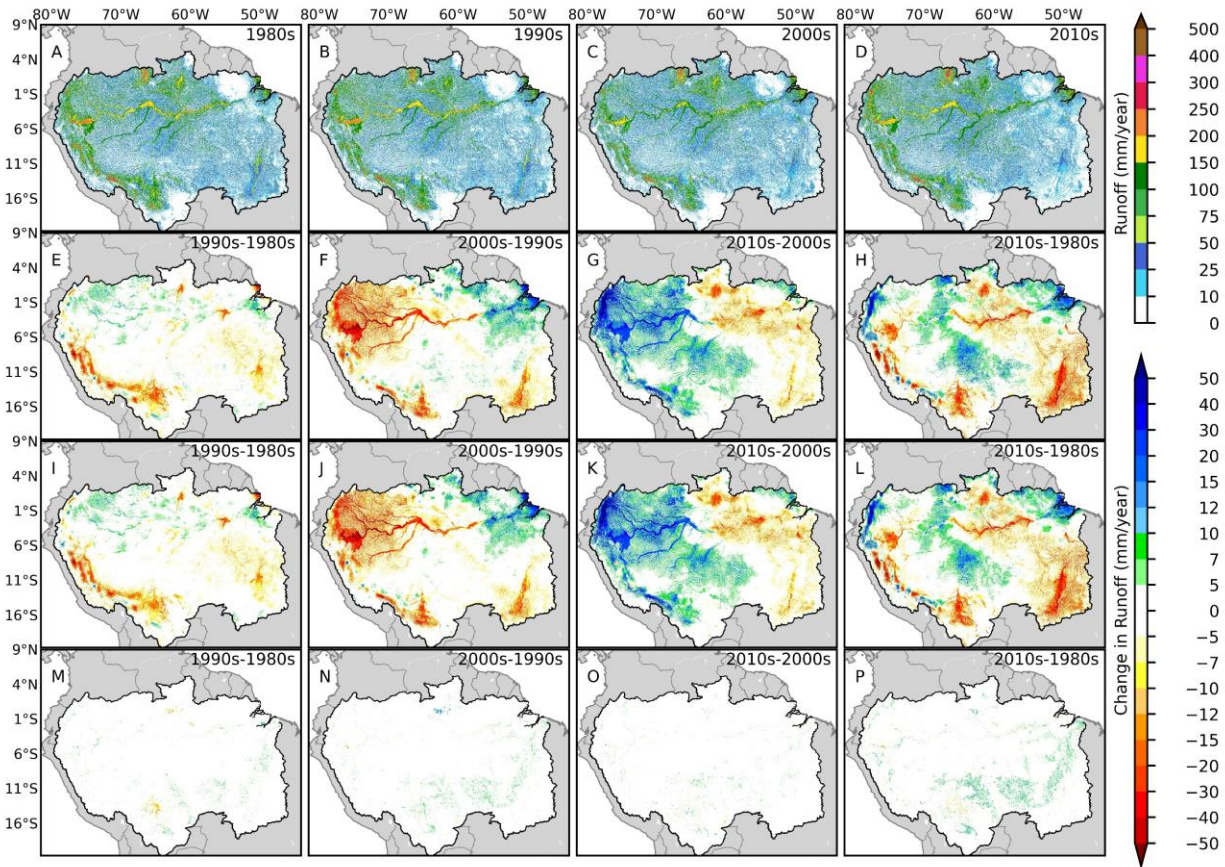


Figure 3-6. Decadal mean of the spatial distribution of runoff in the past four decades (A-D), the decadal changes in runoff due to climate variability and anthropogenic intervention in the 1990s (1991 to 2000) from the 1980s (1981 to 1990), in 2000s (2001 to 2010) from 1990s, in 2010s (2011 to 2020) from 2000s and in 2010s from 1980s (E- H), the decadal changes in runoff due to climate variability in the 1990s from the 1980s, in 2000s from 1990s, in 2010s from 2000s and in 2010s from 1980s (I-L) and the decadal changes in runoff due to deforestation in the 1990s from the 1980s, in 2000s from 1990s, in 2010s from 2000s and in 2010s from 1980s (M-P).

Over the past three decades, the runoff across the ARB has decreased by ~2%. The majority of this decrease occurred in the 1990s (~4% decrease) and 2000s (~8% decrease) due to

multiple major droughts during this period. In the 2010s, the runoff experienced an increase (~11% increase) due to a rise in precipitation, but it could not reach the runoff levels observed in the 1980s. Overall, climate variability contributed to ~75% of the runoff variability, while LULC change contributed to the remaining 25%. At the subbasin scale, the Solimoes subbasin did not experience substantial changes in runoff. On the other hand, the Tocantins, Xingu, and Madeira subbasins witnessed significant runoff decreases of approximately 48%, 18%, and 2%, respectively, with climate variability being the primary driver, accounting for approximately 96%, 82%, and 65% of the variability, mainly attributed to the reduction in precipitation. Conversely, the runoff in the Purus, Japura, Negro, and Tapajos subbasins increased by approximately 15%, 5%, 3%, and 1%, respectively. LULC change played a substantial role in these subbasins, contributing approximately 7%, 9%, 15%, and 58% of the runoff variability, respectively. Tapajos and Xingu subbasins stand out with the highest impact of LULC change, showing runoff increases of more than 5% over the past three decades. These results emphasize the combined influence of climate variability and LULC change in shaping the variability of runoff across different subbasins within the ARB.

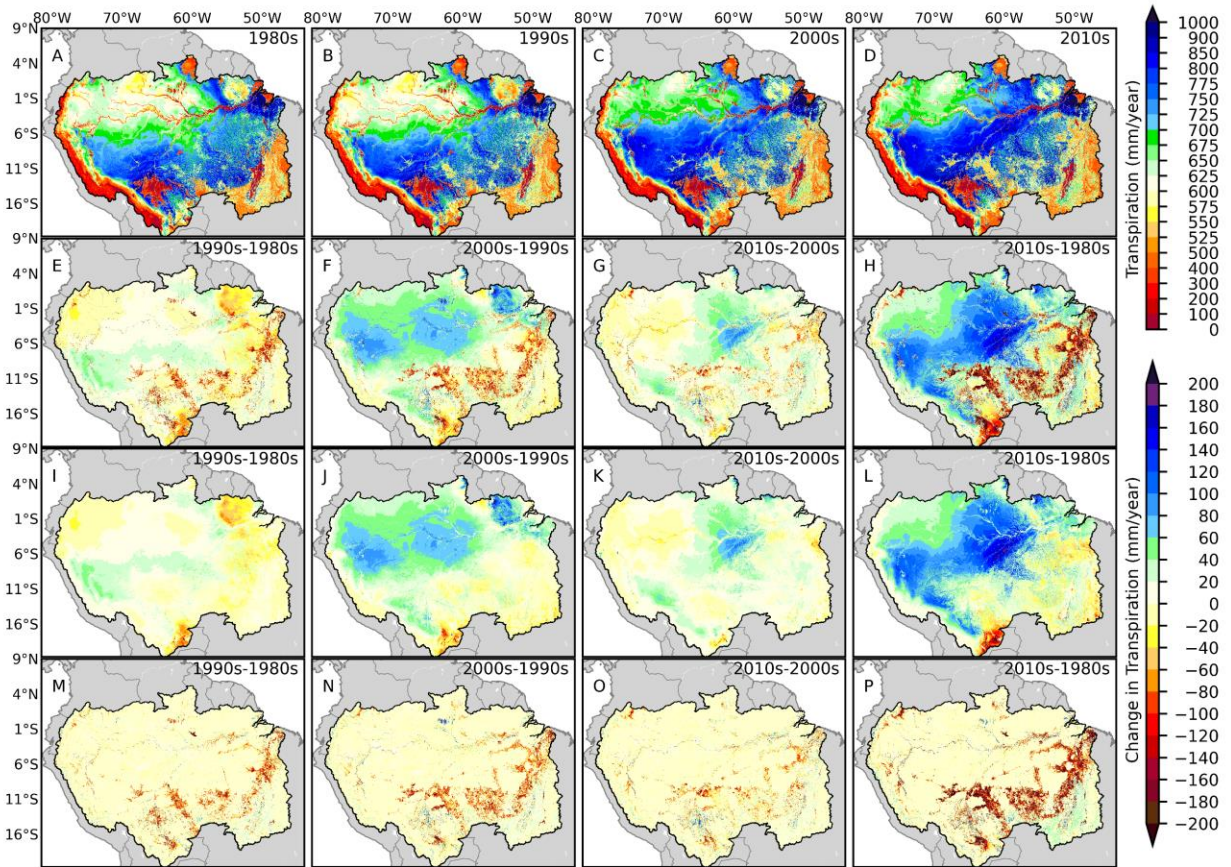


Figure 3-7. Decadal mean of the spatial distribution of transpiration in the past four decades (A to D panels), the decadal changes in transpiration due to climate variability and anthropogenic intervention in the 1990s (1991 to 2000) from the 1980s (1981 to 1990), in 2000s (2001 to 2010) from 1990s, in 2010s (2011 to 2020) from 2000s and in 2010s from 1980s (E to H panels), the decadal changes in transpiration due to climate variability in the 1990s from the 1980s, in 2000s from 1990s, in 2010s from 2000s and in 2010s from 1980s (I to L panels) and the decadal changes in transpiration due to deforestation in the 1990s from the 1980s, in 2000s from 1990s, in 2010s from 2000s and in 2010s from 1980s (M to P panels).

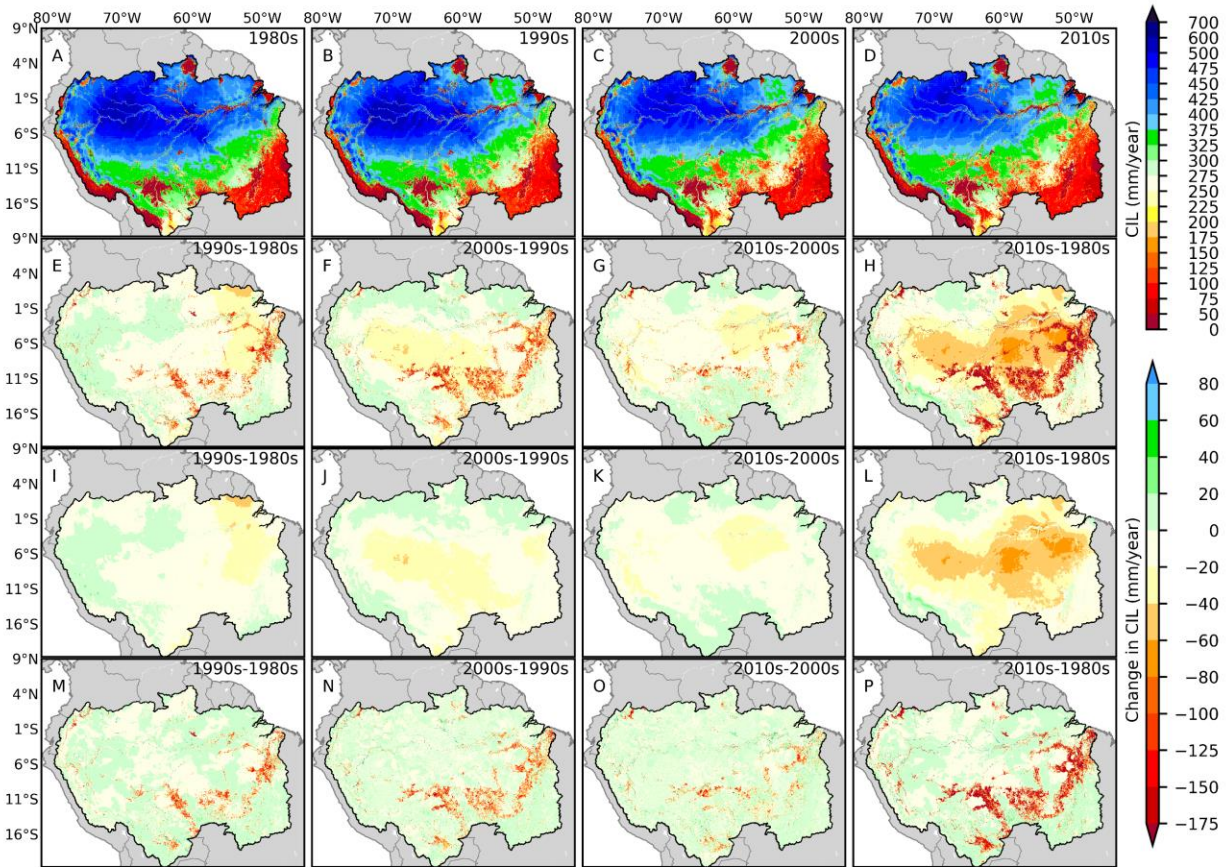


Figure 3-8. Decadal mean of the spatial distribution of canopy interception loss (CIL) in the past four decades (A to D panels), the decadal changes in CIL due to climate variability and anthropogenic intervention in the 1990s (1991 to 2000) from the 1980s (1981 to 1990), in 2000s (2001 to 2010) from 1990s, in 2010s (2011 to 2020) from 2000s and in 2010s from 1980s (E to H panels), the decadal changes in CIL due to climate variability in the 1990s from the 1980s, in 2000s from 1990s, in 2010s from 2000s and in 2010s from 1980s (I to L panels) and the decadal changes in CIL due to deforestation in the 1990s from the 1980s, in 2000s from 1990s, in 2010s from 2000s and in 2010s from 1980s (M to P panels).

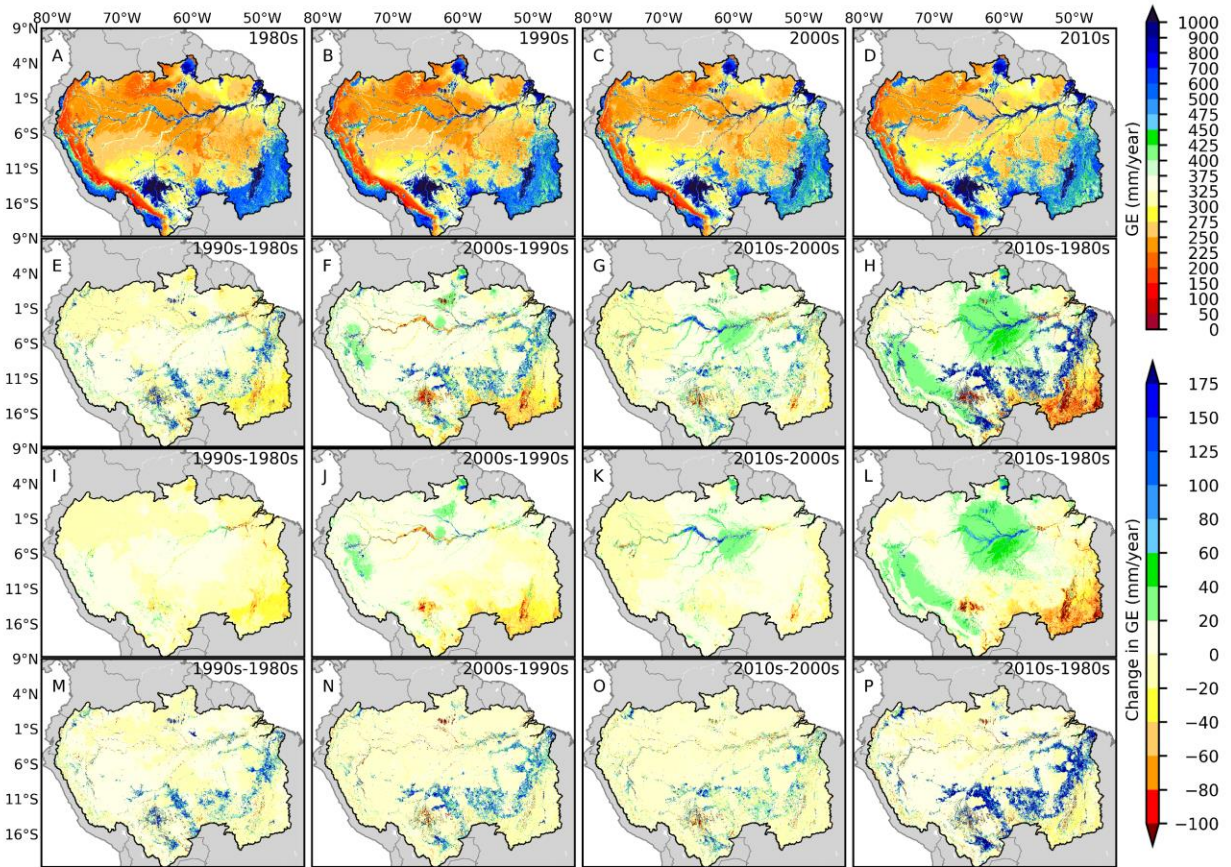


Figure 3-9. Decadal mean of the spatial distribution of ground evaporation (GE) in the past four decades (A to D panels), the decadal changes in GE due to climate variability and anthropogenic intervention in the 1990s (1991 to 2000) from the 1980s (1981 to 1990), in 2000s (2001 to 2010) from 1990s, in 2010s (2011 to 2020) from 2000s and in 2010s from 1980s (E to H panels), the decadal changes in GE due to climate variability in the 1990s from the 1980s, in 2000s from 1990s, in 2010s from 2000s and in 2010s from 1980s (I to L panels) and the decadal changes in GE due to deforestation in the 1990s from the 1980s, in 2000s from 1990s, in 2010s from 2000s and in 2010s from 1980s (M to P panels).

3.4 Conclusions

In conclusion, the analysis of WTD dynamics and its influencing factors across the ARB over the past four decades has revealed substantial variations and their intricate interplay. The basin exhibits diverse vital roles and functions dictated by WTD dynamics, showcasing differences from east to west. Climate variability and anthropogenic impacts, particularly in the form of LULC change, have been significant drivers of these variations. The observed deepening

of the water table across the basin, albeit with certain areas showing shallower water tables, underscores the complexity of the interplay between precipitation, topography, radiation, and human activities. Notable areas with shallower water tables include parts of the Andes and specific southern subbasins, emphasizing the spatial heterogeneity of WTD dynamics. Despite extensive deforestation, climate variability remains the dominant influence on WTD dynamics, especially in the face of frequent droughts in the past two decades.

Spatial distribution of WTD across different regions of the ARB highlighted five distinct structures: waterlogged areas, shallow water tables, transitional zones, deeper water tables, and extremely deep water tables. Each structure plays a crucial role in regulating the hydrological and ecological processes within the basin. Waterlogged areas, particularly along main river channels, have experienced significant changes, with a reduction due to climate variability and a slight expansion attributed to LULC changes. Shallow and transitional water table regions are vital for floodplain dynamics, facilitating critical interactions between floodwater and groundwater, influencing tree growth and survival. The region with deeper water tables significantly contributes to streamflow in the upstream areas.

The impact of climate variability and LULC changes on ET components varied across the basin. Transpiration emerged as a dominant component of ET, and its alteration was primarily driven by climate variability, emphasizing its sensitivity to precipitation and radiation changes. The impacts of LULC changes were more pronounced in ground evaporation, highlighting the complex relationships between LULC alterations and water cycle dynamics. Runoff patterns were intricately tied to precipitation and water table dynamics, demonstrating regional variations influenced by both climate variability and LULC changes. Climate variability had a notable

impact on runoff, particularly during drought periods, while LULC changes exhibited substantial influence in some subbasins, either amplifying or counterbalancing the runoff alterations.

In summary, the ARB showcases a complex and multifaceted relationship between WTD dynamics, climate variability, and anthropogenic influences. Understanding these dynamics is crucial for effective water resource management and sustainable environmental practices in this ecologically significant region. Further research and monitoring are essential to comprehensively unravel the intricate mechanisms driving WTD variations and their implications on the basin's hydrological and ecological systems.

Chapter 4 Tipping Points Associated with Water Table Depth in the Amazon River Basin

Based on: Bagheri, O., and Pokhrel, Y. (202x). Tipping points associated with water table depth in the Amazon River basin. [Under Preparation]

4.1 Introduction

Tipping points (unstable equilibrium states) are defined as phenomena that, beyond a certain threshold, runaway change propels a system to a new state (van Nes et al., 2016; Scheffer et al., 2001). For example, due to deforestation and replacement of forest with pasture ET decreases and water table becomes shallower owing to extra recharge. Then, groundwater causes a positive feedback mechanism (DeAngelis et al., 2012) in further decreasing ET and recharging groundwater and propelling the forest system to an alternative tree species system. Therefore, once a threshold is passed, the dynamics of the system can accelerate dramatically to cause a ‘runaway change’. Two fundamental different ways in which a system can move to another stable state: (i) a change in external conditions (disturbance; e.g., climate change) which in models are represented by parameters, or (ii) a change in the state of the system itself (perturbations; e.g., human activities) which in models is represented by state variables (van Nes et al., 2016). The first type of tipping points are detected by warning signals or resilience indicators because of the gradual erosion of the resilience of the previous state of the system (van Nes et al., 2016).

The ongoing changes in the ARB’s forest system may result in a loss of resilience and surpassing tipping points, triggering a persistent shift to an alternative state within the ecosystem. Over the past six decades, the temperature in the ARB has risen by 1-1.5°C (Nobre et al., 2016), approximately 18% of the forest area has been deforested (Mapbiomas_Amazonia, 2022), forest

degradation has reached 17% (Bullock et al., 2020; Matricardi et al., 2020), forest fires have significantly increased (Aragão et al., 2018), dry season lengths (measured as the number of consecutive days with less than 50mm rainfall) are three to four weeks longer compared to six decades ago (Fu et al., 2013), and dry season water storage deficit is on a divergent trend (Chaudhari et al., 2019). Some studies suggest that the escalating frequency of unprecedented droughts, such as those in 2005, 2010, 2015-16, and 2020, could be signaling the imminent arrival of a tipping point (Bagley et al., 2014; Lovejoy & Nobre, 2019; Walker, 2020). Consequently, there is an imperative need to curtail deforestation in the ARB, rehabilitate the lost forest in its southern and eastern regions, and provide science-based guidelines to inform forest management policies (Lovejoy and Nobre, 2019; Walker, 2020).

Five systemic tipping points are inferred over the ARB including four associated with climate and one associated with human-induced changes (Science Panel for the Amazon, 2021). These tipping points include (1) receiving annual precipitation below 1,000 mm/yr, as inferred from satellite observations of tree cover distributions (Hirota et al., 2011; Staver et al., 2011) or 1,500 mm/yr, as inferred from global climate models (Malhi et al., 2009), (2) a dry season lasting more than seven months, determined from satellite observations of tree cover distributions (Staver et al. 2011), (3) maximum cumulative water deficit values exceeding than 200 mm/yr (Malhi et al. 2009) or 350 mm/yr (Zelazowski et al., 2011) over the ARB lowlands, inferred from various analyses with global climate models, (4) a 2°C increase in the Earth's equilibrium temperature, identified through a coupled climate–vegetation model (Jones et al., 2009), and (5) 20-25% accumulated deforestation of the entire basin, determined through a combination of environmental changes (e.g., increased dry season length), climate projections aligned with the most pessimistic pathway of the Intergovernmental Panel on Climate Change (IPCC), and

human-induced degradation via deforestation (Lovejoy & Nobre, 2019; Carlos A. Nobre et al., 2016).

Tipping points (1) and (2) are determined through a space-for-time substitution method, replacing temporal information on changing conditions and their impacts with observational data on vegetation status across a precipitation gradient at a single snapshot in time (Science Panel for the Amazon, 2021). Tipping points (3) to (5) rely on coupled climate-vegetation models, and the accuracy of their outcomes hinges on a set of parameterizations that may inadequately capture soil-plant-atmosphere interactions (Science Panel for the Amazon, 2021). For instance, in a recent study, Chai et al. (2021) concluded that, even under the most pessimistic IPCC pathway, a basin-wide dieback in the ARB is unlikely to occur following bias correction of future projection models. Hence, further exploration, incorporating a blend of experimental and modeling studies, is essential to validate the thresholds for the aforementioned tipping points.

Existing evidence indicates that, depending on diverse combinations of stressing conditions, disturbances, and feedback mechanisms, the current forest configurations at the local scale, could be replaced by: (i) a seasonally dry, closed-canopy tropical forest with an increasing abundance of deciduous tree species (Dexter et al., 2018; Malhi et al., 2009); (ii) a tropical savanna state dominated by native grass and tree species (Cox et al. 2004; Jones et al. 2009; Hirota et al. 2011; Staver et al. 2011; Lovejoy and Nobre 2019); (iii) an open-canopy degraded state, dominated by invasive alien grasses and native fire-tolerant tree species (Barlow & Peres, 2008; Brando et al., 2012; Flores et al., 2016); and (iv) a closed-canopy secondary forest, dominated by native early successional tree and other plant species (Poorter et al., 2016; Rozendaal et al., 2019).

Given the emergence of novel feedback loops associated with invasive plants and human-modified landscapes, states (iii) and (iv) are more likely to manifest across extensive regions of the ARB, particularly along the "arc of deforestation". However, recent observations suggest that in remote ARB areas, distant from the agricultural frontier, the native savanna state may replace seasonally inundated forests disturbed by wildfires (Science Panel for the Amazon, 2021). Localized forest collapses have the potential to trigger cascading effects on rainfall recycling, intensifying dry seasons and wildfire occurrences. This, in turn, could result in substantial forest loss on a continental scale, particularly in the southwest of the basin. Ecological factors, such as differential tree growth, recruitment, and survival among Amazonian species, play a crucial role in promoting forest resistance to disturbances at local scales and facilitating recovery (Science Panel for the Amazon, 2021).

The likelihood of surpassing these tipping points hinges largely on system-wide heterogeneities, encompassing geological, physical, chemical, and cultural processes that influence connectivity and the probability of contagious disturbances. The probability of reaching such tipping points, specifically due to contagious forest dieback, is influenced by three key mechanisms: (a) environmental heterogeneity and connectivity across the ARB, including geological, physical, chemical, and cultural processes; (b) functional diversity and adaptive capacity of species in different forest types; and (c) the uncertain impact of enhanced CO₂ and nutrient limitations (Science Panel for the Amazon, 2021). The absence of ecological information for many ARB species, uncertainty regarding potential feedback mechanisms, and the need for improved climate change projections hinder the development of robust models for anticipating potential shifts in the ARB's forests. The primary concern is that, beyond these

potential tipping points, the system could enter a cycle of reduced rainfall, increased fire incidence, and forest mortality (Science Panel for the Amazon, 2021).

A recent study showed that groundwater dominates the seasonal dynamics of hydrological fluxes at the basin and subbasins scale, however, the prognostic groundwater components has been absent in the previous studies have been done on tipping points using hydrological models (Bagheri et al., 2024). Another study suggests that the double stress of waterlogging and drought is the primary driver of forest-savanna coexistence with alternating drought and waterlogging at the seasonal scale favoring savanna over forests (Mattos et al., 2023). In this study, we hypothesized that there are tipping points associated with the dynamics of water table depth in the ARB. The present study addresses the aforementioned research and knowledge gaps by answering the following science questions. (1) Are there tipping points associated with dynamics of seasonal water table depth in the ARB? (2) Where the tipping points associated with groundwater stands in comparison to the other inferred tipping points in the literature? (3) How resilient the hydrological system of the ARB is against its groundwater tipping points? In addressing these questions and hypotheses, we first identify the tipping points associated with groundwater seasonal dynamics by using the results from a basin-scale, fully process-based hydrological model, and a dataset of annual times series of tree cover percentage across the ARB. Then, we compare the derived tipping points in this study with the existing inferred tipping points in the literature. Finally, how resilient the ARB is against the groundwater tipping points.

4.2 Methods

The MOD44B Version 6.1 annual product derived from the Moderate Resolution Imaging Spectroradiometer (MODIS) Vegetation Continuous Fields (VCF) was utilized in this

study to determine surface tree coverage over the ARB (Figure 4-1). This data product provides global sub-pixel estimates of three primary land cover components: percent tree cover, percent non-tree vegetation, and percent non-vegetated, all at a spatial resolution of 250 meters since 2000. Moreover, the precipitation data from ERA5 reanalysis (Hersbach et al., 2020), accessible from 1940 to the present, with a spatial resolution of 0.25 degrees and hourly time intervals are integrated. The water table depth (WTD) time series were derived from the outcomes of the high-resolution simulation (~2km) utilizing a fully process-based hydrology model known as LEAF-Hydro-Flood, comprehensively described and validated in Section 2-2 of this dissertation. To ensure consistency among the datasets, WTD and precipitation data were downscaled to achieve a uniform resolution of 250 meters.

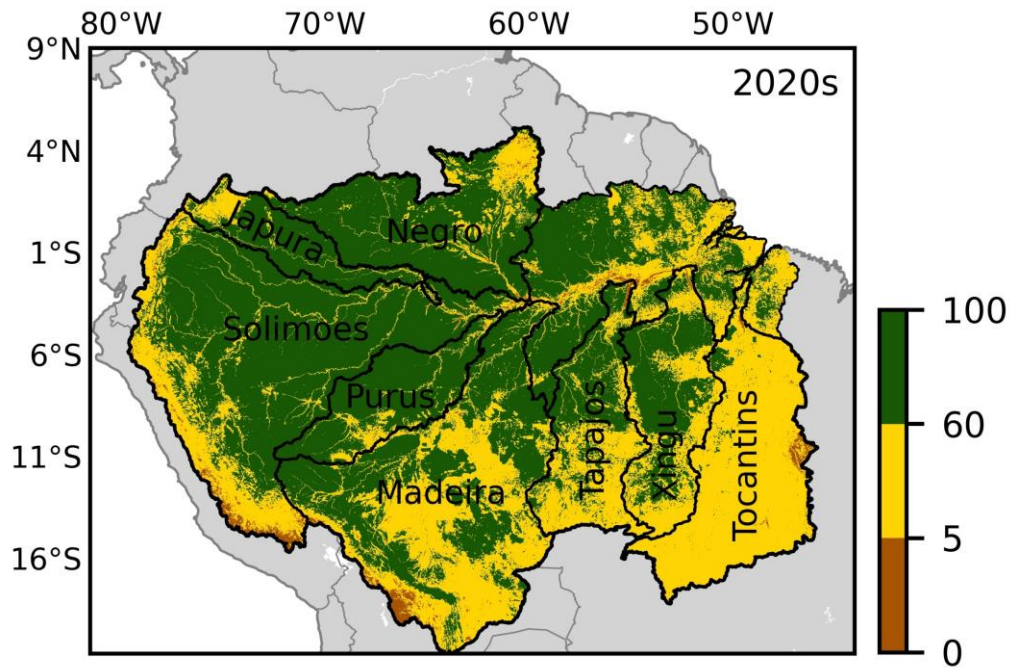


Figure 4-1. MODIS Vegetation Continuous Fields (VCF) data for 2020. Values are showing the tree coverage percentage.

4.3 Results and Discussion

Analyzing the long-term average precipitation and WTD across 5000 randomly sampled grid cells within the ARB reveals a noticeable direct correlation between the two variables (Figure 4-2). Previous studies (Hirota et al., 2011; Staver et al., 2011) have identified tipping points associated with varying levels of precipitation over global tropical forests. Therefore, this finding suggests the possibility of analogous tipping points linked to WTD dynamics. Further investigation into the relationship between WTD and tree cover confirms the presence of distinct patterns (Figure 4-2). When WTD is less than 20m, a wide range of tree cover is feasible across the ARB. However, as the water table deepens, intermediate values of tree coverage decrease, indicating that trees require deep roots or need to be situated in areas with a shorter dry season to survive at depths greater than 20m. To delve deeper into this interaction, we evaluate long-term basin-averaged precipitation rates and water table levels at both basin and sub-basin scales.

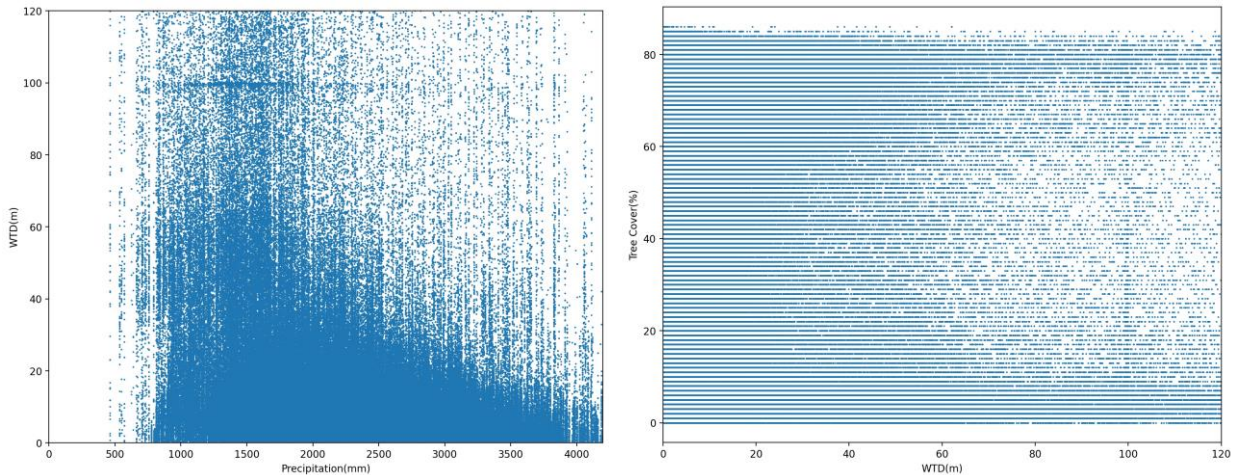


Figure 4-2. The random sample of the interplay of precipitation, WTD and tree coverage over the ARB.

The probability density function (Figure 4-3) representing different levels of precipitation over the ARB is bimodal, highlighting that forest cover (tree coverage > 60%) predominantly occurs in regions receiving an average of more than 1500mm of annual rainfall. Conversely,

savanna cover ($5\% < \text{tree coverage} < 60\%$) predominates in regions with annual rainfall less than 1500mm. In addition, the tree coverages between 20% to 60% are rare over the ARB, indicating existence of stable and unstable states in tree coverage. These results confirm the findings in the previous studies (Hirota et al., 2011; Staver et al., 2011).

The probability density function of precipitation at the subbasin scale shows that the behavior is generally consistent with that of the ARB, however, over some subbasins the distribution is not bimodal (e.g., Purus) or the savanna state happens at a higher tree cover percentage (e.g., Japura). Tocantins does not receive high rates of rainfall and it dominantly falls between 1200 to 2100 mm/year; as a result, only savanna state is present in the probability density function. Negro, Solimoes, Madeira, Tapajos, and Japura subbasins show similar behavior to the ARB, however, the cutoffs for savanna and forest states happen at different precipitation levels over these subbasins. For Negro and Solimoes the cutoff between the two stable states happens around 1800 mm/year, for Madeira and Tapajos it happens around 1200 mm/year, and finally for Japura it occurs around 900 mm/year. Therefore, Japura is the most resilient subbasin in terms of sustaining the forest state. The distribution over Xingu shows that precipitation rates between 1500 to 2400 mm/year result in higher tree coverage in comparison to 2400 to 3000 mm/year, which does not follow the other subbasins. Over Purus only forest state is represented in the distribution because this subbasins generally receives more than 1500 mm/year of precipitation.

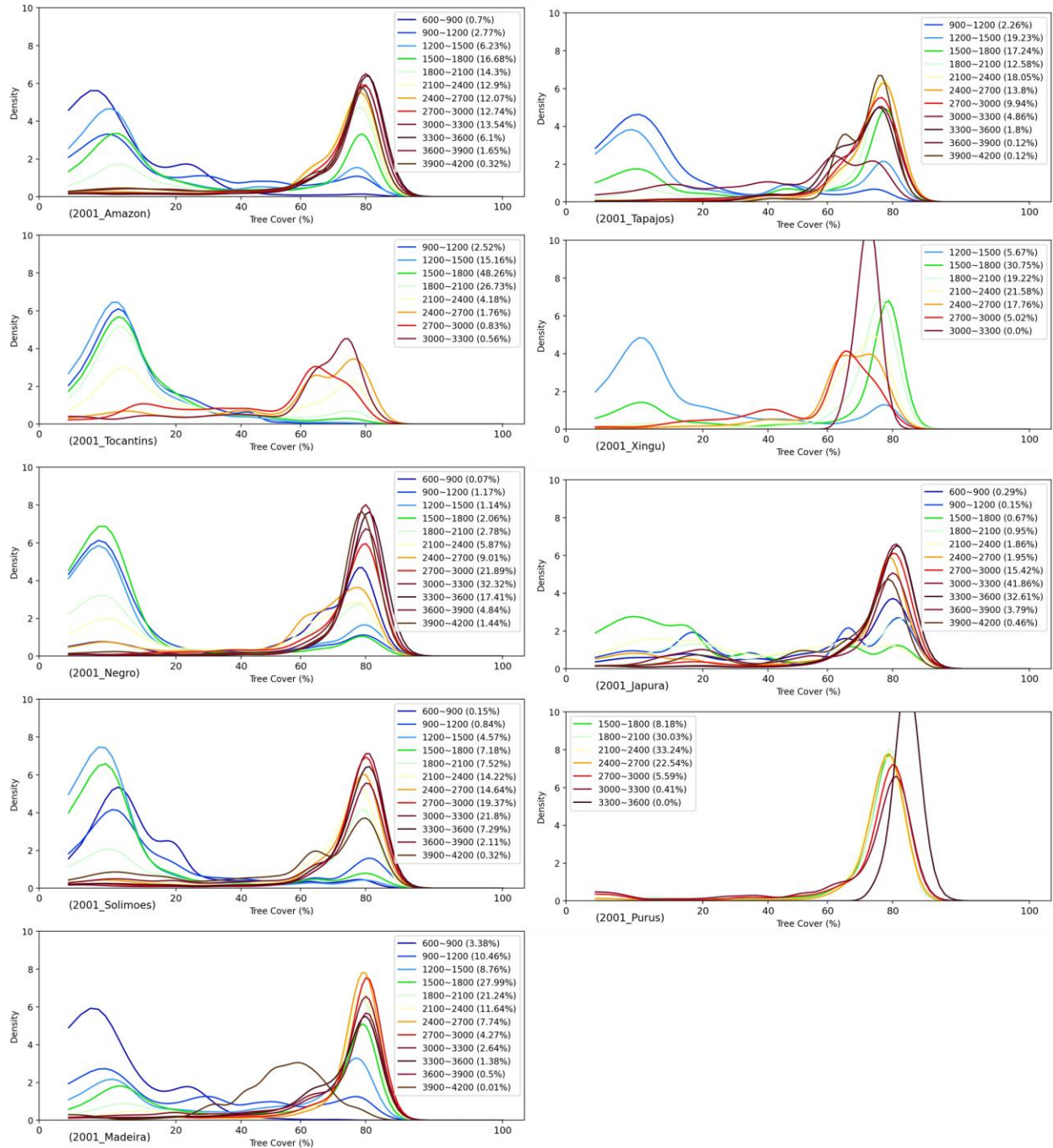


Figure 4-3. The probability density function constructed from 1000 samples of the arcsine transformed data described as the weighted sum for precipitation over the ARB and its subbasins.

Examining the probability density function of various water table levels reveals that forest cover predominantly occurs where WTD is less than 20m, while savanna cover is prevalent in regions with WTD deeper than 20m (Figure 4-4). The probability density function

of WTD at subbasin scale shows that the behavior is generally consistent with that of the ARB, however, Tocantins exhibits a contrasting behavior where conditions favoring forest cover occur in regions typically dominated by savanna. Similar to the probability density function of precipitation, Negro, Solimoes, Madeira, Tapajos, and Japura subbasins show similar behavior to that of the ARB, however, the cutoffs for savanna and forest states happen at different water table levels over these subbasins. The WTD over Negro, Tapajos, Xingu, and Japura subbasins is resilient against favoring savanna state as even at WTD deeper than 40m the distribution favors the forest state. Over Solimoes, $WTD < 20m$ favors the forest state and WTD around 40m defines the cut off level between forest and savanna state over Madeira. Conversely, over Madeira, $WTD > 1m$ are more suitable for forest state than $WTD < 1m$. The reason for this phenomenon needs further investigation. All water table levels over the Purus favor the forest state.

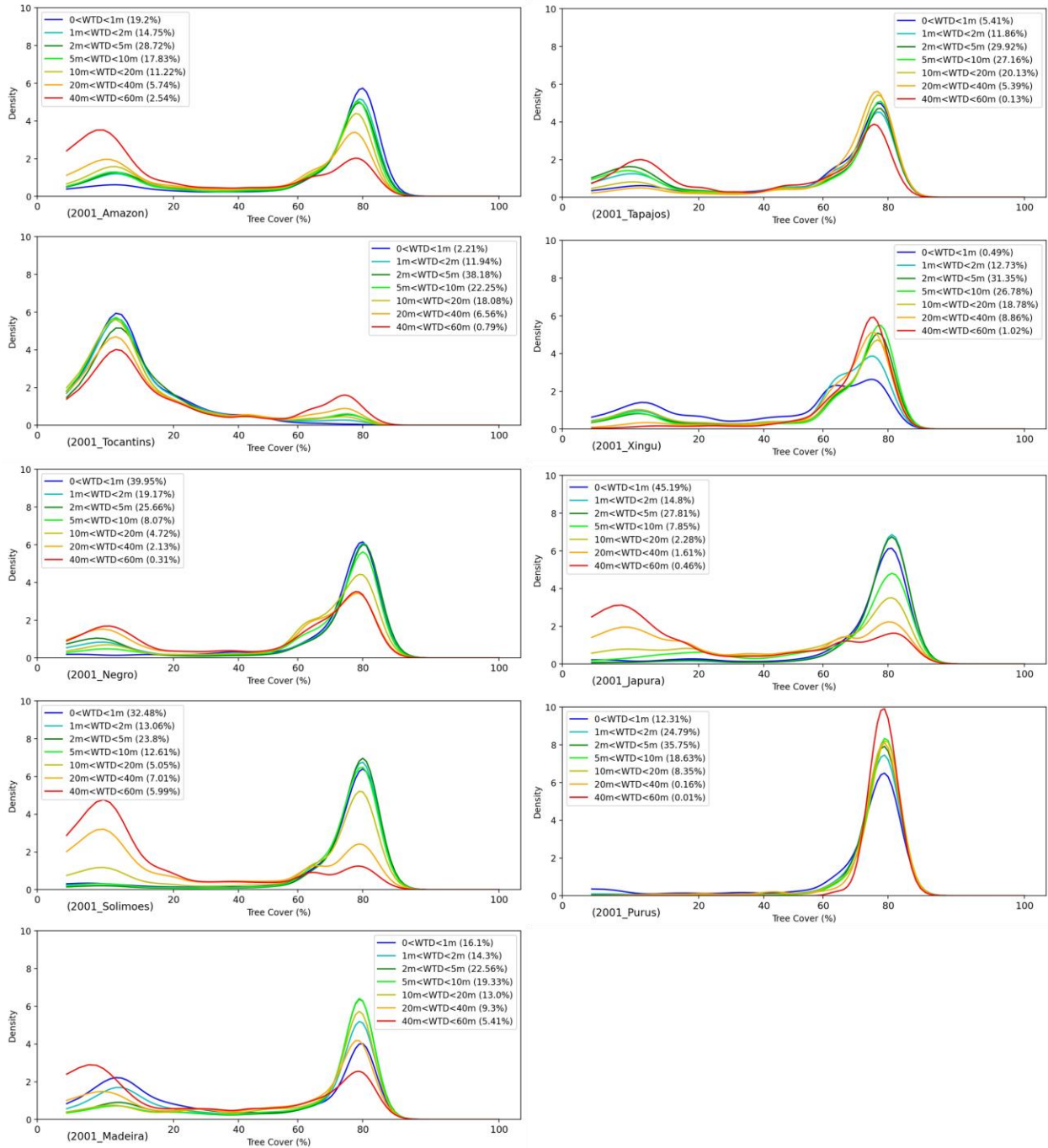


Figure 4-4. The probability density function constructed from 1000 samples of the arcsine transformed data described as the weighted sum for WTD over the ARB and its subbasins.

To investigate the contrasting behavior of the Tocantins subbasin in comparison to the other subbasins, a focused analysis was conducted on grid cells within two random boxes in Tocantins and the western region of the basin (Figure 4-5). Specifically, WTD trajectories were

examined for different tree cover percentages, along with an evaluation of the slope of the change in WTD against the changes in tree cover percentages. The findings revealed a direct relationship between WTD and tree cover change within the western region of the basin.

Conversely, over Tocantins, a reduction in tree cover did not substantially deepen the WTD. This behavior in Tocantins could potentially induce oxidative stress for the forest cover in regions with shallow WTDs, offering an explanation for the absence of forest cover in these areas.

However, further comprehensive assessments of additional components are necessary to validate and confirm this observed behavior.

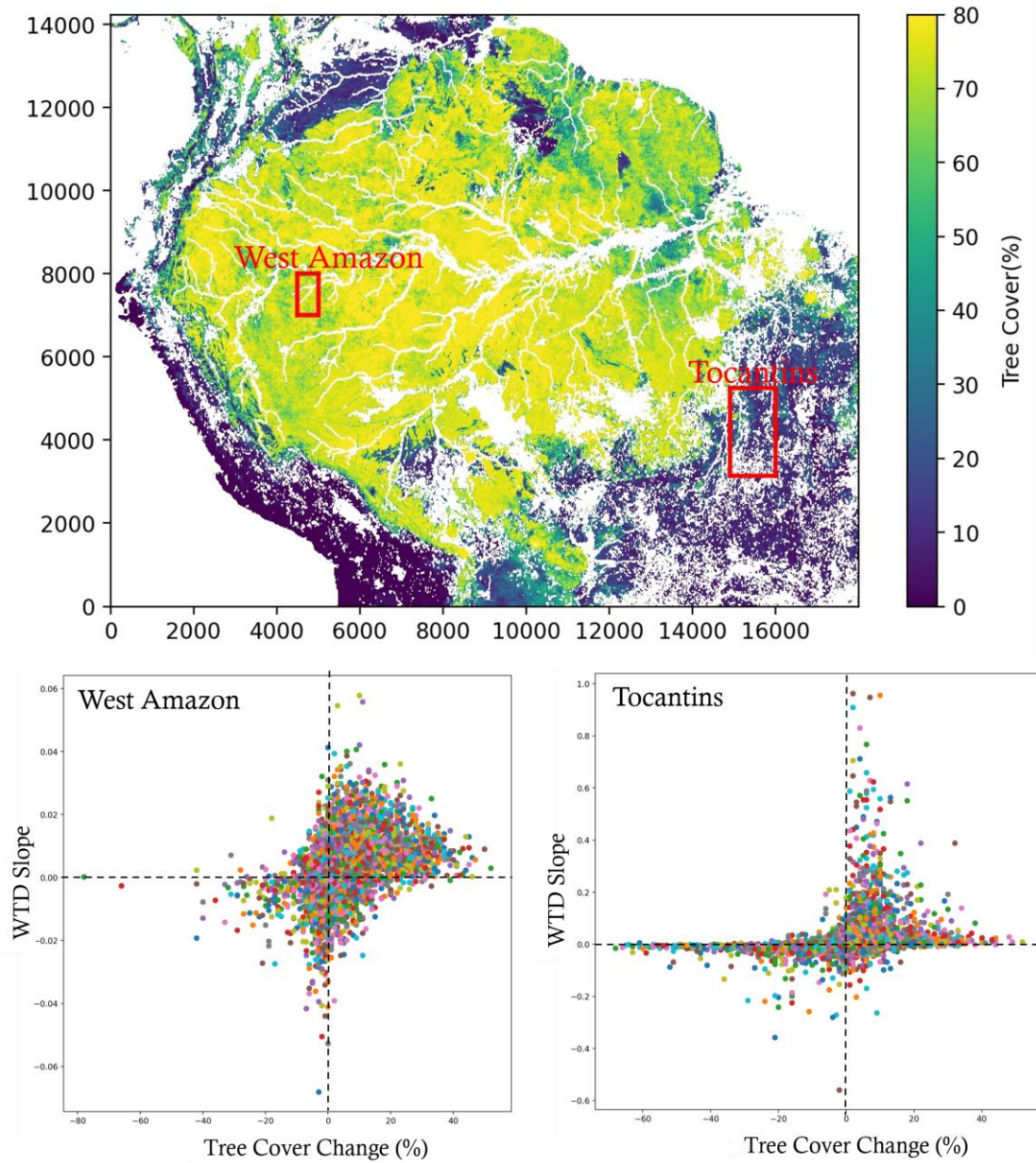


Figure 4-5. The interplay of WTD and tree coverage for two random regions in the forested regions (west Amazon box) and savanna regions (Tocantins box).

4.4 Conclusion

The comprehensive analysis of the ARB highlights a significant correlation between long-term average precipitation and WTD across randomly sampled grid cells. The study suggests the presence of potential tipping points linked to WTD dynamics, akin to those

associated with varying levels of precipitation over tropical forests globally. The relationship between WTD and tree cover demonstrates that as the water table deepens beyond 20 meters, intermediate values of tree coverage decrease, indicating specific requirements for tree survival in drier or deeper conditions.

Further investigation reveals a bimodal probability density function for precipitation, emphasizing that forest cover predominantly occurs in regions receiving over 1500mm of annual rainfall, while savanna cover prevails in drier regions. A reduction in areas conducive to forest coverage due to declining rainfall levels over the past two decades raises concerns. Similarly, the analysis of WTD levels indicates that forest cover is prominent where WTD is less than 5m, emphasizing the importance of shallow water table depths for forest ecosystems. However, a reduction in these favorable regions for forest cover is observed over the same period, suggesting potential discrepancies in existing tipping point assessments.

At a sub-basin scale, the Tocantins subbasin exhibits unique behavior, favoring savanna cover in regions where forest cover is typically expected. The focused analysis of this subbasin reveals a distinct relationship between WTD and tree cover change, offering insights into the potential challenges faced by the forest cover in regions with shallow water table depths. Further research and a more comprehensive assessment of various components are essential to validate and confirm this observed behavior and to better understand the dynamics and complexities of forest-savanna transitions in the ARB.

Chapter 5 Summary and Conclusion

The hydrology of the ARB has been extensively studied; however, critical gaps remain in understanding key processes governing hydrological dynamics and rainforest resilience, disentangling climate and LULC change impacts, and investigating tipping points associated with dominant hydrological processes. This inhibits the understanding of hydrological considerations needed for sustainable forest management under climatic change and growing human stressors.

In Chapter 2, using high resolution (~2km), long-term simulations from a process-based hydrological model (LEAF-Hydro-Flood) and an innovative groundwater area fraction analysis, the dominant hydrological processes across the ARB, their key roles in shaping basin functions, and the decadal evolution therein are investigated. Results indicated that shallow groundwater (<5m deep) strongly modulates the seasonality of the surface fluxes across the ARB. The results indicated that at least 34% of the Amazonian Forest is supported by groundwater during the dry season. A two-month lag between the seasonal peak of ET and river discharge is a key mechanism that potentially prevents the rainforest from tipping into savanna. The ARB is dominantly energy limited; however, the results suggest that in the absence of groundwater support, and with less than ~125 mm/month of precipitation, the ARB could have become water-limited, at least in some regions. The long-term basin-averaged ET—dominated by transpiration—changed with a split pattern of $\pm 9\%$ in the past three decades. Similarly, water table depth ($\pm 19\%$) and runoff ($\pm 29\%$) changed with a heterogenous patterns across the ARB. River discharge did not change substantially due to the crucial buffering role of groundwater. Terrestrial water storage (TWS) decreased (increased) in the 2000s (2010s) compared to that in the 1990s. Although groundwater is the dominant contributor to total TWS, the dynamics of

TWS over the major river channels are controlled by flood water, given relatively shallow groundwater. The chapter provides crucial insights on the dominant hydrological processes in the ARB to inform forest management practices.

In Chapter 3, state-of-the-art model LEAF-Hydro-Flood (LHF), together with developing static and dynamics land use scenarios are used to disentangle the impacts of climate and LULC change. The results showed that despite extensive deforestation, climate variability remains the dominant influence on WTD dynamics; however, the impacts on ET varied across the basin. Runoff patterns were intricately tied to precipitation and water table dynamics, demonstrating regional variations influenced by both climate variability and LULC changes. This chapter provides key insights on the separate role of climate variability and LULC change in the altered water cycle of the ARB over the past four decades.

In Chapter 4, using the simulated WTD from LHF, tree cover from MODIS VCF and precipitation from ERA5 dataset, potential tipping points associated with groundwater over the ARB are investigated. The area fraction analysis of WTD seasonality confirms the existence of tipping points. Further investigation reveals a bimodal probability density function for precipitation and WTD. Emphasizing that forest cover predominantly occurs in regions receiving over 1500mm of annual rainfall and/or where WTD is less than 5m. A reduction in areas conducive to forest coverage due to declining rainfall levels or deepening WTD over the past two decades raises concerns. The different amount of reduction based on rainfall and WTD suggests potential discrepancies in existing tipping point assessments. This chapter provides key insights on the resilience of the Amazonian Forest and highlights the importance of sustainable thresholds in forest management practices.

REFERENCES

- Abril, G., Martinez, J.-M., Artigas, L. F., Moreira-Turcq, P., Benedetti, M. F., Vidal, L., et al. (2014). Amazon River carbon dioxide outgassing fuelled by wetlands. *Nature*, *505*(7483), 395–398.
- Amaral-Zettler, L. A., Zettler, E. R., & Mincer, T. J. (2020). Ecology of the plastisphere. *Nature Reviews Microbiology*, *18*(3), 139–151.
- Anderson, A. B., & Ioris, E. M. (1992). Valuing the rain forest: economic strategies by small-scale forest extractivists in the Amazon estuary. *Human Ecology*, *20*, 337–369.
- Andrade-Filho, J. D., Scholte, R. G. C., Amaral, A. L. G., Shimabukuro, P. H. F., Carvalho, O. dos S., & Caldeira, R. L. (2017). Occurrence and probability maps of *Lutzomyia longipalpis* and *Lutzomyia cruzi* (Diptera: Psychodidae: Phlebotominae) in Brazil. *Journal of Medical Entomology*, *54*(5), 1430–1434.
- Aragão, L. C. E. O. (2012). The rainforest's rain pump. *Nature*, *489*(7415), 217–218.
- Aragão, L. E. O. C., Poulter, B., Barlow, J. B., Anderson, L. O., Malhi, Y., Saatchi, S., et al. (2014). Environmental change and the carbon balance of Amazonian forests. *Biological Reviews*, *89*(4), 913–931. <https://doi.org/10.1111/brv.12088>
- Aragão, L. E. O. C., Anderson, L. O., Fonseca, M. G., Rosan, T. M., Vedovato, L. B., Wagner, F. H., et al. (2018). decline of Amazon deforestation carbon emissions. *Nature Communications*, *9*(1), 1–12. Retrieved from <http://dx.doi.org/10.1038/s41467-017-02771-y>
- Armijos, E., Crave, A., Espinoza, J. C., Filizola, N., Espinoza-Villar, R., Fonseca, P., et al. (2020). Rainfall control on Amazon sediment flux: synthesis from 20 years of monitoring. *Environmental Research Communications*, *2*(5), 51008.
- Arvor, D., Funatsu, B. M., Michot, V., & Dubreui, V. (2017). Monitoring rainfall patterns in the southern amazon with PERSIANN-CDR data: Long-term characteristics and trends. *Remote Sensing*, *9*(9), 889. <https://doi.org/10.3390/rs9090889>
- Bagheri, O., Pokhrel, Y., Moore, N., & Phanikumar, M. S. (2024). Groundwater dominates terrestrial hydrological processes in the Amazon at the basin and subbasin scales. *Journal of Hydrology*, *628*, 130312.
- Bagley, J. E., Desai, A. R., Harding, K. J., Snyder, P. K., & Foley, J. A. (2014). Drought and deforestation: Has land cover change influenced recent precipitation extremes in the Amazon? *Journal of Climate*, *27*(1), 345–361. <https://doi.org/10.1175/JCLI-D-12-00369.1>
- Bala, G., & Nag, B. (2012). Albedo enhancement over land to counteract global warming: impacts on hydrological cycle. *Climate Dynamics*, *39*, 1527–1542.
- Barichivich, J., Gloor, E., Peylin, P., Brienen, R. J. W., Schöngart, J., Espinoza, J. C., & Pattanayak, K. C. (2018). Recent intensification of Amazon flooding extremes driven by

- strengthened Walker circulation. *Science Advances*, 4(9), eaat8785.
- Barkhordarian, A., Saatchi, S. S., Behrangi, A., Loikith, P. C., & Mechoso, C. R. (2019). A Recent Systematic Increase in Vapor Pressure Deficit over Tropical South America. *Scientific Reports*, 9(1), 1–12. <https://doi.org/10.1038/s41598-019-51857-8>
- Barlow, J., & Peres, C. A. (2008). Fire-mediated dieback and compositional cascade in an Amazonian forest. *Philosophical Transactions of the Royal Society B: Biological Sciences*, 363(1498), 1787–1794.
- Barlow, J., Lennox, G. D., Ferreira, J., Berenguer, E., Lees, A. C., Nally, R. Mac, et al. (2016). Anthropogenic disturbance in tropical forests can double biodiversity loss from deforestation. *Nature*, 535(7610), 144–147.
- Barreto, J. R., Berenguer, E., Ferreira, J., Joly, C. A., Malhi, Y., de Seixas, M. M. M., & Barlow, J. (2021). Assessing invertebrate herbivory in human-modified tropical forest canopies. *Ecology and Evolution*, 11(9), 4012–4022.
- Bäse, F., Elsenbeer, H., Neill, C., & Krusche, A. V. (2012). Differences in throughfall and net precipitation between soybean and transitional tropical forest in the southern Amazon, Brazil. *Agriculture, Ecosystems & Environment*, 159, 19–28.
- Bates, P. D., Horritt, M. S., & Fewtrell, T. J. (2010). A simple inertial formulation of the shallow water equations for efficient two-dimensional flood inundation modelling. *Journal of Hydrology*, 387(1–2), 33–45. <https://doi.org/10.1016/j.jhydrol.2010.03.027>
- Berenguer, E., Ferreira, J., Gardner, T. A., Aragão, L. E. O. C., De Camargo, P. B., Cerri, C. E., et al. (2014). A large-scale field assessment of carbon stocks in human-modified tropical forests. *Global Change Biology*, 20(12), 3713–3726.
- Beven, K. J., & Kirkby, M. J. (1979). A physically based, variable contributing area model of basin hydrology. *Hydrological Sciences Bulletin*, 24(1), 43–69. <https://doi.org/10.1080/02626667909491834>
- Bonell, M., Purandara, B. K., Venkatesh, B., Krishnaswamy, J., Acharya, H. A. K., Singh, U. V., et al. (2010). The impact of forest use and reforestation on soil hydraulic conductivity in the Western Ghats of India: Implications for surface and sub-surface hydrology. *Journal of Hydrology*, 391(1–2), 47–62.
- Bosmans, J. H. C., Van Beek, L. P. H., Sutanudjaja, E. H., & Bierkens, M. F. P. (2017). Hydrological impacts of global land cover change and human water use. *Hydrology and Earth System Sciences*, 21(11), 5603–5626. <https://doi.org/10.5194/hess-21-5603-2017>
- Brando, P. M., Nepstad, D. C., Balch, J. K., Bolker, B., Christman, M. C., Coe, M., & Putz, F. E. (2012). Fire-induced tree mortality in a neotropical forest: the roles of bark traits, tree size, wood density and fire behavior. *Global Change Biology*, 18(2), 630–641.
- Brown, E., Johansen, I. C., Bortoleto, A. P., Pokhrel, Y., Chaudhari, S., Cak, A., et al. (2022).

- Feasibility of hybrid in-stream generator–photovoltaic systems for Amazonian off-grid communities. *PNAS Nexus*, 1(3), pgac077. <https://doi.org/10.1093/pnasnexus/pgac077>
- Bruno, R. D., Da Rocha, H. R., De Freitas, H. C., Goulden, M. L., & Miller, S. D. (2006). Soil moisture dynamics in an eastern Amazonian tropical forest. *Hydrological Processes: An International Journal*, 20(12), 2477–2489.
- Builes-Jaramillo, A., Marwan, N., Poveda, G., & Kurths, J. (2018). Nonlinear interactions between the Amazon River basin and the Tropical North Atlantic at interannual timescales. *Climate Dynamics*, 50, 2951–2969.
- Bullock, E. L., Woodcock, C. E., Souza, C., & Olofsson, P. (2020). Satellite-based estimates reveal widespread forest degradation in the Amazon. *Global Change Biology*, 26(5), 2956–2969. <https://doi.org/10.1111/gcb.15029>
- Bustamante, M. G., Cruz, F. W., Vuille, M., Apaéstegui, J., Strikis, N., Panizo, G., et al. (2016). Holocene changes in monsoon precipitation in the Andes of NE Peru based on $\delta^{18}O$ speleothem records. *Quaternary Science Reviews*, 146, 274–287.
- Butt, N., De Oliveira, P. A., & Costa, M. H. (2011). Evidence that deforestation affects the onset of the rainy season in Rondonia, Brazil. *Journal of Geophysical Research Atmospheres*, 116(11). <https://doi.org/10.1029/2010JD015174>
- Callede, J., Cochonneau, G., VIEIRA, A. F., Guyot, J.-L., Guimaraes, V. S., & De Oliveira, E. (2010). The river amazon water contribution to the atlantic Ocean. *J Water Sci*, 23(3), 247–273.
- Campos-Silva, J. V, Peres, C. A., Hawes, J. E., Haugaasen, T., Freitas, C. T., Ladle, R. J., & Lopes, P. F. M. (2021). Sustainable-use protected areas catalyze enhanced livelihoods in rural Amazonia. *Proceedings of the National Academy of Sciences*, 118(40), e2105480118.
- Cerri, C. E. P., Sparovek, G., Bernoux, M., Easterling, W. E., Melillo, J. M., & Cerri, C. C. (2007). Tropical agriculture and global warming: impacts and mitigation options. *Scientia Agricola*, 64, 83–99.
- Chagas, V. B. P., Chaffe, P. L. B., & Blöschl, G. (2022). Climate and land management accelerate the Brazilian water cycle. *Nature Communications*, 13(1), 5136.
- Chaudhari, S., & Pokhrel, Y. (2022). Alteration of River Flow and Flood Dynamics by Existing and Planned Hydropower Dams in the Amazon River Basin. *Water Resources Research*, 58(5), e2021WR030555. <https://doi.org/10.1029/2021WR030555>
- Chaudhari, S., Felfelani, F., Shin, S., & Pokhrel, Y. (2018). Climate and anthropogenic contributions to the desiccation of the second largest saline lake in the twentieth century. *Journal of Hydrology*, 560, 342–353. <https://doi.org/10.1016/j.jhydrol.2018.03.034>
- Chaudhari, S., Pokhrel, Y., Moran, E., & Miguez-Macho, G. (2019). Multi-decadal hydrologic change and variability in the Amazon River basin: Understanding terrestrial water storage

- variations and drought characteristics. *Hydrology and Earth System Sciences*, 23(7), 2841–2862. <https://doi.org/10.5194/hess-23-2841-2019>
- Chaudhari, S., Brown, E., Quispe-Abad, R., Moran, E., Müller, N., & Pokhrel, Y. (2021). In-stream turbines for rethinking hydropower development in the Amazon basin. *Nature Sustainability*, 4(8), 680–687. <https://doi.org/10.1038/s41893-021-00712-8>
- Clark, M. P., Fan, Y., Lawrence, D. M., Adam, J. C., Bolster, D., Gochis, D. J., et al. (2015). Improving the representation of hydrologic processes in Earth System Models. *Water Resources Research*, 51(8), 5929–5956. <https://doi.org/10.1002/2015WR017096>
- Costa, Marcos H., Yanagi, S. N. M., Souza, P. J. O. P., Ribeiro, A., & Rocha, E. J. P. (2007). Climate change in Amazonia caused by soybean cropland expansion, as compared to caused by pastureland expansion. *Geophysical Research Letters*, 34(7). <https://doi.org/10.1029/2007GL029271>
- Costa, Marcos Heil, & Foley, J. A. (1999). Trends in the hydrologic cycle of the Amazon basin. *Journal of Geophysical Research Atmospheres*, 104(D12), 14189–14198. <https://doi.org/10.1029/1998JD200126>
- Costa, Marcos Heil, & Pires, G. F. (2010a). Effects of Amazon and Central Brazil deforestation scenarios on the duration of the dry season in the arc of deforestation. *International Journal of Climatology*, 30(13), 1970–1979.
- Costa, Marcos Heil, & Pires, G. F. (2010b). Effects of Amazon and Central Brazil deforestation scenarios on the duration of the dry season in the arc of deforestation. *International Journal of Climatology*, 30(13), 1970–1979. <https://doi.org/10.1002/joc.2048>
- Cox, P. M., Betts, R. A., Collins, M., Harris, P. P., Huntingford, C., & Jones, C. D. (2004). Amazonian forest dieback under climate-carbon cycle projections for the 21st century. *Theoretical and Applied Climatology*, 78(1–3), 137–156. <https://doi.org/10.1007/s00704-004-0049-4>
- Davidson, E. A., De Araújo, A. C., Artaxo, P., Balch, J. K., Brown, I. F., Mercedes, M. M., et al. (2012). The Amazon basin in transition. *Nature*, 481(7381), 321–328. <https://doi.org/10.1038/nature10717>
- DeAngelis, D. L., Post, W. M., & Travis, C. C. (2012). *Positive feedback in natural systems* (Vol. 15). Springer Science & Business Media.
- Dexter, K. G., Pennington, R. T., Oliveira-Filho, A. T., Bueno, M. L., Silva de Miranda, P. L., & Neves, D. M. (2018). Inserting tropical dry forests into the discussion on biome transitions in the tropics. *Frontiers in Ecology and Evolution*, 6, 104.
- Duponchelle, F., Isaac, V. J., Rodrigues Da Costa Doria, C., Van Damme, P. A., Herrera-R, G. A., Anderson, E. P., et al. (2021). Conservation of migratory fishes in the Amazon basin. *Aquatic Conservation: Marine and Freshwater Ecosystems*, 31(5), 1087–1105. <https://doi.org/10.1002/aqc.3550>

- Eltahir, E. A. B., & Bras, R. L. (1994). Precipitation recycling in the Amazon basin. *Quarterly Journal of the Royal Meteorological Society*, *120*(518), 861–880. <https://doi.org/10.1002/qj.49712051806>
- Endo, W., Peres, C. A., & Hugaasen, T. (2016). Flood pulse dynamics affects exploitation of both aquatic and terrestrial prey by Amazonian floodplain settlements. *Biological Conservation*, *201*, 129–136.
- Van Der Ent, R. J., Savenije, H. H. G., Schaeffli, B., & Steele-Dunne, S. C. (2010). Origin and fate of atmospheric moisture over continents. *Water Resources Research*, *46*(9). <https://doi.org/10.1029/2010WR009127>
- Espinoza Villar, J. C., Ronchail, J., Guyot, J. L., Cochonneau, G., Naziano, F., Lavado, W., et al. (2009). Spatio-temporal rainfall variability in the Amazon basin countries (Brazil, Peru, Bolivia, Colombia, and Ecuador). *International Journal of Climatology: A Journal of the Royal Meteorological Society*, *29*(11), 1574–1594.
- Esquivel-Muelbert, A., Baker, T. R., Dexter, K. G., Lewis, S. L., Brienen, R. J. W., Feldpausch, T. R., et al. (2019). Compositional response of Amazon forests to climate change. *Global Change Biology*, *25*(1), 39–56.
- Fan, Y., & Miguez-Macho, G. (2010). Potential groundwater contribution to Amazon evapotranspiration. *Hydrology and Earth System Sciences*, *14*(10), 2039–2056. <https://doi.org/10.5194/hess-14-2039-2010>
- Fan, Y., Li, H., & Miguez-Macho, G. (2013). Global patterns of groundwater table depth. *Science*, *339*(6122), 940–943. <https://doi.org/10.1126/science.1229881>
- Fan, Ying, Miguez-Macho, G., Jobbágy, E. G., Jackson, R. B., & Otero-Casal, C. (2017). Hydrologic regulation of plant rooting depth. *Proceedings of the National Academy of Sciences of the United States of America*, *114*(40), 10572–10577. <https://doi.org/10.1073/pnas.1712381114>
- Fassoni-Andrade, A. C., Fleischmann, A. S., Papa, F., Paiva, R. C. D. de, Wongchuig, S., Melack, J. M., et al. (2021). Amazon Hydrology From Space: Scientific Advances and Future Challenges. *Reviews of Geophysics*, *59*(4), e2020RG000728. <https://doi.org/10.1029/2020RG000728>
- Felfelani, F., Wada, Y., Longuevergne, L., & Pokhrel, Y. N. (2017). Natural and human-induced terrestrial water storage change: A global analysis using hydrological models and GRACE. *Journal of Hydrology*, *553*, 105–118. <https://doi.org/10.1016/j.jhydrol.2017.07.048>
- Field, C. B., Behrenfeld, M. J., Randerson, J. T., & Falkowski, P. (1998). Primary production of the biosphere: Integrating terrestrial and oceanic components. *Science*, *281*(5374), 237–240. <https://doi.org/10.1126/science.281.5374.237>
- Flores, B. M., Fagoaga, R., Nelson, B. W., & Holmgren, M. (2016). Repeated fires trap Amazonian blackwater floodplains in an open vegetation state. *Journal of Applied Ecology*,

53(5), 1597–1603.

- Foley, J. A., DeFries, R., Asner, G. P., Barford, C., Bonan, G., Carpenter, S. R., et al. (2005). Global consequences of land use. *Science*, 309(5734), 570–574. <https://doi.org/10.1126/science.1111772>
- Frappart, F., Papa, F., Güntner, A., Tomasella, J., Pfeffer, J., Ramillien, G., et al. (2019). The spatio-temporal variability of groundwater storage in the Amazon River Basin. *Advances in Water Resources*, 124, 41–52.
- Fu, R., Yin, L., Li, W., Arias, P. A., Dickinson, R. E., Huang, L., et al. (2013). Increased dry-season length over southern Amazonia in recent decades and its implication for future climate projection. *Proceedings of the National Academy of Sciences of the United States of America*, 110(45), 18110–18115. <https://doi.org/10.1073/pnas.1302584110>
- Gash, J. H. C. (1979). An analytical model of rainfall interception by forests. *Quarterly Journal of the Royal Meteorological Society*, 105(443), 43–55.
- Gatti, L. V., Basso, L. S., Miller, J. B., Gloor, M., Gatti Domingues, L., Cassol, H. L. G., et al. (2021). Amazonia as a carbon source linked to deforestation and climate change. *Nature*, 595(7867), 388–393.
- Getirana, A. C. V., Boone, A., Yamazaki, D., Decharme, B., Papa, F., & Mognard, N. (2012). The hydrological modeling and analysis platform (HyMAP): Evaluation in the Amazon basin. *Journal of Hydrometeorology*, 13(6), 1641–1665.
- Ghimire, C. P., Bruijnzeel, L. A., Bonell, M., Coles, N., Lubczynski, M. W., & Gilmour, D. A. (2014). The effects of sustained forest use on hillslope soil hydraulic conductivity in the Middle Mountains of Central Nepal. *Ecohydrology*, 7(2), 478–495.
- Guan, K., Pan, M., Li, H., Wolf, A., Wu, J., Medvigy, D., et al. (2015). Photosynthetic seasonality of global tropical forests constrained by hydroclimate. *Nature Geoscience*, 8(4), 284–289. <https://doi.org/10.1038/ngeo2382>
- Guilhen, J., Al Bitar, A., Sauvage, S., Parrens, M., Martinez, J.-M., Abril, G., et al. (2020). Denitrification, carbon and nitrogen emissions over the Amazonian wetlands. *Biogeochemistry: Wetlands*. <https://doi.org/10.5194/bg-2020-3>.
- Hassler, S. K., Zimmermann, B., van Breugel, M., Hall, J. S., & Elsenbeer, H. (2011). Recovery of saturated hydraulic conductivity under secondary succession on former pasture in the humid tropics. *Forest Ecology and Management*, 261(10), 1634–1642.
- Heerspink, B. P., Kendall, A. D., Coe, M. T., & Hyndman, D. W. (2020). Trends in streamflow, evapotranspiration, and groundwater storage across the Amazon Basin linked to changing precipitation and land cover. *Journal of Hydrology: Regional Studies*, 32, 100755. <https://doi.org/10.1016/j.ejrh.2020.100755>
- Hersbach, H., B, B., P, B., S, H., A, H., J, M., et al. (2020). The ERA5 global reanalysis.

- Quarterly Journal of the Royal Meteorological Society*, 146(730), 1999–2049.
- Hirota, M., Holmgren, M., Van Nes, E. H., & Scheffer, M. (2011). Global resilience of tropical forest and savanna to critical transitions. *Science*, 334(6053), 232–235.
- Hoek van Dijke, A. J., Herold, M., Mallick, K., Benedict, I., Machwitz, M., Schlerf, M., et al. (2022). Shifts in regional water availability due to global tree restoration. *Nature Geoscience*, 15(5), 363–368. <https://doi.org/10.1038/s41561-022-00935-0>
- Hubbell, S. P., He, F., Condit, R., Borda-de-Água, L., Kellner, J., & Ter Steege, H. (2008). How many tree species are there in the Amazon and how many of them will go extinct? *Proceedings of the National Academy of Sciences*, 105(supplement_1), 11498–11504.
- Jones, C., Lowe, J., Liddicoat, S., & Betts, R. (2009). Committed terrestrial ecosystem changes due to climate change. *Nature Geoscience*, 2(7), 484–487. <https://doi.org/10.1038/ngeo555>
- Junk, W. J., Piedade, M. T. F., Schöngart, J., Cohn-Haft, M., Adeney, J. M., & Wittmann, F. (2011). A classification of major naturally-occurring Amazonian lowland wetlands. *Wetlands*, 31, 623–640.
- Kendall, M. G. (1948). Rank correlation methods.
- Khanna, J., Medvigy, D., Fueglistaler, S., & Walko, R. (2017). Regional dry-season climate changes due to three decades of Amazonian deforestation. *Nature Climate Change*, 7(3), 200–204. <https://doi.org/10.1038/nclimate3226>
- Kirschke, S., Bousquet, P., Ciais, P., Saunoy, M., Canadell, J. G., Dlugokencky, E. J., et al. (2013). Three decades of global methane sources and sinks. *Nature Geoscience*, 6(10), 813–823.
- Kumagai, T., Kanamori, H., & Yasunari, T. (2013). Deforestation-induced reduction in rainfall. *Hydrological Processes*, 27(25), 3811–3814.
- Lanckriet, S., Araya, T., Cornelis, W., Verfaillie, E., Poesen, J., Govaerts, B., et al. (2012). Impact of conservation agriculture on catchment runoff and soil loss under changing climate conditions in May Zeg-zeg (Ethiopia). *Journal of Hydrology*, 475, 336–349.
- Laurance, W. F., Cochrane, M. A., Bergen, S., Fearnside, P. M., Delamônica, P., Barber, C., et al. (2001). The future of the Brazilian Amazon. *Science*, 291(5503), 438–439. <https://doi.org/10.1126/science.291.5503.438>
- Laurance, William F., Lovejoy, T. E., Vasconcelos, H. L., Bruna, E. M., Didham, R. K., Stouffer, P. C., et al. (2002). Ecosystem decay of Amazonian forest fragments: A 22-year investigation. *Conservation Biology*, 16(3), 605–618. <https://doi.org/10.1046/j.1523-1739.2002.01025.x>
- Lavagnini, I., Badocco, D., Pastore, P., & Magno, F. (2011). Theil–Sen nonparametric regression technique on univariate calibration, inverse regression and detection limits. *Talanta*, 87,

180–188.

- Lawrence, D. M., Fisher, R. A., Koven, C. D., Oleson, K. W., Swenson, S. C., Bonan, G., et al. (2019). The Community Land Model Version 5: Description of New Features, Benchmarking, and Impact of Forcing Uncertainty. *Journal of Advances in Modeling Earth Systems*, *11*(12), 4245–4287. <https://doi.org/10.1029/2018MS001583>
- Legates, D. R., & McCabe, G. J. (1999). Evaluating the use of “goodness-of-fit” measures in hydrologic and hydroclimatic model validation. *Water Resources Research*, *35*(1), 233–241. <https://doi.org/10.1029/1998WR900018>
- Leite-Filho, A. T., de Sousa Pontes, V. Y., & Costa, M. H. (2019). Effects of Deforestation on the Onset of the Rainy Season and the Duration of Dry Spells in Southern Amazonia. *Journal of Geophysical Research: Atmospheres*, *124*(10), 5268–5281. <https://doi.org/10.1029/2018JD029537>
- Lenton, T. M., Held, H., Kriegler, E., Hall, J. W., Lucht, W., Rahmstorf, S., & Schellnhuber, H. J. (2008). Tipping elements in the Earth’s climate system. *Proceedings of the National Academy of Sciences*, *105*(6), 1786–1793.
- Levy, M. C., Lopes, A. V., Cohn, A., Larsen, L. G., & Thompson, S. E. (2018). Land use change increases streamflow across the arc of deforestation in Brazil. *Geophysical Research Letters*, *45*(8), 3520–3530.
- Lewinsohn, T. M., & Prado, P. I. (2005). How many species are there in Brazil? *Conservation Biology*, *19*(3), 619–624.
- Li, F., Zhang, G., & Xu, Y. J. (2014). Spatiotemporal variability of climate and streamflow in the Songhua River Basin, northeast China. *Journal of Hydrology*, *514*, 53–64.
- Longo, M., Saatchi, S., Keller, M., Bowman, K., Ferraz, A., Moorcroft, P. R., et al. (2020). Impacts of degradation on water, energy, and carbon cycling of the Amazon tropical forests. *Journal of Geophysical Research: Biogeosciences*, *125*(8), e2020JG005677.
- Longuevergne, L., Scanlon, B. R., & Wilson, C. R. (2010). GRACE hydrological estimates for small basins: Evaluating processing approaches on the High Plains aquifer, USA. *Water Resources Research*, *46*(11). <https://doi.org/10.1029/2009WR008564>
- Lovejoy, T. E., & Nobre, C. (2019). Amazon tipping point: Last chance for action. *Science Advances*. American Association for the Advancement of Science. <https://doi.org/10.1126/sciadv.aba2949>
- Maeda, E. E., Ma, X., Wagner, F. H., Kim, H., Oki, T., Eamus, D., & Huete, A. (2017). Evapotranspiration seasonality across the Amazon Basin. *Earth System Dynamics*, *8*(2), 439–454. <https://doi.org/10.5194/esd-8-439-2017>
- Malhi, Y., Wood, D., Baker, T. R., Wright, J., Phillips, O. L., Cochrane, T., et al. (2006). The regional variation of aboveground live biomass in old-growth Amazonian forests. *Global*

Change Biology, 12(7), 1107–1138.

- Malhi, Y., Roberts, J. T., Betts, R. A., Killeen, T. J., Li, W., & Nobre, C. A. (2008). Climate change, deforestation, and the fate of the Amazon. *Science*, 319(5860), 169–172. <https://doi.org/10.1126/science.1146961>
- Malhi, Y., Aragão, L. E. O. C., Galbraith, D., Huntingford, C., Fisher, R., Zelazowski, P., et al. (2009). Exploring the likelihood and mechanism of a climate-change-induced dieback of the Amazon rainforest. *Proceedings of the National Academy of Sciences*, 106(49), 20610–20615.
- Mann, H. B. (1945). Nonparametric tests against trend. *Econometrica: Journal of the Econometric Society*, 245–259.
- Mapbiomas_Amazonia. (2022). *Collection 2.0 of annual maps of land cover, land use and land use changes between 1985 to 2018 in the Pan-Amazon. The Amazonian Network of Georeferenced Socio-Environmental Information (RAISG)*. Retrieved from <https://amazonia.mapbiomas.org/>
- Marengo, Jose A., Souza, C. M., Thonicke, K., Burton, C., Halladay, K., Betts, R. A., et al. (2018). Changes in Climate and Land Use Over the Amazon Region: Current and Future Variability and Trends. *Frontiers in Earth Science*, 6, 228. <https://doi.org/10.3389/feart.2018.00228>
- Marengo, Jose Antonio, Tomasella, J., Soares, W. R., Alves, L. M., & Nobre, C. A. (2012). Extreme climatic events in the Amazon basin Climatological and hydrological context of recent floods. *Theoretical and Applied Climatology*, 107(1–2), 73–85.
- Marengo, José Antonio, & Espinoza, J. C. (2016). Extreme seasonal droughts and floods in Amazonia: causes, trends and impacts. *International Journal of Climatology*, 36(3), 1033–1050.
- Martens, B., Miralles, D. G., Lievens, H., Van Der Schalie, R., De Jeu, R. A. M., Fernández-Prieto, D., et al. (2017). GLEAM v3: Satellite-based land evaporation and root-zone soil moisture. *Geoscientific Model Development*, 10(5), 1903–1925.
- Matricardi, E. A. T., Skole, D. L., Costa, O. B., Pedlowski, M. A., Samek, J. H., & Miguel, E. P. (2020). Long-term forest degradation surpasses deforestation in the Brazilian Amazon. *Science*, 369(6509), 1378–1382. <https://doi.org/10.1126/SCIENCE.ABB3021>
- Mattos, C. R. C., Hirota, M., Oliveira, R. S., Flores, B. M., Miguez-Macho, G., Pokhrel, Y., & Fan, Y. (2023). Double stress of waterlogging and drought drives forest–savanna coexistence. *Proceedings of the National Academy of Sciences*, 120(33), e2301255120.
- Melack, J. M., Hess, L. L., Gastil, M., Forsberg, B. R., Hamilton, S. K., Lima, I. B. T., & Novo, E. M. L. M. (2004). Regionalization of methane emissions in the Amazon Basin with microwave remote sensing. *Global Change Biology*, 10(5), 530–544.

- Mercedes, G., & Montenegro, L. (2005). Globalwarming and Tropical Land-Use Change: Greenhouse Gas Emissions Frombiomass Burning, Decomposition and Soils in Forest Conversion, Shifting Cultivation and Secondaryvegetation. *Climatic Change*, 46(1), 115–158.
- Miguez-Macho, G., & Fan, Y. (2012). The role of groundwater in the Amazon water cycle: 2. Influence on seasonal soil moisture and evapotranspiration. *Journal of Geophysical Research Atmospheres*, 117(15). <https://doi.org/10.1029/2012JD017540>
- Miguez-Macho, G., Fan, Y., Weaver, C. P., Walko, R., & Robock, A. (2007). Incorporating water table dynamics in climate modeling: 2. Formulation, validation, and soil moisture simulation. *Journal of Geophysical Research Atmospheres*, 112(13). <https://doi.org/10.1029/2006JD008112>
- Miralles, D. G., Holmes, T. R. H., De Jeu, R. A. M., Gash, J. H., Meesters, A., & Dolman, A. J. (2011). Global land-surface evaporation estimated from satellite-based observations. *Hydrology and Earth System Sciences*, 15(2), 453–469.
- Mishra, V., Cherkauer, K. A., Niyogi, D., Lei, M., Pijanowski, B. C., Ray, D. K., et al. (2010). A regional scale assessment of land use/land cover and climatic changes on water and energy cycle in the upper Midwest United States. *International Journal of Climatology*, 30(13), 2025–2044.
- Monteith, J. L. (1965). Evaporation and environment. In *Symposia of the society for experimental biology* (Vol. 19, pp. 205–234). Cambridge University Press (CUP) Cambridge.
- Moore, N., Arima, E., Walker, R., & Ramos da Silva, R. (2007). Uncertainty and the changing hydroclimatology of the Amazon. *Geophysical Research Letters*, 34(14). <https://doi.org/10.1029/2007GL030157>
- Moran, E. F. (1993). Deforestation and land use in the Brazilian Amazon. *Human Ecology*, 21, 1–21.
- Morrison, E. B., & Lindell, C. A. (2011). Active or Passive Forest Restoration? Assessing Restoration Alternatives with Avian Foraging Behavior. *Restoration Ecology*, 19(201), 170–177. <https://doi.org/10.1111/j.1526-100X.2010.00725.x>
- Morton, D. C., DeFries, R. S., Shimabukuro, Y. E., Anderson, L. O., Arai, E., Del Bon Espirito-Santo, F., et al. (2006). Cropland expansion changes deforestation dynamics in the southern Brazilian Amazon. *Proceedings of the National Academy of Sciences of the United States of America*, 103(39), 14637–14641. <https://doi.org/10.1073/pnas.0606377103>
- Muma, M., Assani, A. A., Landry, R., Quessy, J.-F., & Mesfioui, M. (2011). Effects of the change from forest to agriculture land use on the spatial variability of summer extreme daily flow characteristics in southern Quebec (Canada). *Journal of Hydrology*, 407(1–4), 153–163.

- Nagy, L., Artaxo, P., & Forsberg, B. R. (2016). Interactions between biosphere, atmosphere, and human land use in the Amazon basin: an introduction. *Interactions Between Biosphere, Atmosphere and Human Land Use in the Amazon Basin*, 3–15.
- Neill, C., Coe, M. T., Riskin, S. H., Krusche, A. V., Elsenbeer, H., Macedo, M. N., et al. (2013). Watershed responses to Amazon soya bean cropland expansion and intensification. *Philosophical Transactions of the Royal Society B: Biological Sciences*, 368(1619), 20120425.
- Nepstad, D. C., Stickler, C. M., Filho, B. S.-, & Merry, F. (2008). Interactions among Amazon land use, forests and climate: prospects for a near-term forest tipping point. *Philosophical Transactions of the Royal Society B: Biological Sciences*, 363(1498), 1737–1746.
- van Nes, E. H., Arani, B. M. S., Staal, A., van der Bolt, B., Flores, B. M., Bathiany, S., & Scheffer, M. (2016). What do you mean, ‘tipping point’? *Trends in Ecology & Evolution*, 31(12), 902–904.
- Nobre, Carlos A., Sellers, P. J., & Shukla, J. (1991). Amazonian Deforestation and Regional Climate Change. *Journal of Climate*, 4(10), 957–988. [https://doi.org/10.1175/1520-0442\(1991\)004<0957:adarcc>2.0.co;2](https://doi.org/10.1175/1520-0442(1991)004<0957:adarcc>2.0.co;2)
- Nobre, Carlos A., Sampaio, G., Borma, L. S., Castilla-Rubio, J. C., Silva, J. S., & Cardoso, M. (2016). Land-use and climate change risks in the amazon and the need of a novel sustainable development paradigm. *Proceedings of the National Academy of Sciences of the United States of America*, 113(39), 10759–10768. <https://doi.org/10.1073/pnas.1605516113>
- Nobre, Carlos Afonso, & Borma, L. D. S. (2009). “Tipping points” for the Amazon forest. *Current Opinion in Environmental Sustainability*, 1(1), 28–36. <https://doi.org/10.1016/j.cosust.2009.07.003>
- De Paiva, R. C. D., Buarque, D. C., Collischonn, W., Bonnet, M., Frappart, F., Calmant, S., & Bulhões Mendes, C. A. (2013). Large-scale hydrologic and hydrodynamic modeling of the Amazon River basin. *Water Resources Research*, 49(3), 1226–1243.
- Pangala, S. R., Enrich-Prast, A., Basso, L. S., Peixoto, R. B., Bastviken, D., Hornibrook, E. R. C., et al. (2017). Large emissions from floodplain trees close the Amazon methane budget. *Nature*, 552(7684), 230–234.
- Parrotta, J. A., Wildburger, C., & Mansourian, S. (2012). *Understanding relationships between biodiversity, carbon, forests and people: the key to achieving REDD+ objectives. A global assessment report prepared by the Global Forest Expert Panel on Biodiversity, Forest Management and REDD+*. (Vol. 31). IUFRO (International Union of Forestry Research Organizations) Secretariat.
- Pfeffer, J., Seyler, F., Bonnet, M., Calmant, S., Frappart, F., Papa, F., et al. (2014). Low-water maps of the groundwater table in the central Amazon by satellite altimetry. *Geophysical Research Letters*, 41(6), 1981–1987.

- Phillips, J. N., & Derryberry, E. P. (2017). Equivalent effects of bandwidth and trill rate: support for a performance constraint as a competitive signal. *Animal Behaviour*, *132*, 209–215.
- Pielke, R. A., Cotton, W. R., Walko, R. L., Tremback, C. J., Lyons, W. A., Grasso, L. D., et al. (1992). A comprehensive meteorological modeling system-RAMS. *Meteorology and Atmospheric Physics*, *49*(1–4), 69–91. <https://doi.org/10.1007/BF01025401>
- Pison, I., Ringeval, B., Bousquet, P., Prigent, C., & Papa, F. (2013). Stable atmospheric methane in the 2000s: key-role of emissions from natural wetlands. *Atmospheric Chemistry and Physics*, *13*(23), 11609–11623.
- Pokhrel, Y. N., Fan, Y., Miguez-Macho, G., Yeh, P. J. F., & Han, S. C. (2013). The role of groundwater in the Amazon water cycle: 3. Influence on terrestrial water storage computations and comparison with GRACE. *Journal of Geophysical Research Atmospheres*, *118*(8), 3233–3244. <https://doi.org/10.1002/jgrd.50335>
- Pokhrel, Y. N., Fan, Y., & Miguez-Macho, G. (2014). Potential hydrologic changes in the Amazon by the end of the 21st century and the groundwater buffer. *Environmental Research Letters*, *9*(8), 84004. <https://doi.org/10.1088/1748-9326/9/8/084004>
- Poorter, L., Bongers, F., Aide, T. M., Almeyda Zambrano, A. M., Balvanera, P., Becknell, J. M., et al. (2016). Biomass resilience of Neotropical secondary forests. *Nature*, *530*(7589), 211–214.
- Poorter, L., Craven, D., Jakovac, C. C., van der Sande, M. T., Amissah, L., Bongers, F., et al. (2021). Multidimensional tropical forest recovery. *Science*, *374*(6573), 1370–1376.
- Poveda, G., Jaramillo, L., & Vallejo, L. F. (2014). Seasonal precipitation patterns along pathways of South American low-level jets and aerial rivers. *Water Resources Research*, *50*(1), 98–118.
- Priestley, C. H. B., & Taylor, R. J. (1972). On the assessment of surface heat flux and evaporation using large-scale parameters. *Monthly Weather Review*, *100*(2), 81–92.
- Putz, F. E., & Redford, K. H. (2010). The importance of defining ‘forest’: Tropical forest degradation, deforestation, long-term phase shifts, and further transitions. *Biotropica*, *42*(1), 10–20.
- Raymond, P. A., Hartmann, J., Lauerwald, R., Sobek, S., McDonald, C., Hoover, M., et al. (2013). Global carbon dioxide emissions from inland waters. *Nature*, *503*(7476), 355–359.
- Reis, A., Magne, K., Massot, S., Tallini, L. R., Scopel, M., Bastida, J., et al. (2019). Amaryllidaceae alkaloids: identification and partial characterization of montanine production in *Rhodophiala bifida* plant. *Scientific Reports*, *9*(1), 8471.
- Richey, J. E., Melack, J. M., Aufdenkampe, A. K., Ballester, V. M., & Hess, L. L. (2002). Outgassing from Amazonian rivers and wetlands as a large tropical source of atmospheric CO₂. *Nature*, *416*(6881), 617–620.

- Rozendaal, D. M. A., Bongers, F., Aide, T. M., Alvarez-Dávila, E., Ascarrunz, N., Balvanera, P., et al. (2019). Biodiversity recovery of Neotropical secondary forests. *Science Advances*, 5(3), eaau3114.
- Running, S., Mu, Q., Zhao, M., & Moreno, A. (2021). *MODIS/Terra Net Evapotranspiration 8-Day L4 Global 500m SIN Grid V061. NASA EOSDIS Land Processes DAAC*. Retrieved from <https://doi.org/10.5067/MODIS/MOD16A3GF.061>
- Rutishauser, E., Hérault, B., Baraloto, C., Blanc, L., Descroix, L., Sotta, E. D., et al. (2015). Rapid tree carbon stock recovery in managed Amazonian forests. *Current Biology*, 25(18), R787–R788.
- Saatchi, S. S., Harris, N. L., Brown, S., Lefsky, M., Mitchard, E. T. A., Salas, W., et al. (2011). Benchmark map of forest carbon stocks in tropical regions across three continents. *Proceedings of the National Academy of Sciences*, 108(24), 9899–9904.
- Salati, E., Dall'Olio, A., Matsui, E., & Gat, J. R. (1979). Recycling of water in the Amazon basin: an isotopic study. *Water Resources Research*, 15(5), 1250–1258.
- Sampaio, G., Nobre, C., Costa, M. H., Satyamurty, P., Soares-Filho, B. S., & Cardoso, M. (2007). Regional climate change over eastern Amazonia caused by pasture and soybean cropland expansion. *Geophysical Research Letters*, 34(17). <https://doi.org/10.1029/2007GL030612>
- Santoro, M., Kirches, G., Wevers, J., Boettcher, M., Brockmann, C., Lamarche, C., & Defourny, P. (2017). Land cover CCI: Product user guide version 2.0. *Climate Change Initiative Belgium*.
- Satyamurty, P., da Costa, C. P. W., & Manzi, A. O. (2013). Moisture source for the Amazon Basin: a study of contrasting years. *Theoretical and Applied Climatology*, 111, 195–209.
- Scheffer, M., Carpenter, S., Foley, J. A., Folke, C., & Walker, B. (2001). Catastrophic shifts in ecosystems. *Nature*, 413(6856), 591–596.
- Schellnhuber, H. J. (2009). Tipping elements in the Earth System. *Proceedings of the National Academy of Sciences of the United States of America*, 106(49), 20561–20563. <https://doi.org/10.1073/pnas.0911106106>
- Sen, P. K. (1968). Estimates of the regression coefficient based on Kendall's tau. *Journal of the American Statistical Association*, 63(324), 1379–1389.
- Shukla, J., Nobre, C., & Sellers, P. (1990). Amazon deforestation and climate change. Shukla, J., Nobre, C., Sellers, P., 1990. Amazon deforestation and climate change. *Science* (80-.). 247, 1322–1325. <https://doi.org/10.1126/science.247.4948.1322>. *Science*, 247(4948), 1322–1325. <https://doi.org/10.1126/science.247.4948.1322>
- Silva, B. N., Khan, M., & Han, K. (2018). Towards sustainable smart cities: A review of trends, architectures, components, and open challenges in smart cities. *Sustainable Cities and*

Society, 38, 697–713.

- Siqueira, V. A., Paiva, R. C. D., Fleischmann, A. S., Fan, F. M., Ruhoff, A. L., Pontes, P. R. M., et al. (2018). Toward continental hydrologic-hydrodynamic modeling in South America. *Hydrology and Earth System Sciences*, 22(9), 4815–4842. <https://doi.org/10.5194/hess-22-4815-2018>
- Smith, C. C., Healey, J. R., Berenguer, E., Young, P. J., Taylor, B., Elias, F., et al. (2021). Old-growth forest loss and secondary forest recovery across Amazonian countries. *Environmental Research Letters*, 16(8), 85009.
- Soares-Filho, B., Moutinho, P., Nepstad, D., Anderson, A., Rodrigues, H., Garcia, R., et al. (2010). Role of Brazilian Amazon protected areas in climate change mitigation. *Proceedings of the National Academy of Sciences of the United States of America*, 107(24), 10821–10826. <https://doi.org/10.1073/pnas.0913048107>
- Soares-Filho, B. S., Nepstad, D. C., Curran, L. M., Cerqueira, G. C., Garcia, R. A., Ramos, C. A., et al. (2006). Modelling conservation in the Amazon basin. *Nature*, 440(7083), 520–523. <https://doi.org/10.1038/nature04389>
- Souza Jr, C. M., Z. Shimbo, J., Rosa, M. R., Parente, L. L., A. Alencar, A., Rudorff, B. F. T., et al. (2020). Reconstructing three decades of land use and land cover changes in Brazilian biomes with Landsat archive and Earth Engine. *Remote Sensing*, 12(17), 2735.
- Spracklen, D. V., Arnold, S. R., & Taylor, C. M. (2012). Observations of increased tropical rainfall preceded by air passage over forests. *Nature*, 489(7415), 282–285. <https://doi.org/10.1038/nature11390>
- Spracklen, Dominick V, Arnold, S. R., & Taylor, C. M. (2012). Observations of increased tropical rainfall preceded by air passage over forests. *Nature*, 489(7415), 282–285.
- Staal, A., Tuinenburg, O. A., Bosmans, J. H. C., Holmgren, M., Van Nes, E. H., Scheffer, M., et al. (2018). Forest-rainfall cascades buffer against drought across the Amazon. *Nature Climate Change*, 8(6), 539–543. <https://doi.org/10.1038/s41558-018-0177-y>
- Staal, A., Fetzer, I., Wang-Erlandsson, L., Bosmans, J. H. C., Dekker, S. C., van Nes, E. H., et al. (2020). Hysteresis of tropical forests in the 21st century. *Nature Communications*, 11(1), 1–8. <https://doi.org/10.1038/s41467-020-18728-7>
- Staver, A. C., Archibald, S., & Levin, S. A. (2011). The global extent and determinants of savanna and forest as alternative biome states. *Science*, 334(6053), 230–232. <https://doi.org/10.1126/science.1210465>
- Sterling, S. M., Ducharme, A., & Polcher, J. (2013). The impact of global land-cover change on the terrestrial water cycle. *Nature Climate Change*, 3(4), 385–390. <https://doi.org/10.1038/nclimate1690>
- Theil, H. (1950). A rank-invariant method of linear and polynomial regression analysis.

Indagationes Mathematicae, 12(85), 173.

- Tropek, R., Sedláček, O., Beck, J., Keil, P., Musilová, Z., Šimová, I., & Storch, D. (2014). Comment on “High-resolution global maps of 21st-century forest cover change.” *Science*, 344(6187), 850–853. <https://doi.org/10.1126/science.1248753>
- Walker, R. T. (2020). Collision Course: Development Pushes Amazonia Toward Its Tipping Point. *Environment*, 63(1), 15–25. <https://doi.org/10.1080/00139157.2021.1842711>
- Walko, R. L., Band, L. E., Baron, J., Kittel, T. G. F., Lammers, R., Lee, T. J., et al. (2000). Coupled atmosphere-biophysics-hydrology models for environmental modeling. *Journal of Applied Meteorology*, 39(6), 931–944. [https://doi.org/10.1175/1520-0450\(2000\)039<0931:CABHMF>2.0.CO;2](https://doi.org/10.1175/1520-0450(2000)039<0931:CABHMF>2.0.CO;2)
- Weng, W., Luedeke, M., Zemp, D., Lakes, T., & Kropp, J. (2018). Aerial and surface rivers: Downwind impacts on water availability from land use changes in Amazonia. *Hydrology and Earth System Sciences*, 22(1), 911–927. <https://doi.org/10.5194/hess-22-911-2018>
- Werth, D., & Avissar, R. (2005). The local and global effects of Southeast Asian deforestation. *Geophysical Research Letters*, 32(20), 1–4. <https://doi.org/10.1029/2005GL022970>
- Wohl, E., Barros, A., Brunsell, N., Chappell, N. A., Coe, M., Giambelluca, T., et al. (2012). The hydrology of the humid tropics. *Nature Climate Change*, 2(9), 655–662. <https://doi.org/10.1038/nclimate1556>
- Wright, J. S., Fu, R., Worden, J. R., Chakraborty, S., Clinton, N. E., Risi, C., et al. (2017). Rainforest-initiated wet season onset over the southern Amazon. *Proceedings of the National Academy of Sciences*, 114(32), 8481–8486.
- Xu, D., Agee, E., Wang, J., & Ivanov, V. Y. (2019). Estimation of evapotranspiration of Amazon rainforest using the maximum entropy production method. *Geophysical Research Letters*, 46(3), 1402–1412.
- Yamazaki, D., Kanae, S., Kim, H., & Oki, T. (2011). A physically based description of floodplain inundation dynamics in a global river routing model. *Water Resources Research*, 47(4). <https://doi.org/10.1029/2010WR009726>
- Zak, R., & Nippert, J. B. (2012). Comment on “Global resilience of tropical forest and Savanna to critical transitions.” *Science*, 336(6081), 232–235. <https://doi.org/10.1126/science.1219346>
- Zelazowski, P., Malhi, Y., Huntingford, C., Sitch, S., & Fisher, J. B. (2011). Changes in the potential distribution of humid tropical forests on a warmer planet. *Philosophical Transactions of the Royal Society A: Mathematical, Physical and Engineering Sciences*, 369(1934), 137–160.
- Zemp, D C, Schleussner, C.-F., Barbosa, H. M. J., Van der Ent, R. J., Donges, J. F., Heinke, J., et al. (2014). On the importance of cascading moisture recycling in South America.

Atmospheric Chemistry and Physics, 14(23), 13337–13359.

Zemp, Delphine Clara, Schleussner, C. F., Barbosa, H. M. J., Hirota, M., Montade, V., Sampaio, G., et al. (2017). Self-amplified Amazon forest loss due to vegetation-atmosphere feedbacks. *Nature Communications*, 8(1), 1–10. <https://doi.org/10.1038/ncomms14681>

Zeng, N. (1999). Seasonal cycle and interannual variability in the Amazon hydrologic cycle. *Journal of Geophysical Research Atmospheres*, 104(D8), 9097–9106. <https://doi.org/10.1029/1998JD200088>

Zeng, N., Dickinson, R. E., & Zeng, X. (1996). Climatic impact of Amazon deforestation - A mechanistic model study. *Journal of Climate*, 9(4), 859–883. [https://doi.org/10.1175/1520-0442\(1996\)009<0859:CIOADM>2.0.CO;2](https://doi.org/10.1175/1520-0442(1996)009<0859:CIOADM>2.0.CO;2)